İZMİR KÂTİP ÇELEBİ ÜNİVERSİTESİ
2010
GRADUATE SCHOOL OF NATURAL AND APPLIED SCIENCES

Investigation of Process Conditions in the Preparation of Biobased Polyethylene Masterbatch and Development of Innovative Masterbatches

Materials Science and Engineering

Doctoral Thesis

Mert Yücetürk

ORCID 0000-0002-9692-0893

Advisor: Prof. Dr. M. Özgür Seydibeyoğlu

June, 2025

This is to certify that we have read the thesis **Investigation of process conditions in the preparation of biobased polyethylene masterbatch and development of innovative masterbatches** submitted by **Mert Yücetürk**, and it has been judged to be successful, in scope and in quality, at the defense exam and accepted by our jury as a DOCTORAL THESIS.

APPROVED BY:

Advisor: **Prof. Dr. Mehmet Özgür Seydibeyoğlu**
İzmir Kâtip Çelebi University

Committee Members:

Prof. Dr. Gül Yılmaz Atay
İzmir Kâtip Çelebi University

Prof. Dr. Ümit Halis Erdoğan
Dokuz Eylül University

Prof. Dr. Mustafa Erol
Dokuz Eylül University

Assoc. Prof. Dr. İsmail Doğan Külcü
İzmir Kâtip Çelebi University

Date of Defense: June 30, 2025

Declaration of Authorship

I, **Mert Yücetürk**, declare that this thesis titled **Investigation of process conditions in the preparation of biobased polyethylene masterbatch and development of innovative masterbatches** and the work presented in it are my own. I confirm that:

- This work was done wholly or mainly while in candidature for the Doctoral degree at this university.
- Where any part of this thesis has previously been submitted for a degree or any other qualification at this university or any other institution, this has been clearly stated.
- Where I have consulted the published work of others, this is always clearly attributed.
- Where I have quoted from the work of others, the source is always given. This thesis is entirely my own work, with the exception of such quotations.
- I have acknowledged all major sources of assistance.
- Where the thesis is based on work done by myself jointly with others, I have made clear exactly what was done by others and what I have contributed myself.

Date: 30.06.2025

_____

Investigation of process conditions in the preparation of biobased polyethylene masterbatch and development of innovative masterbatches

Abstract

This doctoral thesis presents a comprehensive investigation into the properties and processing characteristics of biobased polyethylene in comparison with petroleum-based polyethylene. Life cycle assessment data demonstrate the environmental advantage of biobased polyethylene, which removes approximately 2.12 metric tons of CO_2-equivalent per metric ton of polymer, while conventional petroleum-based polyethylene emits around 3.10 metric tons, yielding a net benefit of 5.2 metric tons of CO_2-equivalent.

The research covers three main areas: pigment dispersion in masterbatches, development of biobased films with natural pigments, and evaluation of recycling performance.

In the first phase, pigment dispersion in polyethylene masterbatches was investigated using a Taguchi L9 design. Key processing parameters, including wax type, were optimized to enhance dispersion of copper phthalocyanine blue. The application of micronized wax led to the lowest observed filter pressure (approximately 1.45 bar/g) and the highest color strength (114.7%), whereas homopolymer wax exhibited comparatively lower performance. Although additives increased stiffness (up to 0.57

GPa), they significantly reduced elongation at break, indicating a trade-off between rigidity and ductility.

In the second phase, environmentally friendly packaging films were produced by incorporating 10% plant-derived pigments into biobased polyethylene through blown film extrusion. Pigments such as yellow mignonette and pomegranate significantly altered the mechanical, optical, and surface properties of the films. Yellow mignonette produced the highest haze (99.8%) and yellowness (b* = 26.0), while pomegranate improved stiffness (elastic modulus up to 246 MPa) but reduced tensile strength and elongation. Pigments also acted as nucleating agents, increasing the crystallization temperature and enhancing barrier and slip properties.

In the third phase, the recycling performance of biobased and petroleum-based polyethylene was evaluated through multiple extrusion cycles simulating industrial reuse conditions. Biobased polyethylene, derived from renewable resources, exhibited a higher reduction in molecular weight (18.6%) and a more pronounced decrease in melt flow index (16.3%) compared to petroleum-based polyethylene (8.5% and 6.4%, respectively). These results indicated that chain scission and viscosity loss were more prominent in biobased polyethylene, suggesting greater sensitivity to thermal and oxidative stress.

In conclusion, this study offers a comprehensive evaluation of process optimization, material performance, and recyclability of biobased polyethylene. The results highlight the significance of wax selection in masterbatch formulations, the role of natural pigments in modulating film functionality, and the necessity of implementing stabilization strategies to mitigate degradation during recycling. These findings contribute to the development of sustainable polymer systems and indicate the potential for broader implementation of biobased polyethylene in commercial applications.

Keywords: Biobased Polymers, Polyethylene, Masterbatch Formulation, Pigment Dispersion, Natural Pigments, Biobased Packaging Films, Recycling Performance, Sustainable Materials, Process Optimization

Biyoesaslı polietilen konsantre boya hazırlanmasında proses şartlarının incelenmesi ve yenilikçi biyoesaslı konsantre boyaların geliştirilmesi

Öz

Bu doktora tezi, petrol bazlı polietilene sürdürülebilir bir alternatif olarak biyoesaslı polietilenin özelliklerini ve işlenme davranışını kapsamlı bir şekilde incelemektedir. Yaşam döngüsü analizlerine göre, şeker kamışından elde edilen biyoesaslı polietilenin bir tonunun üretimi atmosferden yaklaşık 2,12 ton CO_2 eşdeğeri uzaklaştırmakta; buna karşılık, geleneksel petrol bazlı polietilenin üretimi ise yaklaşık 3,10 ton CO_2 eşdeğeri salımına neden olmaktadır. Bu fark, polimerin her bir tonu için net 5,2 ton CO_2 eşdeğeri düzeyinde avantaj sunmakta ve biyoesaslı seçeneğin iklim değişikliğiyle mücadeledeki potansiyel katkısını ortaya koymaktadır.

Araştırma üç ana başlıkta yapılandırılmıştır: konsantre boyalarda (masterbatch) pigment dispersiyonu, biyoesaslı polietilen kullanılarak doğal pigmentli ambalaj filmi üretimi ve her iki malzemenin geri dönüşüm performansının değerlendirilmesi.

İlk aşamada, Taguchi L9 deney tasarımı kullanılarak %25 bakır ftalosiyanin mavisi içeren konsantre boya üretiminde işleme parametrelerinin pigment dispersiyonu üzerindeki etkisi incelenmiştir. Wax (mum) tipi en kritik değişken olarak belirlenmiştir. Mikronize wax, dispersiyonu önemli ölçüde iyileştirerek yaklaşık 1,45 bar/g filtre basıncı sağlamış, homopolimer wax ise 6 bar/g üzerinde değerlerle daha

zayıf performans sergilemiştir. Ayrıca, mikronize wax ile biyo-esaslı polietilende %114,7'ye kadar, homopolimer wax ile ise yaklaşık %93,1 renk şiddeti elde edilmiştir. Katkı maddeleri Young modülünü belirgin şekilde artırmış (mikronize wax ile 0,57 GPa; katkısız sistemde 0,22 GPa), kopma uzamasında %95–98 oranında azalma gözlenmiştir.

İkinci aşamada, %10 doğal pigment içeren çevre dostu gıda ambalaj filmleri, şişirme film ekstrüzyonu yöntemiyle üretilmiştir. Bu pigmentler, filmlerin optik, mekanik ve yüzey özelliklerini etkilemiştir. Muhabbet çiçeği pigmenti %99,8 pusluluk ve 26.0 sarılık değeri sağlamıştır. Nar bazlı filmler ise 246 MPa elastik modül ile daha yüksek rijitlik sergilemiş, ancak çekme dayanımı ve esneklik azalmıştır. Bloklaşma kuvveti yaklaşık 440 gf/100 cm^2'ye kadar düşmüştür. Ayrıca, pigmentlerin kristalleşme sıcaklığını artırdığı, dolayısıyla çekirdeklenme ajanı gibi davrandığı gözlenmiştir.

Üçüncü aşamada, biyoesaslı ve petrol bazlı polietilenin geri dönüşüm performansı, endüstriyel yeniden kullanım koşullarını simüle eden çoklu ekstrüzyon çevrimleriyle değerlendirilmiştir. Yenilenebilir kaynaklı biyoesaslı polietilen, petrol bazlı muadiliyle karşılaştırıldığında daha yüksek oranda moleküler ağırlık kaybı (%18,6) ve daha belirgin bir ergime akış indeksi azalışı (%16,3) göstermiştir (petrol bazlı için sırasıyla %8,5 ve %6,4). Bu bulgular, zincir kırılmalarının ve viskozite kayıplarının biyoesaslı polietilende daha belirgin olduğunu ve malzemenin termal ve oksidatif gerilimlere karşı daha duyarlı olduğunu ortaya koymuştur.

Sonuç olarak, bu tez; pigment dispersiyonunda mikronize wax'ın olumlu etkisini, doğal pigmentlerin sürdürülebilir ambalaj üretimindeki rolünü ve biyoesaslı polietilenin geri dönüşüm sürecindeki zayıf yönlerini ortaya koymaktadır. Gelecek araştırmalar, stabilizasyon ve uyumlaştırma stratejileri üzerine yoğunlaşarak bu malzemenin endüstriyel performansını artırmaya yönelik çözümler geliştirmelidir.

Anahtar Kelimeler: Biyoesaslı Polietilen, Petrol Bazlı Polietilen, Masterbatch Formülasyonu, Pigment Dispersiyonu, Doğal Pigmentler, Ambalaj Filmleri, Geri Dönüşüm Performansı, Sürdürülebilir Malzemeler, Proses Optimizasyonu

Acknowledgment

I would like to express my sincere thanks to all the individuals and institutions who supported and contributed to the completion of this doctoral dissertation.

First and foremost, I am deeply grateful to my advisor, Prof. Dr. Mehmet Özgür Seydibeyoğlu, for his constant guidance, expertise, and encouragement throughout my doctoral journey. His support was essential in shaping and completing this study.

I sincerely appreciate the valuable support and guidance of Prof. Dr. Gül Yılmaz Atay and Prof. Dr. Ümit Halis Erdoğan, who supported me both as members of my thesis monitoring committee and defense jury. Their feedback and encouragement played an important role throughout this process. I am also grateful to Prof. Dr. Mücahit Sütçü for his support and contributions.

I would like to thank Prof. Dr. Mustafa Erol and Assoc. Prof. Dr. İsmail Doğan Külcü, who were members of the defense jury and provided helpful feedback.

I am thankful to Hakan Budin and Okan Budin for their support during my Ph.D. studies. I am especially grateful to my dear colleagues at the Budin R&D team, Vahap Emektar, Samet Yunar, Mert Tozaraydın, Gizem Yegane, Ecenur Aksoy, and Cihan Köse, for their teamwork, help, and all the moments we shared during this process.

Special thanks to Oğuzhan Ay from the Bilim Lab for his technical support during the lab work.

I would like to thank my wife, Buket Yücetürk, for her endless patience, love, and support throughout this journey. Her presence gave me strength when I needed it most and helped me keep going during difficult times.

Finally, I would like to express my heartfelt gratitude to my beloved mother, Tangül Yücetürk. Her love, strength, and values have always been with me, and I respectfully dedicate this work to her memory.

Table of Contents

List of Figures

List of Tables

List of Abbreviations

ANOVA	Analysis of Variance
ASTM	American Society for Testing and Materials
ATR	Attenuated Total Reflectance
CI	Color Index
DSC	Differential Scanning Calorimetry
FPV	Filter Pressure Value
FTIR	Fourier-Transform Infrared Spectroscopy
GPC	Gel Permeation Chromatography
HDPE	High-Density Polyethylene
ICI	Imperial Chemical Industries
LDPE	Low-Density Polyethylene
LLDPE	Linear Low-Density Polyethylene
MD	Machine Direction
MFI	Melt Flow Index
RCS	Relative Color Strength
Rpm	Revolutions per Minute
SEM	Scanning Electron Microscopy
S/N	Signal-to-Noise
TD	Transverse Direction
UTS	Ultimate Tensile Strength
UV	Ultraviolet

List of Symbols

%	Percent
°C	Celsius degree
a*	Redness (CIE Lab)
b*	Yellowness (CIE Lab)
Da	Dalton
F	Force [N]
g	Gram
gf	Gram force
GPa	Gigapascal
K	Absorption coefficient
kN	Kilonewton
kV	Kilovolt
L*	Lightness (CIE Lab)
mg	Milligram
min	Minute
mm	Millimeter
M_n	Number average molecular weight
MPa	Megapascal
M_w	Weight average molecular weight
nm	Nanometer
P_1	Initial pressure
P_2	Maximum pressure

S	Scattering coefficient
T_c	Crystallization temperature
T_m	Melting temperature
ΔE	Total color difference
ΔH_c	Enthalpy of crystallization
ΔH_m	Enthalpy of melting
λ	Wavelength
μ	Friction coefficient
σ_0	Initial stress [MPa]
μL	Microliter
μm	Micrometer
χ_c	Degree of crystallization (%)

Chapter 1

1 General Introduction

1.1 Historical Development and Industrial Use of Polyethylene

Plastic materials, and polyethylene (PE) in particular, have significantly transformed modern industry and daily life. Polyethylene is one of the most widely used thermoplastics globally, found in applications ranging from packaging films and grocery bags to automotive parts and construction materials (Cheng et al., 2024; Soo et al., 2024). This polymer was synthesized in 1933 by Gibson and Fawcett at Imperial Chemical Industries (ICI). Commercial production of polyethylene began in 1939 (Kannan et al., 2025). The subsequent development of Ziegler–Natta catalysts in the 1950s enabled more controlled polymerization at lower pressures, greatly improving production efficiency and yielding various grades of polyethylene such as high-density polyethylene (HDPE) and low-density polyethylene (LDPE) (Granados-Carrera et al., 2025; Vanli & Karakaya, 2025).

These innovations, for which Karl Ziegler and Giulio Natta received the Nobel Prize, established polyethylene as a cornerstone polymer of the 20th century. Chemically, PE consists of long CH_2–CH_2 chains, a simple structure that provides versatility, hydrophobicity, and resistance to chemicals. It can be manufactured with different densities and branching configurations, resulting in materials ranging from flexible films (LDPE) and rigid plastics (HDPE) to elastomeric polymers. These attributes, along with cost-effective mass production, have led to the widespread use of PE in both consumer and industrial products (Joo et al., 2024).

1.2 Environmental Impact of Petroleum-Based Polyethylene

Despite its widespread use, petroleum-based polyethylene raises substantial environmental concerns. Conventional petroleum-based PE is derived from fossil fuels and is extremely durable and therefore does not readily degrade in the environment. Discarded plastics can persist for decades, fragmenting into microplastics that pose serious ecological and health risks (Dolza et al., 2021). The accumulation of non-degradable plastic waste and extremely low recycling rates for certain PE products have raised global concern. Plastics manufacturing and disposal are also associated with greenhouse gas emissions and pollution in waterways and oceans (Bajpai, 2019; Shen et al., 2020).

In response, governments and international organizations have enacted regulations to reduce plastic waste and encourage sustainability. For instance, the European Union's recent strategies, including the Single-Use Plastics Directive and the Circular Economy Action Plan, aim to curb disposable plastics and boost recycling (Foschi & Bonoli, 2019). These efforts underscore an urgent need for more sustainable alternatives to traditional plastics.

1.3 Biobased Polyethylene: Chemistry, Production, and Development

Biobased polyethylene is chemically identical to conventional polyethylene but is produced using ethylene derived from renewable resources rather than petrochemical sources. Its development has been driven by growing concerns regarding the environmental impact of plastic waste and the depletion of fossil fuel reserves. These concerns have made its commercial production increasingly viable. Currently, the production of polyethylene from sugarcane and corn is expanding in countries such as Brazil, the United States, and several European nations.

The production of biobased polyethylene involves three key stages, as illustrated in Figure 1.1.

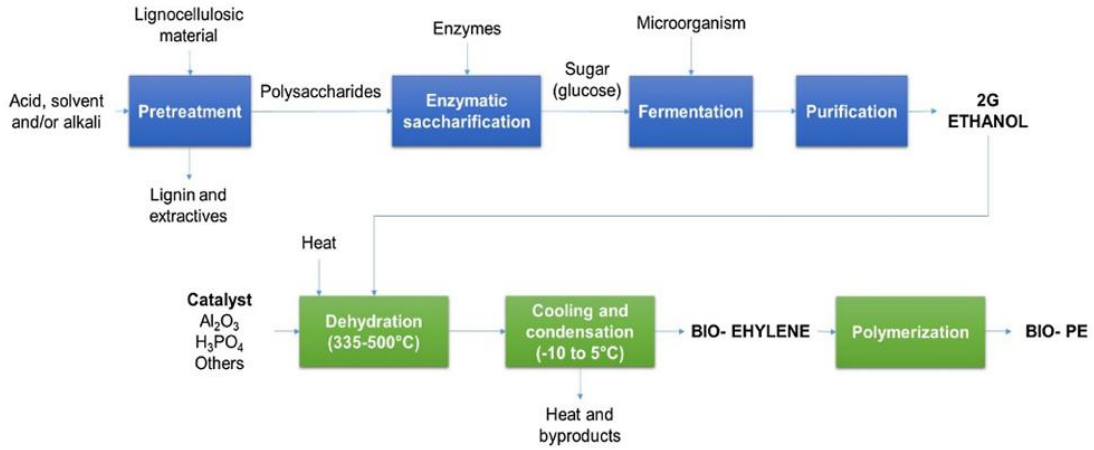

Figure 1.1: Biobased polyethylene production process from lignocellulosic biomass (Mendieta et al., 2020)

In the first stage, glucose from renewable sources such as sugarcane, corn starch, or lignocellulosic biomass is fermented into ethanol (C_2H_5OH) by microorganisms such as *Saccharomyces cerevisiae*. The process begins with biomass hydrolysis, during which enzymes such as cellulase and amylase break down complex carbohydrates into fermentable sugars.

In the second stage, ethanol is converted into ethylene through a catalytic dehydration process. Catalysts commonly used in this step include zeolite, alumina, and phosphoric acid. The process is conducted at temperatures between 300 and 500 °C, during which water is removed from the ethanol molecules to yield high-purity ethylene.

The third stage is polymerization, where the biobased ethylene is polymerized using the same types of catalysts employed in conventional polyethylene production. These include Ziegler-Natta and metallocene catalysts. Polymerization can be achieved through either high-pressure radical mechanisms or low-pressure catalytic processes. As a result, biobased ethylene can be transformed into high-density polyethylene, low-density polyethylene, or linear low-density polyethylene (LLDPE) (Blanco et al., 2017; Siracusa & Blanco, 2020).

The primary distinction between biobased and petroleum-based polyethylene lies in the origin of their raw materials. However, there are also differences in production processes. For example, life cycle assessments have shown that biobased polyethylene typically requires less energy than petroleum-based equivalents. Specifically, the energy demand for producing biobased low-density polyethylene has been reported as

73.6 MJ/kg, compared to 78.05 MJ/kg for its petroleum-based counterpart (Benavides et al., 2020).

One of the key advantages of biobased polyethylene is its lower carbon footprint. Renewable feedstocks such as sugarcane absorb carbon dioxide (CO_2) during cultivation, contributing to the overall environmental benefit of the material. Life cycle assessments consistently show that producing one metric ton of sugarcane-based polyethylene removes approximately 2.12 metric tons of CO_2 equivalent from the atmosphere. In contrast, producing one metric ton of petroleum-based polyethylene results in emissions of 3.10 metric tons of CO_2 equivalent. Therefore, the net climate benefit of using biobased polyethylene is approximately 5.2 metric tons of CO_2 equivalent per metric ton of polymer produced (Suarez et al., 2023; Tsiropoulos et al., 2015).

While conventional polyethylene is synthesized from ethylene obtained via steam cracking of petroleum-derived feedstocks, biobased polyethylene is produced from ethanol obtained through fermentation. This distinction makes biobased polyethylene a renewable and sustainable alternative.

However, the growing demand for biobased plastics has raised concerns about the use of agricultural resources. Cultivating sugarcane or corn for polymer production may compete with food supply chains, prompting debates over food security and land-use ethics. These concerns have led to criticism, particularly in regions with limited arable land (Saeaung et al., 2021).

From an industrial perspective, biobased low-density polyethylene is already used in applications such as packaging films, food bags, agricultural covers, and automotive parts. Its adoption is particularly notable in food packaging, beverage containers, and cosmetic products. A key advantage is its structural compatibility with existing recycling systems, as it is chemically identical to conventional polyethylene.

Commercial-scale production of biobased polyethylene began in the late 2000s. A notable example is Braskem, a Brazilian company that pioneered industrial-scale bio-polyethylene manufacturing around 2010, using sugarcane ethanol as the primary feedstock (Hellvig & Flores-Sahagun, 2023). Since then, production facilities have

been established in several regions, including Brazil, the United States, and Europe. Technology continues to gain momentum due to its potential to reduce greenhouse gas emissions and dependence on fossil resources (Jaiswal et al., 2017; Petrielli et al., 2023).

Plants cultivated for biobased polyethylene production absorb CO_2 through photosynthesis, helping to offset emissions associated with polymer synthesis. For instance, Braskem's green polyethylene is estimated to sequester approximately 2.15 kilograms of CO_2 per kilogram of resin, making the production process carbon-negative up to the factory gate (Jorda-Reolid et al., 2021; Kikuchi et al., 2013; Siracusa & Blanco, 2020).

Biobased polyethylene also contributes to the diversification of the raw material supply chain. By relying on agricultural feedstocks, it reduces dependence on the volatile petroleum market. Moreover, it is fully recyclable within existing infrastructure, which is essential for maintaining material circularity. It is important to note that being biobased does not imply biodegradability. Like conventional polyethylene, biobased polyethylene persists in the environment under natural conditions and does not readily decompose. Therefore, its environmental benefit stems from its renewable origin and improved carbon balance rather than its degradability. As such, responsible waste management remains essential (Mecking, 2020).

In future scenarios, advances in biotechnology and process engineering are expected to reduce production costs, improve efficiency, and enable the use of second-generation feedstocks. Agricultural residues and non-food biomass represent promising alternatives that may further improve the sustainability profile of biobased polyethylene.

1.4 Performance Characteristics and Material Compatibility of Biobased Polyethylene

Initial studies comparing Bio-PE and petroleum-based PE suggest that the two materials exhibit similar physical and mechanical properties. This outcome is expected, as both polymers consist of chemically identical polyethylene chains. For

example, biobased high-density polyethylene shows comparable density, melting point, crystallinity, and tensile properties to its petroleum-derived counterpart (Burelo et al., 2023). Any minor differences generally result from impurities or processing variations rather than differences in the polymer backbone.

Therefore, in terms of functionality and performance, Bio-PE can serve as a substitute for conventional PE in many applications. A milk bottle or packaging film made from Bio-PE performs similarly to one made from petroleum-based PE. This equivalence represents a significant advantage, as it enables manufacturers to adopt Bio-PE without modifying production lines or compromising product quality (Rahman & Bhoi, 2021). However, Bio-PE development still faces several challenges, one of which is economic scalability. Producing polyethylene from biomass has historically been more costly due to feedstock cultivation expenses, additional processing steps, and limited economies of scale. Although technological advancements have improved the process, the production cost of biobased polyethylene remains relatively high, and its global output represents only a small fraction of total polyethylene production. As of 2024, bioplastics including Bio-PE account for only about 1% of the global plastics market by volume (Jaiswal et al., 2017; Siracusa & Blanco, 2020).

Bio-PE also faces concerns regarding feedstock sustainability. The use of food crops such as sugarcane or corn raises questions about land use and competition with food production (Bos et al., 2012). Current research is focusing on second-generation feedstocks, such as agricultural residues and non-food biomass, with ongoing efforts to improve biorefinery efficiency.

1.5 Coloration and Pigment Use in Polyethylene

The coloration of polyethylene is a significant design parameter, contributing not only to aesthetic appeal but also to functional performance across various applications. Colorants are incorporated into plastics to meet branding and consumer preferences, while also serving specific functional purposes. For instance, dark pigments such as carbon black are used in agricultural films and outdoor pipes to absorb ultraviolet (UV) radiation and enhance weather resistance. In food packaging, opaque or colored layers protect contents from light-induced degradation. In industrial settings, colored plastics

assist in the sorting and identification of materials (Bigger & Delatycki, 1989; Maalihan & Pajarito, 2015).

Achieving consistent and high-quality color in PE typically involves incorporating insoluble pigments or soluble dyes into the polymer matrix. In practice, pigments are more commonly used in PE due to its non-polar and hydrophobic nature, which makes water-soluble dyes impractical. Pigments are solid particles, often inorganic compounds or stable organic molecules, that are dispersed throughout the polymer to impart color. Inorganic pigments such as titanium dioxide (TiO_2) or iron oxide (Fe_2O_3) are preferred for their excellent heat stability, lightfastness, and opacity. Organic pigments such as phthalocyanines or quinacridone red offer a wider range of bright, saturated colors but may have lower thermal stability and are susceptible to aggregation (Christie & Abel, 2022; Lomax, 2005).

The choice of pigment depends on the desired shade, performance requirements, and regulatory constraints such as avoiding heavy metals. One of the main challenges is achieving uniform dispersion of the pigment within the polyethylene matrix.

1.6 Masterbatch Technology and Pigment Dispersion

Directly mixing raw pigment powder with polymer melt is inefficient and hazardous. The plastics industry relies on masterbatch technology. A color masterbatch is a concentrated formulation of pigments and additives dispersed in a carrier polymer at varying ratios, depending on the application requirements (Weinmann, 2007). The carrier is typically a polyethylene or compatible wax that mixes into the bulk PE. Masterbatches are produced by pre-mixing pigments with the carrier resin using compounding equipment. The output is pelletized, producing colored masterbatch pellets that are blended with natural polyethylene pellets during manufacturing.

This approach simplifies the coloring process and enhances handling safety. Using masterbatches also improves pigment dispersion because the pigments are already pre-dispersed in the carrier during production. It enables color consistency across large material volumes and eliminates the need to handle raw pigments (C. yao Chen et al., 2018; Wong et al., 1997).

However, high-quality color masterbatch requires attention to dispersion and compatibility. Poor dispersion leads to visible specks or streaks, color inconsistencies, and compromised mechanical properties. Achieving good dispersion is challenging because many pigments have different surface chemistries from the non-polar PE chains (Yücetürk & Seydibeyoğlu, 2020).

To address this, dispersing agents or compatibilizers are added. Polyethylene waxes or surfactants improve the wetting of pigment particles. Sufficient shear mixing is needed to effectively disperse pigment agglomerates without degrading the materials. Processing temperature must ensure polymer fluidity while avoiding thermal degradation. Low-molecular-weight PE wax is often included to enhance the flow and dispersion of pigment particles during mixing (AlMaadeed et al., 2015; Desidery & Lanotte, 2021).

1.7 Natural Pigments in Biobased Polyethylene Systems

There is growing interest in natural pigments for coloring polyethylene. Natural pigments are derived from renewable sources like plants or algae. Examples include carotenoids, chlorophyll, anthocyanins, curcumin, or tannins. Their appeal is attributed to their renewability, potential biodegradability, and reduced toxicity (Giuliani et al., 2015; Ibáñez-García et al., 2024).

Recent efforts have incorporated natural pigments such as spirulina or turmeric into biopolymers like polylactic acid (PLA) and polybutylene succinate (PBS). In PE, natural pigments continue to provide renewable sourcing advantages. However, they are not as thermally stable as inorganic pigments. Many degrade or discolor at PE processing temperatures of 180–220 °C (Rodriguez-Amaya, 2019). They also contain organic components such as cellulose or proteins that may change polymer properties. High loadings may lead to increased stiffness at the expense of ductility. Their irregular particle shape and size pose challenges for achieving uniform dispersion. Moisture must be managed to avoid foaming. Some pigments may impart odor or chemically interact with the polymer or additives.

Despite these challenges, successful incorporation of natural pigments could yield masterbatches that are both aesthetically appealing and environmentally advantageous. Natural pigments may also increase opacity or UV absorption due to polyphenols (Wijesekara & Xu, 2024).

1.8 Recyclability of Biobased and Petroleum-Based Polyethylene

Recycling plays a fundamental role in promoting sustainability within plastic applications, as it extends the material life cycle and mitigates environmental impacts. Both petroleum-based polyethylene and its biobased equivalent undergo degradation during repeated melt processing, primarily due to prolonged exposure to elevated temperatures and oxygen. This degradation is characterized by polymer chain scission, which results in a decline in molecular weight and corresponding changes in mechanical properties and melt flow (MFI) behavior. Preserving polymer integrity over multiple recycling cycles is essential for materials intended to be incorporated into a circular economy framework. Although numerous studies report that biobased polyethylene exhibits degradation behavior similar to its petroleum-derived counterpart, some have observed a slightly greater reduction in molecular weight in the biobased variant. This difference may be attributed to variations in antioxidant content, the presence of residual impurities, or catalyst residues associated with the polymerization of bio-derived ethylene. Ensuring that biobased polyethylene offers comparable recyclability to petroleum-based polyethylene is therefore critical for its broader industrial utilization and contribution to sustainable material strategies (Lee et al., 2022; Trucillo et al., 2024; Zaman & Newman, 2021).

1.9 Scope and Structure of the Thesis

Given the background above, the main objective of this study was to evaluate biobased polyethylene in comparison with its fossil-derived counterpart across the entire value chain. The research was structured in three principal parts:

• Chapter 2 - Optimization of Biobased Polyethylene Masterbatches:

The influence of pigment type, wax structure, functional additives, and processing parameters on pigment dispersion and mechanical performance was systematically explored in this section. Masterbatches prepared from both biobased and petroleum-based polyethylene were evaluated through filter pressure tests, colorimetry, scanning electron microscopy (SEM), and tensile testing.

• Chapter 3 - Biobased Polyethylene Films with Natural Pigments:

Prototype polyethylene films incorporating plant-derived pigments were developed and assessed for their optical clarity, mechanical strength, crystallization behavior, and surface properties, with a particular focus on their applicability in sustainable packaging.

• Chapter 4 - Recyclability of Biobased and Petroleum-Based Polyethylene:

Recyclability was examined by simulating five extrusion cycles and monitoring molecular degradation in both types of polyethylene. Characterization techniques included MFI analysis, gel permeation chromatography (GPC), differential scanning calorimetry (DSC), Fourier-transform infrared spectroscopy (FTIR), and tensile testing.

A schematic overview (Figure 1.2) linked these stages in sequence, and the next chapter applied this background to the practical challenge of pigment dispersion in Bio-PE masterbatch formulations.

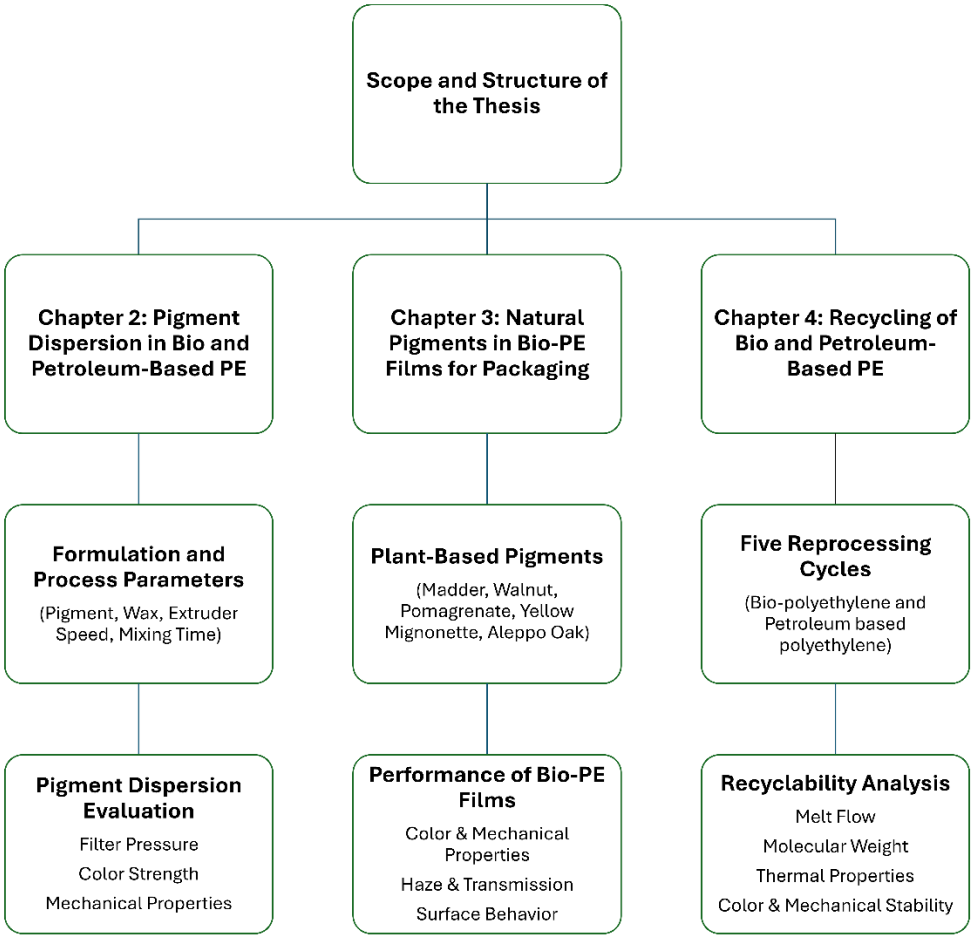

Figure 1.2: Overview of thesis structure highlighting studies on pigment dispersion, natural pigmentation, and recycling

Chapter 2

2 Pigment Dispersion Optimization in Biobased Polyethylene Masterbatches

2.1 Introduction

Color in the polymer industry is not only an aesthetic element but also a key factor influencing product functionality and performance. It affects consumer perception, reinforces brand identity, and fulfills specific roles based on the intended application. In sectors such as packaging, automotive, textiles, and consumer products, properties like color stability, light fastness, and chemical resistance are essential. In outdoor applications, maintaining color stability is crucial to ensure long-term durability.

The incorporation of pigments and dyes into plastic materials significantly influences both the aesthetic appeal and the functional performance of the final product. Proper pigment dispersion enhances polymer performance and facilitates the achievement of target color strength. In addition, maintaining color uniformity during production minimizes material loss and defects, while also supporting efficient recycling.

With advancing technology, colorants used in polymer materials are designed to impart not only visual elements but also additional properties such as heat stability, UV resistance and chemical resistance. Pigments used in polymers can cause problems such as fading, oxidation or mechanical weakening over time when exposed to light. Therefore, pigments with high light resistance should be preferred to increase color

stability (Barbas et al., 2014; Lertwimolnun & Vergnes, 2006; Martin, 2013; Wagner et al., 2013).

A masterbatch is a concentrated mixture of polymer carrier, pigment, wax, and additives. It is used to impart color and functionality to plastic materials. These granules contain a high concentration of pigment and are blended with the base polymer at predetermined ratios depending on application requirements. The resulting mixtures are melted and processed at elevated temperatures and pressures using extrusion equipment. Dispersion may vary depending on the selected processing parameters at this stage. The main factors affecting dispersion include mixing time, extruder temperature profile, feed rate, screw speed, screw design, shear stress, and the presence of dispersing agents (Alsadi, 2021; Bardet et al., 2013).

Masterbatch technology offers significant advantages in terms of cost and production efficiency. It also enables the delivery of desired color and functional properties to polymers. This technology enables more uniform color distribution compared to traditional pigment blends, achieving effective coloration with reduced pigment loadings. Masterbatches are widely preferred in the production of high-performance plastics, especially in the automotive and packaging industries. In addition, sustainable masterbatch solutions have been developed for biodegradable plastics, contributing to environmentally friendly production by enhancing compatibility with recyclable materials (Demir & Wegner, 2012; Neo et al., 2023).

The coloring performance of biobased and petroleum-based polyethylene varies according to the structural characteristics and dispersion parameters of the carrier polymer. Bio-PE offers certain advantages and disadvantages in pigment dispersion due to its low crystalline structure (Aguado et al., 2022; Bos et al., 2012; Garcia-Garcia et al., 2016; Leppäkoski et al., 2023; Quiles-Carrillo et al., 2019; Siracusa & Blanco, 2020).

To explore these differences more systematically, the dispersion of Color Index (CI) Pigment Blue 15:1, an alpha-crystalline modification of copper phthalocyanine, was investigated. This pigment has excellent acid-base resistance, high light fastness and temperature resistance (McKeown, 1998; Yücetürk & Seydibeyoğlu, 2020). The study focused on evaluating the dispersion efficiency of this pigment in a biobased

polyethylene carrier. To provide a comparative assessment, the same experimental methodology was also applied to a petroleum-based polyethylene carrier. The results from both systems were analyzed to identify the processing parameters with the most significant influence on pigment distribution.

The issue of dispersion is often overlooked in many scientific studies. The study aimed to optimize processing parameters that are typically considered trade secrets by masterbatch manufacturers and are seldom addressed in scientific literature, while also eliminating unnecessary variables. Thus, it is aimed to provide more accurate data and save time for scientific studies. Comparative analysis of pigment dispersion in both polymer types was conducted to enhance overall color performance. Experiments were designed to evaluate the effects of various wax types, as well as specific mixing and extrusion parameters. The collected data were statistically analyzed using the orthogonal Taguchi method. Variables were systematically analyzed and reported using Minitab 21.1.1 software.

The findings were evaluated to assess the feasibility of utilizing biobased polymers in masterbatch applications. This study was expected to support the development of innovative plastic coloring technologies and serve as a valuable reference for advancing sustainable production processes by clarifying the distinctions between biobased and petroleum-based polymers. Building on these insights, Chapter 3 investigated the incorporation of naturally derived plant pigments into Bio-PE films and evaluated their optical, mechanical, and surface properties.

2.2 Materials and Methods

2.2.1 Biobased Polyethylene and Petroleum-Based Polyethylene

The Bio-PE resin (SEB853/72) produced by Braskem (Brazil) has at least 95% biobased carbon content. This polymer has a melt flow rate of 2.7 g/10 min (190 °C, 2.16 kg) and a density of 0.923 g/cm³. It exhibits high optical clarity, favorable mechanical strength, and low gel content. The tensile strength at break is 25 MPa in the machine direction (MD) and 20 MPa in the transverse direction (TD), with

elongation at break values of 350% and 1050%, respectively. Tear strength is measured as 580 gf in the MD direction and 210 gf in the TD direction. Dart impact strength is 70 g, and the haze value is 7%.

PETİLEN F2-12 (PB-PE), an LDPE resin produced by Petkim (Türkiye), is manufactured using a high-pressure autoclave process. This petroleum-based polymer has a melt flow rate of 2.5 g/10 min (190 °C, 2.16 kg) and a density of 0.920 g/cm³. The tensile strength at break is determined as 23 MPa in the MD direction and 17 MPa in the TD direction, and the elongation at break values are above 200% and 500%, respectively. Tear strength is measured as 337 gf in the MD direction and 245 gf in the TD direction. Dart impact strength is 120 g, and the haze value is 6.3% (Table 2.1).

Both polymer grades offer high processability, optical transparency, and mechanical strength in blown film extrusion applications. Melting temperature and extrusion parameters have been optimized to ensure homogeneous film properties are maintained.

Table 2.1: Properties of biobased polyethylene and petroleum-based polyethylene

Product	Density (g/cm^3)	Melt Flow Rate (g/10 min)	Haze (%)
Braskem SEB853/72	0.92	2.7	7.0
Petkim F2-12	0.92	2.5	6.3

2.2.2 Pigments and Additives Used in Masterbatch Formulations

C.I. Pigment Blue 15:1 (74160), Alpha Blue AGK (alpha modification of copper phthalocyanine) was supplied by Alliance Organics LLP (Mumbai, India). This pigment has a specific gravity of 1.60 and an oil absorption value of 37 cc/100 g. Its heat stability was measured at 280 °C, and it exhibits high resistance to chemicals such as water, acids, and bases. Light fastness was rated 8 on a scale of 1 to 8. The pigment's limited water solubility (1%) and good solvent resistance ensure long-term stability in polymer applications (Table 2.2).

Table 2.2: Technical data for Pigment Blue 15:1

Product	Color Index Number	Chemical Class	Average Particle Size (µm)	Density (g/cm^3)	Heat Stability (°C/5min)	Light Fastness (scale of 1-8)
Pigment blue 15:1	74160	Copper phthalocyanine, alpha	5	1.60	280	8

Three different polyethylene-based waxes were used to enhance pigment dispersion and ensure homogeneous distribution. Luwax A is a homopolymer polyethylene wax (HW) produced by BASF (Germany) with a D50 particle size of 500 µm. It has a melting point between 101-109°C and a dropping point between 107-114°C. Its melt viscosity at 120°C was measured in the range of 950-1550 mm^2/s and contributes to the effective dispersion of pigments due to its good miscibility with polymers and low viscosity.

Ceretan MX 9815 (MW), a micronized polyolefin-based wax, is manufactured by Münzing (Germany) and has a D50 particle size of 15 µm. Its drop point was 111°C and its density was 0.94 g/cm^3. Its spherical particle shape provides high scratch and abrasion resistance, improves dispersion properties, and reduces dust formation.

Finally, Hordamer PE 02 wax emulsion (WE) was used to improve pigment dispersion. Produced by BYK Additives & Instruments (Germany), it is an anionic polyethylene emulsion with a D50 particle size of 130 nm. Hordamer PE 02 offers advantages such as low viscosity, high spreadability and surface lubricity in polymer and pigment dispersions. In addition, it exhibits a stable structure against heat and mechanical effects and increases the dispersion efficiency of pigments (Table 2.3).

Table 2.3: Technical specifications of polyethylene waxes used as dispersants

Product	Form	Average Particle Size (μm)	Drop Point (ºC)	Density (g/cm^3)
Luwax A	Powder	<500	107- 114	0.91- 0.93
Ceretan MX 9815	Powder	<15	111- 119	0.94- 0.95
Hordamer PE 02	Liquid	<130	-	0.96- 0.98

2.2.3 Masterbatch Production Process

Taguchi orthogonal arrays are a method of experimental design that allow researchers to analyze the influence of multiple factors simultaneously. Unlike traditional full factorial designs, which evaluate all possible combinations and are costly in terms of time and resources, Taguchi arrays enable the examination of factor effects with a reduced number of experiments.

In this study, a Taguchi L9 orthogonal array was constructed using the Minitab program for the masterbatch production process (Table 2.4). Four basic parameters were considered at this stage: type of wax used, extruder speed, mixing time, and extruder temperature profile. For each parameter, experiments were performed at three distinct levels.

After the experiments, the signal-to-noise ratio (S/N) (smaller is better) (Equation 2.1) was analyzed based on the filter pressure value (FPV). This analysis was considered important, as lower filter pressure indicates improved dispersion.

The S/N ratio is used to measure the robustness of a system's performance under variable conditions. This ratio evaluates the relationship between desired performance (signal) and unwanted variability (noise). In this context, 'n' represents the number of measurements and 'Y' represents the value of each measurement. A high S/N ratio indicates that the system performs effectively without being affected by unwanted changes. Therefore, the levels with the highest S/N ratio are regarded as optimal.

$$\frac{S}{N} = -10 \log\left(\Sigma \frac{Y^2}{n}\right) \quad (2.1)$$

Table 2.4: Parameter table according to Taguchi L9 orthogonal array

Sample	Wax Type	Extruder Speed (Rpm)	Mixer Time (Min)	Extruder Temperature (ºC)
BIO-PE/HW/01	Homopolymer	100	5	160
BIO-PE/HW/02	Homopolymer	200	10	200
BIO-PE/HW/03	Homopolymer	300	20	240
BIO-PE/MW/01	Micronized	100	10	240
BIO-PE/MW/02	Micronized	200	20	160
BIO-PE/MW/03	Micronized	300	5	200
BIO-PE/WE/01	Emulsion	100	20	200
BIO-PE/WE/02	Emulsion	200	5	240
BIO-PE/WE/03	Emulsion	300	10	160
PB-PE/HW/01	Homopolymer	100	5	160
PB-PE/HW/02	Homopolymer	200	10	200
PB-PE/HW/03	Homopolymer	300	20	240
PB-PE/MW/01	Micronized	100	10	240
PB-PE/MW/02	Micronized	200	20	160
PB-PE/MW/03	Micronized	300	5	200
PB-PE/WE/01	Emulsion	100	20	200
PB-PE/WE/02	Emulsion	200	5	240
PB-PE/WE/03	Emulsion	300	10	160

In masterbatch production, the percentage of formulation components was kept constant. In this way, the effect of wax type and process parameters could be observed (Table 2.5). In order to obtain a more homogeneous mixture, Bio-PE was crushed in a grinder.

Pigment, polymer powder and wax were added simultaneously into a laboratory turbo mixer (Labtech Engineering, Thailand) and mixed at 1500 revolutions per minute (rpm) for 5 to 20 minutes depending on the parameters. The resulting mixture was then transferred to a 20 mm diameter twin-screw laboratory extruder (Labtech Engineering, Thailand) with a 44:1 L/D ratio.

The extrusion temperature profile ranged from 160 to 240 °C, and the screw speed was maintained between 100 and 300 rpm. After extrusion, the masterbatch samples were cooled to room temperature and dried in a hot air oven at 80 °C for 8 hours.

Table 2.5: Masterbatch formulations

Sample	Bio-PE (wt.%)	PB-PE (wt.%)	Pigment Blue 15:1 (wt.%)	Homopolymer Wax (wt.%)	Micronized Wax (wt.%)	Wax Emulsion (wt.%)
BIO-PE/HW/01	60	-	25	15	-	-
BIO-PE/HW/02	60	-	25	15	-	-
BIO-PE/HW/03	60	-	25	15	-	-
BIO-PE/MW/01	60	-	25	-	15	-
BIO-PE/MW/02	60	-	25	-	15	-
BIO-PE/MW/03	60	-	25	-	15	-
BIO-PE/WE/01	60	-	25	-	-	15
BIO-PE/WE/02	60	-	25	-	-	15
BIO-PE/WE/03	60	-	25	-	-	15
PB-PE/HW/01	-	60	25	15	-	-
PB-PE/HW/02	-	60	25	15	-	-
PB-PE/HW/03	-	60	25	15	-	-
PB-PE/MW/01	-	60	25	-	15	-
PB-PE/MW/02	-	60	25	-	15	-
PB-PE/MW/03	-	60	25	-	15	-
PB-PE/WE/01	-	60	25	-	15	-
PB-PE/WE/02	-	60	25	-	15	-
PB-PE/WE/03	-	60	25	-	15	-

2.2.4 Preparation of Molded Color Samples

To determine the color strength, the masterbatch samples were mixed with titanium dioxide in a thermokinetic mixer (Gülnar, Türkiye) at a ratio of 1:10. The mixer does not have a direct heating element; however, as a result of its specially designed blades

and a 2000 rpm mixing speed, the barrel temperature rose to 190 °C through the mechanical impact applied to the granules, causing the mixture to melt.

The melt was then molded using a compression molding machine (Labtech Engineering, Thailand). The relative color strength (RCS) of the samples was calculated by comparing their Kubelka-Munk (K/S) ratio with a standard reference (Equation 2.2).

$$RCS = \frac{\left(\frac{K}{S}\right)Sample}{\left(\frac{K}{S}\right)Reference} \times 100 \quad (2.2)$$

The K/S value was determined based on the Kubelka-Munk equation. In Equation 2.3, K is the absorption coefficient, S is the scattering coefficient, and Rλ represents the light reflectance at a given wavelength (λ) from the masterbatch plate. All samples were prepared in five replicates and measured independently.

$$\frac{K}{S} = \frac{(1 - R\lambda)^2}{2R\lambda} \quad (2.3)$$

2.2.5 Blown Film Production

To observe the presence of agglomerated particles in the masterbatch samples, film samples with a thickness of 100 µm were produced. During this process, 4% masterbatch was incorporated into the mixture, and the films were processed using a blown film machine manufactured by Labtech Engineering (Thailand). Additionally, film samples were prepared to investigate the distribution and dispersion of pigments within the masterbatch. These samples, containing 4% masterbatch, were examined under intense fluorescent light to assess pigment dispersion in detail. These investigations provided important insights regarding the homogeneous distribution of pigments and the identification of potential agglomerates.

2.2.6 Injection Molding of Mechanical Test Samples

The tensile test specimens were produced in accordance with ASTM D638 Type 1, using an injection molding machine (Haitian, China) with a clamping force of 600 kN. During specimen production, injection temperatures were maintained within the range of 210–230 °C. The samples were molded directly without dilution or blending with additional polymer. The aim of this process was to evaluate the mechanical properties of the compounds produced under the selected processing conditions. Additionally, the effects of the production process on the material were assessed. Variables such as temperature, pressure, and molding time were carefully controlled during production. The prepared specimens were used for tensile testing in subsequent stages to investigate the mechanical performance of the material.

2.2.7 Characterization Techniques

2.2.7.1 Fourier Transform Infrared Spectroscopy Analysis

Fourier transform infrared spectra of the masterbatch samples were obtained using an IR spectrometer (Bruker ALPHA-II, Germany) equipped with an attenuated total reflection (ATR) crystal. The spectra were recorded in the wavelength range from 4000 cm^{-1} to 450 cm^{-1} with a data interval of 1 cm^{-1} and a resolution of 4 cm^{-1}. A background scan was performed prior to each sample measurement. This step aimed to determine the functional groups and chemical composition of the masterbatch. The obtained spectra were evaluated for structural analysis and to identify possible chemical changes within the material.

2.2.7.2 Color Strength Analysis

Color strength measurements were performed using an X-Rite Ci64 (USA) spherical spectrophotometer. Five replicate samples were prepared for each formulation and analyzed individually. The average value was calculated to improve the accuracy of the results. Measurements were conducted under a D65 light source and a 10° observation angle. The instrument operates with d/8° spherical geometry and a spectral range of 400–700 nm. The measurement aperture was set to 8 mm.

2.2.7.3 Filter Pressure Value Measurement

A higher FPV value indicates lower dispersion, resulting in a greater presence of undispersed coarse particles within the matrix. The dispersion quality of the masterbatches was evaluated using a filter tester (Labtech Engineering, Thailand) in accordance with ISO 23900-5. This test measures the pressure generated by the agglomerated coarse particles in the material and the result is reported as the FPV in bar/g (Equation 2.4). Here, P_1 represents the initial pressure of the melt, P_2 the maximum pressure reached, and M the total amount of pigment in the mix.

$$FPV = \frac{P2 - P1}{M} \tag{2.4}$$

Since masterbatches contain 25% pigment, mixtures prepared with 50 grams of masterbatches contain 12.5 grams of pigment. During the test, a standard three-layer 15 μm filter was used. To evaluate the effect of the processing parameters on dispersion, each test was repeated five times.

2.2.7.4 Mechanical Testing

Mechanical tests were performed using a universal testing machine (Devotrans, Türkiye) with a capacity of 10 kN. The tensile strength and elongation at break of the specimens were determined in accordance with ASTM D638. The tests were performed at a speed of 50 mm/min and the specimens were carefully monitored until failure. During the tensile test, the mechanical behavior of the specimens under load was monitored and the stress-strain curves were recorded and analyzed.

Each test was repeated five times, and the results were statistically evaluated. Specimens with values exceeding the standard deviation range were identified and retested to ensure measurement accuracy.

2.2.7.5 Morphological Analysis by Scanning Electron Microscopy

Fractographic analysis was conducted on the fracture surfaces of masterbatch specimens following tensile testing, using a scanning electron microscope (SEM) to obtain high-resolution images. To improve the surface conductivity and obtain high-

resolution images, the samples were gold coated. Images were taken at various magnifications using a Carl Zeiss 300VP (Germany) SEM, with the accelerating voltage set to 5 kV.

The Carl Zeiss 300VP is a SEM with variable pressure mode and is capable of operating in both low vacuum and high vacuum modes. This feature enables detailed morphological analysis, particularly in polymer-based samples, while minimizing surface charging effects. Thanks to its high signal-to-noise (S/N) ratio detectors, the device is capable of precisely imaging details in fine structures.

Within the scope of the analysis, pigment distribution and dispersion within the matrix were examined and compared with results from the blown film and filter pressure tests. The morphology of the fracture surfaces was assessed to determine whether pigments were homogeneously dispersed or tended to form agglomerates.

2.3 Results and Discussion

2.3.1 Fourier Transform Infrared Spectroscopy

A comparative analysis of the FTIR spectra of Bio-PE and PB-PE (Figure 2.1) reveals several common spectral features. The bands in the 2917-2848 cm^{-1} and 2911-2844 cm^{-1} ranges indicate methylene group vibrations for both Bio-PE and PB-PE (Calabrò & Magazù, 2013; Wu et al., 2005). A prominent band at 1643 cm^{-1}, associated with amine vibrations from HALS-type UV stabilizers, was observed in both polymeric samples (Javadi et al., 2014; Salem et al., 2002). However, shifts in these bands occurred in masterbatch formulations. CH_2 shear vibrations were observed at 1417 cm^{-1} for Bio-PE and 1469 cm^{-1} for PB-PE. CH_2 oscillation vibrations were observed in the region of 719 cm^{-1} in both samples (Karlsen & Spanget-Larsen, 2009). In the masterbatch samples, the presence of phthalocyanine pigment led to the appearance of C=N bonds at 1506 cm^{-1} and 1510 cm^{-1}. In addition, C–H groups attached to the aromatic ring, C–C and C–N bonds from isoindole, Cu–ligand vibrations, and metal–oxygen bonds were evident in the masterbatch forms of both samples (Andrew & Ajibade, 2018a). The comparative analysis highlights the spectral effects of pigments and additives on both Bio-PE and PB-PE. Due to the pigment in the masterbatch,

differences in the spectral profiles of both samples were observed. These included band shifts and the formation of new bands.

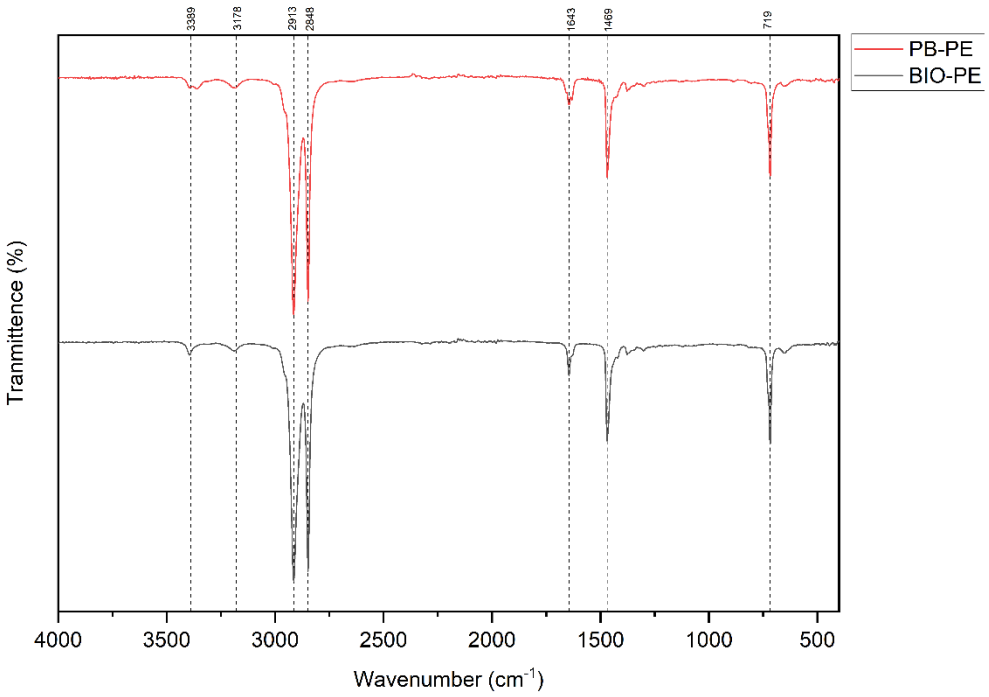

Figure 2.1: Fourier transform infrared spectroscopy spectra comparing biobased polyethylene with petroleum-based polyethylene

The FTIR spectrum of Bio-PE (Figure 2.2) displays strong asymmetric and symmetric CH_2 stretching vibrations between 2917-2848 cm^{-1}, which are characteristic of polyethylene structures. These bands are associated with the methylene group (CH_2) and show the characteristic features of the polymer structure (Calabrò & Magazù, 2013). The 1643 cm^{-1} band, which is prominently observed in the Bio-PE pure sample, indicates characteristic vibrations of amine groups originating from HALS-type UV stabilizers (Javadi et al., 2014). In the masterbatch samples, this band exhibited slight shifts, likely due to pigment dispersion or additive interactions with the matrix. The band observed in the 1417 cm^{-1} region corresponds to CH_2 shear vibrations, while the sharp band at 719 cm^{-1} wavelength is associated with CH_2 oscillatory vibrations (Karlsen & Spanget-Larsen, 2009). In the masterbatch samples, the presence of phthalocyanine pigment led to the formation of some new structure-specific bands.

The C=N bond vibration at 1506 cm^{-1} wavelength is due to the components of the pigment containing aromatic systems. In addition, the broad band between 1460-754 cm^{-1} represents C-H groups from the aromatic ring, the 1417-1331 cm^{-1} band represents C-C bonds from isoindole and the 1284-1167 cm^{-1} range represents C-N bonds from isoindole. Furthermore, C-H bonds in the 1118-1090 cm^{-1} region, Cu-ligand vibrations in the 899-862 cm^{-1} range and metal-oxygen bonds in the 569-502-430 cm^{-1} range were observed (Andrew & Ajibade, 2018b). These spectral changes provide valuable information to evaluate the extent to which the pigment is dispersed in the polymer matrix and how it interacts with the additives.

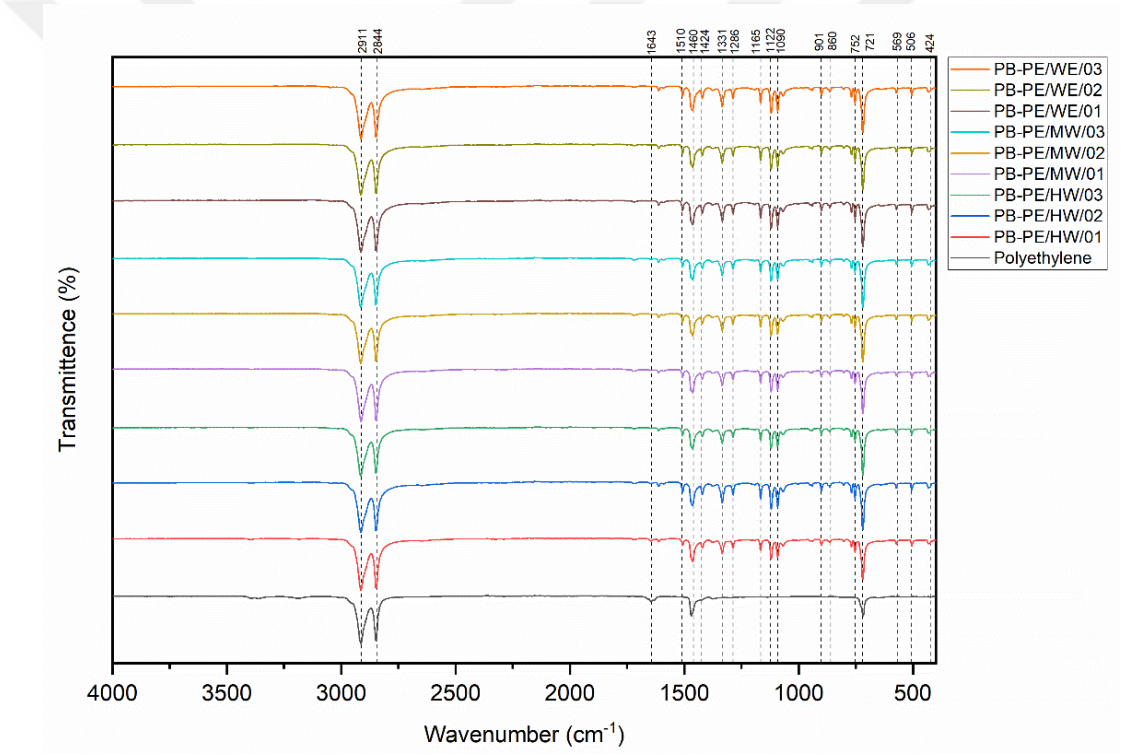

Figure 2.2: Fourier transform infrared spectra of petroleum-based polyethylene masterbatches

An analysis of the PB-PE FTIR spectrum reveals similarities to certain characteristic bands observed in Bio-PE samples (Figure 2.3). The bands located between 2911 cm^{-1} and 2844 cm^{-1} correspond to methylene group vibrations, indicating hydrocarbon components within the polymeric structure. A distinct peak was also noted at 1643 cm^{-1} in the PB-PE samples; however, this peak underwent shifts in the masterbatch form.

This phenomenon is attributed to interactions of additives or pigments within the matrix. The band at 1469 cm^{-1} signifies CH_2 scissoring vibrations, while the band at 719 cm^{-1} is associated with CH_2 rocking vibrations. In the masterbatch formulation, C=N bonding was observed at 1510 cm^{-1} due to the phthalocyanine pigment. Additionally, C-H vibrations linked to the aromatic ring were identified in the 1460-752 cm^{-1} region, C-C bonds from isoindole in the 1424-1331 cm^{-1} region, and C-N bonds from isoindole in the 1286-1165 cm^{-1} region. Furthermore, C-H bonding was detected in the 1122-1090 cm^{-1} region, Cu-ligand vibrations in the 901-860 cm^{-1} range, and metal-oxygen bonding in the 569-506-424 cm^{-1} range. These findings clearly illustrate the impact of pigments and additives on the spectral characteristics of PB-PE samples. The pigments and additives in the masterbatch composition led to the emergence of new bands that were not present in the pure PB-PE spectrum.

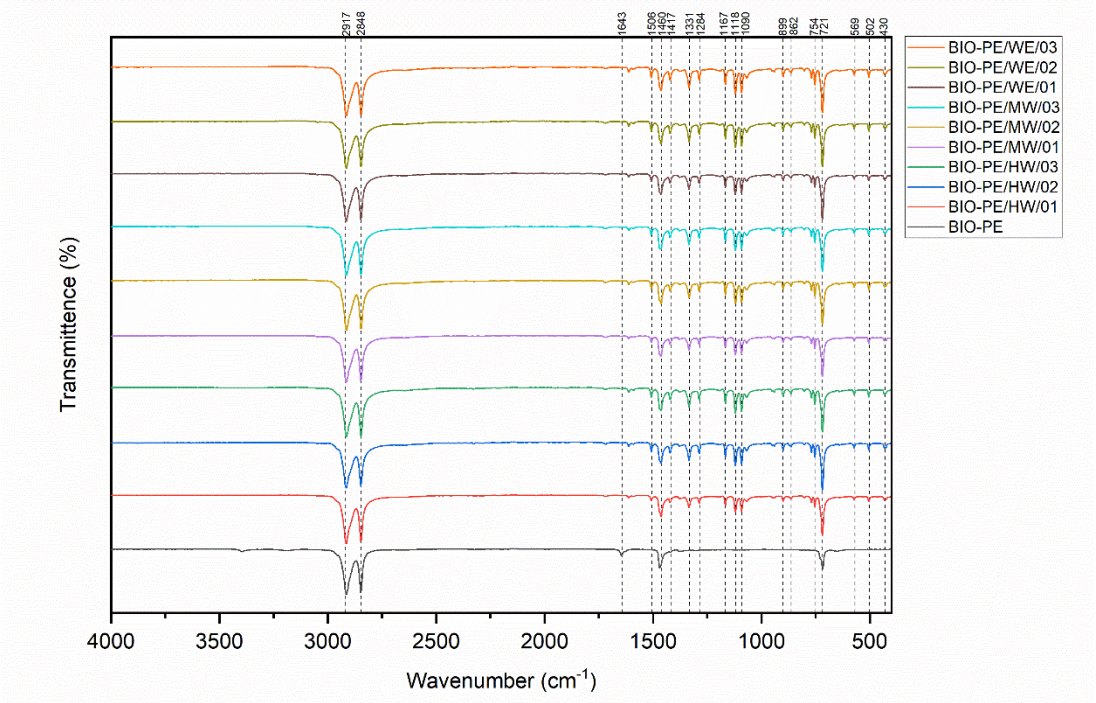

Figure 2.3: Fourier transform infrared spectra of biobased polyethylene masterbatches

2.3.2 Color Strength Analysis

Phthalocyanine Blue is one of the most difficult pigments to disperse and is widely used in the plastics industry. Color strength can be increased by reducing the pigment to smaller particles and ensuring homogeneous dispersion within the polymer matrix. The effect of different polymer matrices (Bio-PE and PB-PE) and wax types on pigment dispersion is illustrated in Figure 2.4.

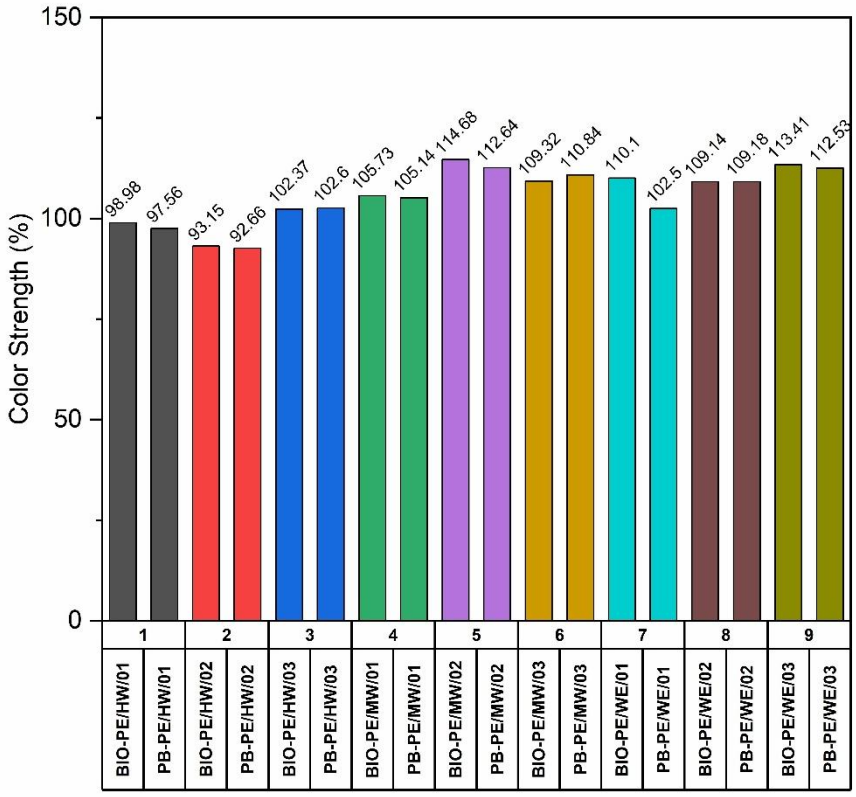

Figure 2.4: Relative color strength of masterbatch samples

In samples containing homopolymer wax, the color strength for both Bio-PE and PB-PE based systems was found to be lower than for other formulations. Color strength values of 98.98%, 97.56%, 93.15% and 92.66% were obtained for BIO-PE/HW/01, PB-PE/HW/01, BIO-PE/HW/02 and PB-PE/HW/02 samples, respectively. Among the samples with homopolymer wax, both polymers showed similar trends, although PB-PE systems generally exhibited slightly lower color strength values than Bio-PE. The color strength of the BIO-PE/HW/03 and PB-PE/HW/03 samples was 102.37% and

102.6%, and higher color strength was observed in both formulations compared to the previous samples containing homopolymer wax. However, in general, the use of homopolymer wax results in lower color strength compared to other wax types.

Improved pigment dispersion was observed in the samples containing micronized wax. BIO-PE/MW/01 and PB-PE/MW/01 samples gave color strength values of 105.73% and 105.14% respectively. Similarly, the color strength of BIO-PE/MW/02 and PB-PE/MW/02 samples were 114.68% and 112.64%. These results suggest that micronized wax facilitates finer particle size and more uniform dispersion of the pigment within the polymer matrix. Color strength values of 109.32% and 110.84% were measured in BIO-PE/MW/03 and PB-PE/MW/03 samples.

Formulations containing emulsion wax had high levels of color strength. The BIO-PE/WE/01 sample had a color strength value of 110.1%, while this value was 102.5% for the PB-PE/WE/01 sample. Similarly, color strength values of 109.14% and 109.18% were obtained in BIO-PE/WE/02 and PB-PE/WE/02 samples. These values indicate that the pigment dispersion was homogeneous and similar color strength was obtained in both polymer matrices. BIO-PE/WE/03 and PB-PE/WE/03 samples measured 113.41% and 112.53% color strength, respectively. PB-PE systems containing emulsion waxes presented similar color strength values to Bio-PE based systems indicating that successful pigment distribution was achieved.

The findings demonstrate that wax type has a direct effect on pigment dispersion, with similar trends observed in both Bio-PE and PB-PE matrices. Systems containing homopolymer wax showed the lowest color strength values, while a significant increase in color strength was observed in systems containing micronized and emulsion wax. Especially formulations containing emulsion wax contributed to the highest levels of color strength by providing better dispersion of the pigment. While there were no major differences between the Bio-PE and PB-PE based samples in general, it is noteworthy that the PB-PE systems containing micronized wax exhibited slightly higher color strength values than their Bio-PE counterparts.

2.3.3 Blown Film Dispersion Analysis

In blown film tests, samples containing 4% masterbatch were evaluated under a fluorescent light source to examine pigment distribution and dispersion quality. Visual observations were consistent with the color strength data obtained by a spectrophotometer. Especially the samples containing homopolymer wax showed low color strength, which was confirmed by the presence of large pigment clusters on the film. In such samples, the hue was lighter and uneven; the pigment was not sufficiently dispersed, as evidenced by the density differences and particle residues on the film surface.

In the images of Bio-PE based samples (Figure 2.5), the presence of large pigment particles is similarly noticeable in BIO-PE/HW/01, BIO-PE/HW/02 and BIO-PE/HW/03 samples. Among them, the BIO-PE/HW/02 sample was notable for its low color strength and significant dispersion issues. In contrast, the BIO-PE/MW/02 sample containing micronized wax showed darker shades and higher particle density, indicating that the pigment is both smaller and more homogeneously dispersed in this sample. This sample also stood out as one of the samples with the highest color strength in the spectrophotometric results. BIO-PE/WE/03, one of the samples containing emulsion wax, showed a more stable and homogeneous color distribution on the film and no noticeable large particle formations were observed on the surface. This example demonstrated that the use of emulsion wax optimized dispersion and improved the overall appearance of the film.

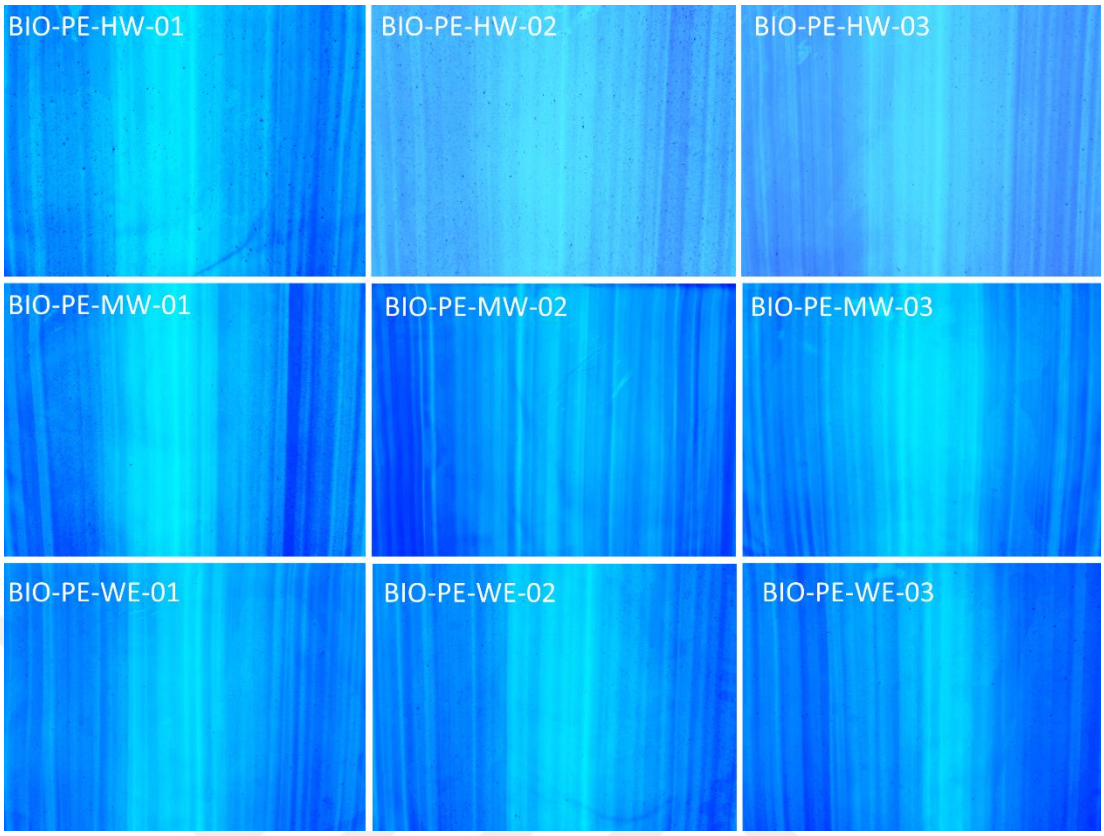

Figure 2.5: Visual assessment of pigment dispersion in biobased polyethylene masterbatch films

Similar trends were observed in PB-PE based samples (Figure 2.6). Similar to BIO-PE, PB-PE/HW/01, PB-PE/HW/02 and PB-PE/HW/03 samples contained coarse pigment particles and obvious traces of agglomeration. The PB-PE/HW/02 sample, with its irregular distribution and light tint, indicates insufficient dispersion.

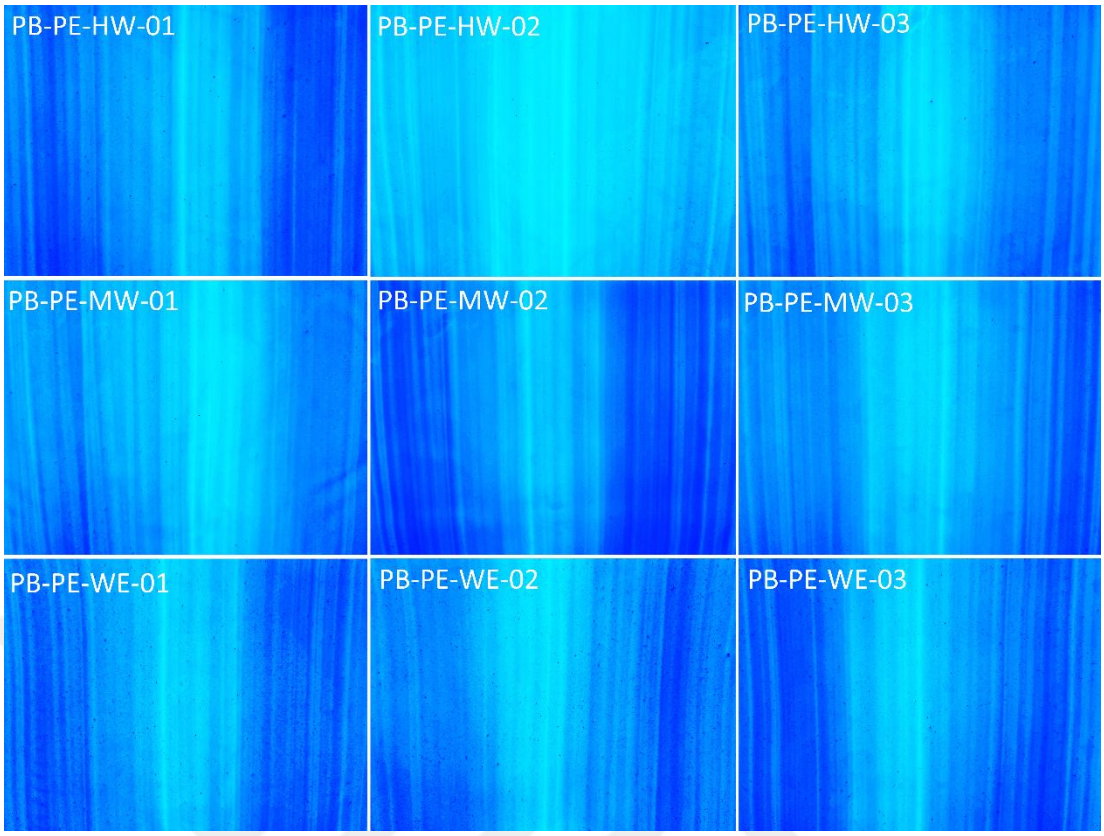

Figure 2.6: Visual assessment of pigment dispersion in petroleum-based polyethylene masterbatch films

PB-PE/MW/01, MW/02, and MW/03 samples containing micronized wax showed more homogeneous dispersion and stronger color appearance. The more successful dispersion in these samples was evident from the color consistency on the film surface and the smaller particle size. The PB-PE/MW/03 sample exhibits a visually darker and cleaner appearance, which supports the spectrophotometric results of high color intensity.

The PB-PE samples containing emulsion waxes generally distributed the pigment well and were among the samples without large particles on the surface. The PB-PE/WE/03 sample exhibited notable dispersion uniformity and tonal depth, indicating good compatibility between the emulsion wax and the PB-PE matrix.

In conclusion, the use of homopolymer waxes in both Bio-PE and PB-PE based systems performed poorly in terms of dispersion, while micronized and especially emulsion waxes provided better dispersion of the pigment. Visual inspections

confirmed the dispersion quality in agreement with the color strength data and clearly demonstrated the decisive role of additive type on film quality.

2.3.4 Filter Pressure Analysis

The data obtained from the filter tests (Figure 2.7) were consistent with the color strength and blown film test results presented in the previous sections. The filter pressure values measured during the filtration tests are particularly important for revealing the influence of wax type on pigment dispersion. All Bio-PE and PB-PE samples containing homopolymer wax showed the poorest dispersion performance with both higher FPV values and lower color strength. The FPV values of BIO-PE/HW/01 and PB-PE/HW/01 samples were measured as 6.24 bar/g and 7.60 bar/g, respectively. These high values indicate the presence of significant amounts of coarse pigment agglomerates in the polymer matrix. These particles rapidly clogged the filter pores, resulting in a significant rise in pressure values.

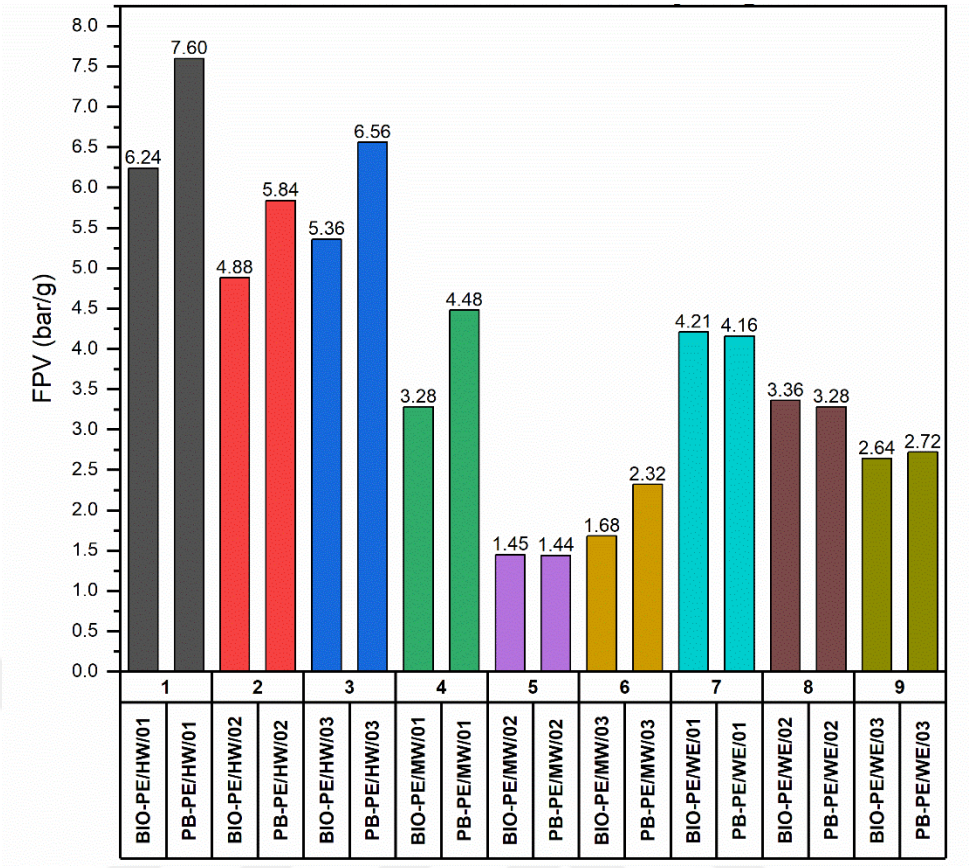

Figure 2.7: Filter pressure values of masterbatches

Similarly high FPV values were found in the other samples containing homopolymer wax, namely BIO-PE/HW/02 (4.88 bar/g), PB-PE/HW/02 (5.84 bar/g), BIO-PE/HW/03 (5.36 bar/g) and PB-PE/HW/03 (6.56 bar/g). These results are in agreement with the low color strength and uneven pigment distribution observed in the blown film samples. This indicates that homopolymer wax does not sufficiently improve pigment dispersion and adversely affects processability.

The lowest FPV values were obtained in samples containing micronized wax. Especially BIO-PE/MW/02 (1.45 bar/g) and PB-PE/MW/02 (1.44 bar/g) samples showed the best filter performance among all samples. These values indicate that the pigment was homogeneously dispersed as fine particles within the polymer matrix, thereby minimizing the risk of filter clogging. The other micronized wax-containing samples, BIO-PE/MW/01 (3.28 bar/g), PB-PE/MW/01 (4.48 bar/g), BIO-PE/MW/03 (2.32 bar/g) and PB-PE/MW/03 (1.68 bar/g) also have low FPV values. These results confirmed previous observations that such waxes optimize pigment dispersion. In

addition to the wax type, the FPV's were also notably influenced by processing parameters such as extruder screw speed, barrel temperature, and mixing time. Among these, screw speed had the most pronounced effect. The results indicated that a screw speed of 200 rpm consistently yielded lower FPV's compared to 100 rpm or 300 rpm. This intermediate speed appears to offer an optimal balance between adequate shear force and controlled thermal exposure. It facilitates pigment agglomerate breakdown while minimizing degradation or re-agglomeration. Notably, the BIO-PE/MW/02 and PB-PE/MW/02 samples, both of which exhibited the lowest FPV's, were processed at 200 rpm, reinforcing the conclusion that moderate shear enhances dispersion efficiency.

Barrel temperature was another critical factor affecting pigment dispersion. Lower extrusion temperatures, particularly 160°C, resulted in significantly lower FPV values. This can be attributed to the increased melt viscosity at lower temperatures, which generates higher shear stress within the extruder. Such conditions are favorable for dispersing pigments like phthalocyanine blue that require high mechanical energy to achieve fine and uniform particle distribution. Higher temperatures, while potentially improving polymer flow, were less effective in dispersing the pigment due to reduced shear intensity.

Mixing time, on the other hand, exhibited the least influence among all parameters. While longer mixing durations, such as 20 minutes, led to slight improvements in dispersion, the differences among mixing durations were relatively minor. This suggests that once a sufficient initial blend is achieved before extrusion, extending the mixing time does not substantially affect pigment breakdown or distribution. Therefore, from a processing efficiency standpoint, shorter mixing times can be preferred without sacrificing dispersion quality. These findings collectively indicate that although wax type is the dominant factor, optimizing screw speed and temperature settings can further enhance pigment dispersion, reduce FPV, and improve overall masterbatch processability.

Although samples containing emulsion waxes showed lower FPV values compared to those containing homopolymer waxes, they presented higher values compared to samples containing micronized waxes. In particular, BIO-PE/WE/01 and PB-PE/WE/01 samples showed values of 4.21 bar/g and 4.16 bar/g respectively, while

BIO-PE/WE/02 and PB-PE/WE/02 samples showed values of 3.36 bar/g and 3.28 bar/g, respectively. It is understood that the pigment is more homogeneously dispersed in these samples, but larger particles are still present in places compared to micronized wax. While emulsion waxes improve dispersion to some extent, micronized waxes are notably more effective, especially in applications requiring enhanced performance. Relatively low FPV values were obtained in BIO-PE/WE/03 (2.64 bar/g) and PB-PE/WE/03 (2.72 bar/g) samples. This indicates that the pigment distribution in these samples is more balanced, and the formation of coarse particles is reduced.

These results also highlight the influence of processing parameters beyond wax type. Specifically, BIO-PE/WE/03 and PB-PE/WE/03 were both processed at a higher screw speed of 300 rpm and a lower extrusion temperature of 160°C. The combination of increased mechanical shear and elevated melt viscosity contributed to the enhanced dispersion observed in these samples. In contrast, samples such as BIO-PE/WE/01 and PB-PE/WE/01, processed at lower screw speeds and higher temperatures, exhibited higher FPV values, indicating less effective pigment breakdown. These findings demonstrate that not only the physical form of wax but also the interplay between shear force and thermal conditions during extrusion plays a decisive role in pigment dispersion. Furthermore, mixing time showed marginal effect, yet samples subjected to 10 minutes of mixing tended to exhibit slightly improved dispersion, possibly due to sufficient initial homogenization prior to extrusion. Thus, optimizing the full set of process parameters alongside wax selection is critical for achieving superior dispersion performance in masterbatch formulations.

When the results of the filter pressure tests are interpreted in conjunction with the color strength measurements and visual assessments of blown film samples, it becomes evident that the type of wax used in the masterbatch formulation plays a decisive role in determining pigment dispersion quality. Among all evaluated parameters, the physical and chemical nature of the wax exhibits a more substantial influence on dispersion and filter pressure than the applied process conditions. This suggests that the interaction between the wax and pigment, particularly in terms of particle size, polarity, and compatibility with the polymer matrix, governs the degree to which pigment agglomerates can be broken down and uniformly distributed.

This conclusion is partially consistent with the findings reported by Buccella et al. (2018) who demonstrated that repeated extrusion of copper phthalocyanine pigment in polyamide-based masterbatches resulted in increased color strength and reduced filter pressure values due to improved dispersion. While their approach relied on mechanical refinement through successive processing, the present study shows that comparable dispersion quality can be achieved in a single-pass extrusion process by selecting a suitable additive system, particularly using micronized wax. This suggests that fine particle size and improved compatibility with the polymer matrix can enable effective pigment breakdown without the need for multiple processing cycles.

In the current work, this principle was validated using micronized wax, which enabled excellent pigment dispersion without the need for multiple processing cycles. Its fine particle size and high compatibility with the polymer matrix contributed to efficient pigment wetting and breakdown during a single-pass extrusion. As a result, masterbatch samples containing micronized wax consistently exhibited lower FPV's, higher color strength, and more uniform pigment distribution in blown film samples. These findings reinforce the notion that optimizing additive morphology, particularly wax structure, is more influential than processing conditions in the design of high-performance masterbatches.

2.3.5 Mechanical Properties Analysis

A detailed evaluation of the mechanical test results presented in Table 2.6 revealed a clear increasing trend in the Young's modulus values of all masterbatch samples compared to the neat polymers. Specifically, the incorporation of solid additives such as pigments, minerals, and waxes into the polymer matrix has consistently increased the stiffness of the material. This behavior can be attributed to the restriction of polymer chain mobility by the dispersed phase, which leads to a more rigid structure. The elevated Young's modulus values observed across all modified samples are consistent with similar findings reported in various studies (Kuan et al., 2021; Lapčík et al., 2018; Leong et al., 2004; Liang & Li, 2000; Mahdi & Dean, 2020; Pérez et al., 2013; Shirvanimoghaddam et al., 2021).

Table 2.6: Mechanical properties of masterbatch specimens

Sample	Young's Modulus (GPa)	Tensile Strength (MPa)	Elongation at Break (%)
BIO-PE	0.22 ± 0.04	10.87 ± 0.05	115.03 ± 6.49
BIO-PE/HW/01	0.35 ± 0.05	7.27 ± 0.77	6.51 ± 1.94
BIO-PE/HW/02	0.33 ± 0.04	7.62 ± 0.31	6.34 ± 1.08
BIO-PE/HW/03	0.37 ± 0.02	7.90 ± 0.25	6.40 ± 0.80
BIO-PE/MW/01	0.41 ± 0.08	8.49 ± 0.55	4.11 ± 1.11
BIO-PE/MW/02	0.57 ± 0.04	10.23 ± 0.79	4.10 ± 0.75
BIO-PE/MW/03	0.54 ± 0.07	9.72 ± 0.37	4.35 ± 1.44
BIO-PE/WE/01	0.36 ± 0.04	8.66 ± 0.50	4.48 ± 1.03
BIO-PE/WE/02	0.39 ± 0.09	9.25 ± 0.06	4.75 ± 1.27
BIO-PE/WE/03	0.36 ± 0.06	8.63 ± 0.24	4.30 ± 0.70
PB-PE	0.26 ± 0.02	10.95 ± 0.04	109.94 ± 3.65
PB-PE/HW/01	0.34 ± 0.01	8.27 ± 0.12	6.63 ± 0.45
PB-PE/HW/02	0.37 ± 0.01	8.18 ± 0.14	9.23 ± 0.52
PB-PE/HW/03	0.37 ± 0.01	8.62 ± 0.10	6.40 ± 0.38
PB-PE/MW/01	0.39 ± 0.04	8.88 ± 0.11	8.02 ± 0.60
PB-PE/MW/02	0.42 ± 0.02	8.70 ± 0.08	2.09 ± 0.22
PB-PE/MW/03	0.40 ± 0.05	9.49 ± 0.14	2.20 ± 0.19
PB-PE/WE/01	0.39 ± 0.02	9.26 ± 0.09	4.35 ± 0.35
PB-PE/WE/02	0.43 ± 0.03	8.23 ± 0.13	5.28 ± 0.42
PB-PE/WE/03	0.46 ± 0.01	8.88 ± 0.12	4.99 ± 0.39

The highest Young's modulus values were observed in the formulations containing micronized wax (MW), reaching up to 0.57 GPa in the case of BIO-PE/MW/02 and 0.42 GPa in PB-PE/MW/02. These findings suggest that micronized wax particles not only dispersed more homogeneously within the polymer matrix but also interacted more effectively with the polymer chains, thereby enhancing stiffness. This improvement in rigidity was particularly pronounced in PB-PE samples, which

exhibited a higher baseline modulus (0.26 GPa) than Bio-PE (0.22 GPa), indicating the inherently stiffer nature of this polymer compared to Bio-PE.

Despite the significant improvements in stiffness, the tensile strength values of the samples did not follow a similar progressive trend. While both Bio-PE and PB-PE showed initial values of 10.87 MPa and 10.95 MPa respectively, most masterbatch formulations demonstrated a decrease in tensile strength. For example, BIO-PE/HW/01 and PB-PE/HW/02 exhibited reduced tensile strengths of 7.27 MPa and 8.18 MPa, respectively. This decline can be interpreted as the outcome of particle agglomeration or weak interfacial adhesion between the matrix and the filler phase, both of which limit stress transfer under load.

Interestingly, among the PB-PE-based samples, formulations incorporating micronized wax (PB-PE/MW/03: 9.49 MPa) showed more tensile strength retention, approaching that of the neat polymer. This is further evidence that good dispersion plays a critical role in preserving tensile properties. In contrast, some BIO-PE-based masterbatches, despite their increased stiffness, did not show comparable strength retention, suggesting matrix-filler incompatibility or dispersion issues.

A critical drawback observed in all modified samples was the substantial reduction in ductility. While the raw Bio-PE sample demonstrated an elongation at break of 115.03%, and PB-PE followed closely with 109.94%, almost all masterbatch formulations exhibited substantially reduced elongation values. This brittleness was especially evident in the PB-PE/MW/02 (2.09%) and PB-PE/MW/03 (2.20%) samples, which fractured shortly after the onset of plastic deformation. The significant reduction in elongation, particularly evident in specimens exhibiting the highest Young's modulus, underscores the inherent inverse relationship between stiffness and ductility in polymeric composite systems.

Furthermore, the samples containing homopolymer wax generally performed poorly in all three measured properties. For instance, BIO-PE/HW/01 and PB-PE/HW/01 not only had lower tensile strengths (7.27 MPa, 8.27 MPa) but also limited elongation at break (6.51%, 6.63%) and modest modulus improvements. These results strongly indicate poor filler dispersion, which is likely caused by interfacial incompatibility, which hinders mechanical interlocking and effective stress transfer. This interpretation

aligns with the work of Ersoy & Köse (2020) who observed similar mechanical deficiencies in polypropylene composites containing uncoated $CaCO_3$ due to insufficient dispersion and weak interfacial bonding.

In contrast, the better overall performance of PB-PE-based samples, especially in Young's modulus and tensile strength, can be explained by the polyethylene carrier's higher inherent crystallinity and strength. However, the samples still exhibited poor ductility regardless of additive type, confirming the universal tendency of fillers to embrittle the polymer matrix regardless of base polymer type.

In summary, although the introduction of solid additives led to clear improvements in stiffness (as reflected by higher Young's modulus values), this enhancement came at the cost of tensile strength in several formulations and significantly compromised ductility in all cases. The most promising results were achieved in micronized wax formulations, which offered a balanced improvement in modulus and acceptable tensile strength due to superior dispersion characteristics. Nevertheless, the marked reduction in elongation at break across all samples underscores the need for further optimization. In particular, improving additive-polymer compatibility is essential if the material is to be used in applications requiring flexibility or high impact resistance.

2.3.6 Scanning Electron Microscopy

SEM analysis of the fracture surfaces of the specimens after mechanical testing is presented in Figure 2.8. Examination of the images revealed a brittle fracture mechanism on the fracture surfaces of all specimens. This finding coincides with the low elongation at break values obtained from tensile tests. In particular, all modified Bio-PE-based specimens exhibited a clear loss of ductility, as sudden fracture occurs before passing into the plastic deformation zone.

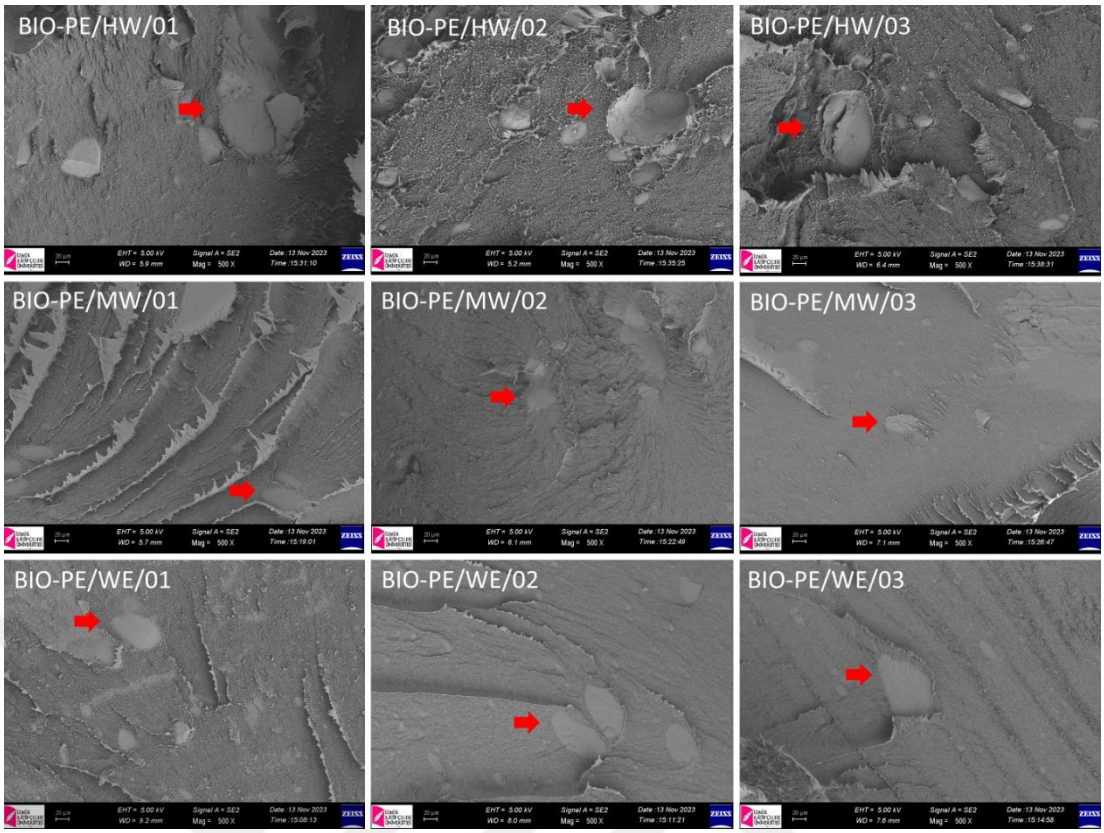

Figure 2.8: Scanning electron microscopy images of fracture surfaces of masterbatch specimens

In formulations containing homopolymer wax (BIO-PE/HW/01, HW/02, and HW/03) and wax emulsion (BIO-PE/WE/01, WE/02, and WE/03), many irregular particle structures larger than 20 micrometers were observed. These particles, marked with red arrows, suggest poor dispersion and weak bonding at the matrix–filler interface. These structures were also retained in 15 µm filters during the FPV tests, resulting in elevated filter pressure values. This indicates that the dispersion quality is low, and the pigments or fillers are not homogeneously dispersed in the matrix.

In contrast, samples containing micronized wax (BIO-PE/MW/01, MW/02, and MW/03) showed distinct differences in particle density and size compared to the other formulations. Especially in the BIO-PE/MW/03 sample, the fracture surface is very smooth, laminar, and linear, indicating a good dispersion quality. Smaller and more homogeneously dispersed particles were observed in these samples containing micronized wax, which is consistent with the higher Young's modulus and color strength values obtained from mechanical testing. Improved dispersion quality led to

enhanced rigidity and increased color strength. However, since these structural improvements are accompanied by a loss of ductility, a balance must be established based on the intended application.

In conclusion, the SEM images are in good agreement with the tensile tests and FPV analysis. The particle structures observed on the fracture surfaces show significant differences depending on the type and distribution of the filler. Samples containing micronized wax exhibited more homogeneous and fine structures, while dense agglomerations were observed in homopolymer wax and emulsion wax samples. These observations reveal that not only the chemical structure of the additives but also their size and dispersion characteristics critically influence the overall performance of the composite material.

2.3.7 Design of Experiment: Analysis of Variance and Regression

This comprehensive analysis systematically evaluated four critical output parameters: Filter pressure value (FPV), ultimate tensile strength (UTS), elongation at break (EAB), and relative color strength (RCS) in both biobased and petroleum-based polyethylene masterbatch systems. The study was structured using a Taguchi orthogonal experimental design, which allowed for efficient optimization by minimizing the number of trials while capturing the main factor interactions. The factors examined included wax type, screw speed, mixing time, and extruder temperature.

These parameters were analyzed using signal-to-noise ratio graphs, which provided insights into both the main effects and the robustness of each parameter. The outcomes of the experiments provided valuable guidelines for future industrial and academic applications aiming to improve dispersion and mechanical performance of masterbatches.

In the FPV analysis (Figure 2.9), the "smaller is better" criterion was adopted, reflecting the goal of minimizing filter clogging due to undispersed particles.

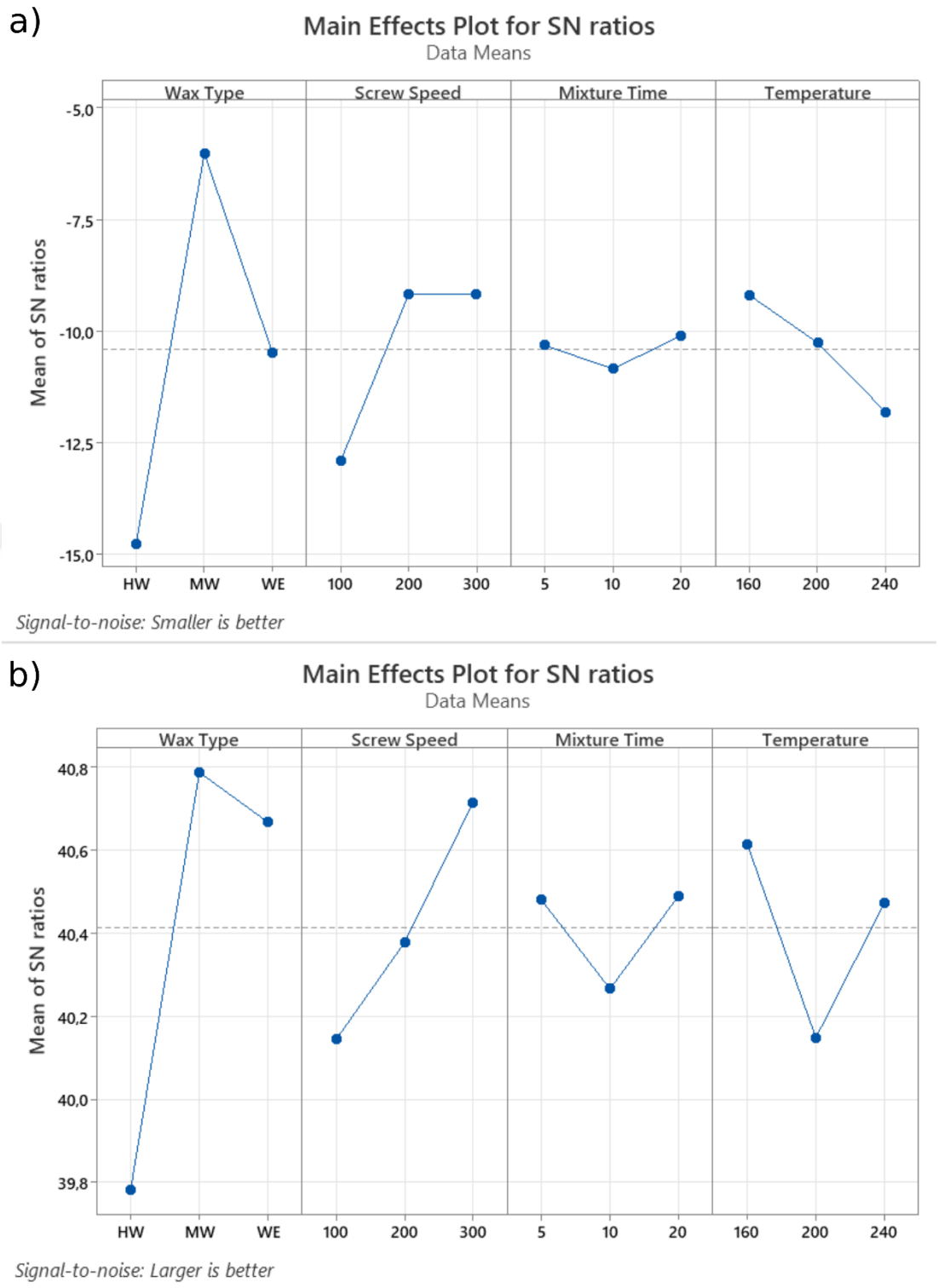

Figure 2.9: Signal-to-noise ratio graph for filter pressure value: (a) biobased polyethylene and (b) petroleum-based polyethylene

Micronized wax resulted in the lowest FPV values, which confirmed its superior dispersion performance in both polymer matrices. Conversely, homopolymer wax

(HW) resulted in significantly higher FPV values, indicating poor dispersion likely caused by its larger particle size and lower compatibility with the polymer-pigment matrix.

Among the process parameters, a screw speed of 200 rpm was found to be optimal. A mixing time of 10 minutes and an extruder temperature around 200°C also improved dispersion, although their influence was less significant than that of wax type. PB-PE exhibited more stable and consistent S/N trends than BIO-PE, suggesting enhanced process robustness in petroleum-based systems.

When examining UTS (Figure 2.10), the “larger is better” approach was utilized, emphasizing mechanical reinforcement.

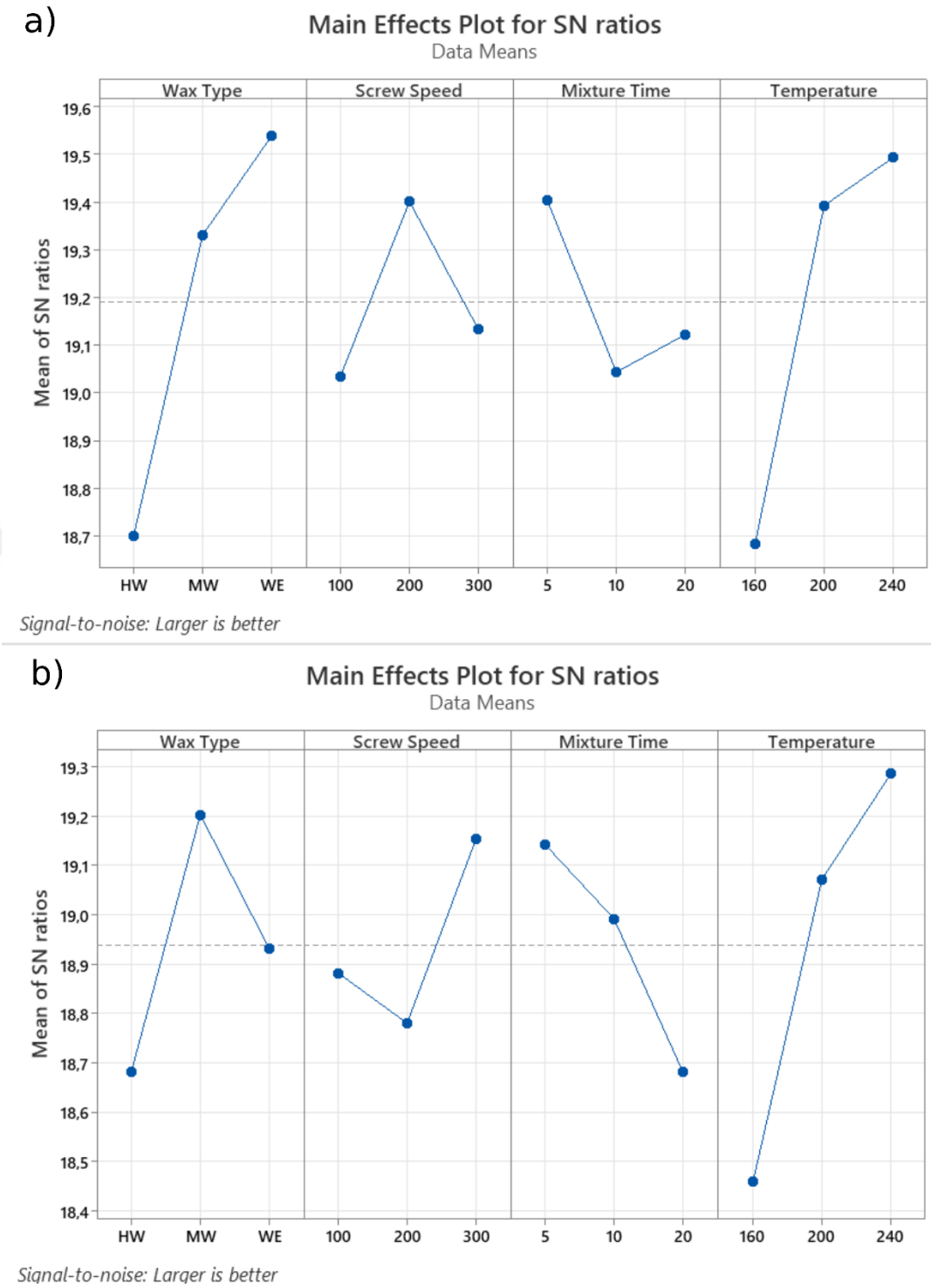

Figure 2.10: Signal-to-noise ratio graph for ultimate tensile strength: (a) biobased polyethylene and (b) petroleum-based polyethylene

MW again yielded the highest S/N ratios, underlining its dual benefit in both dispersion and tensile performance. Screw speed had a more pronounced effect on UTS than on FPV, with 200 rpm providing optimal results. At 100 rpm, especially in the PB-PE

matrix, mechanical performance significantly decreased, which was likely due to incomplete mixing or phase separation.

Mixing time and processing temperature also influenced UTS. A mixing time of 10 minutes was found to balance shear forces without inducing polymer degradation. Temperatures between 200°C and 240°C supported improved interfacial bonding, which resulted in higher tensile strength in both systems.

Elongation at break (EAB), (Figure 2.11), a key indicator of ductility, was evaluated using the "larger is better" criterion.

Figure 2.11: Signal-to-noise ratio graph for elongation at break: (a) biobased polyethylene and (b) petroleum-based polyethylene

However, the results revealed that micronized wax (MW) and extrusion at 200°C or higher consistently resulted in lower EAB values, indicating reduced ductility. While MW enhanced pigment dispersion and tensile strength, it likely introduced stiffness

and brittleness to the matrix, limiting polymer chain mobility. Similarly, prolonged thermal exposure at elevated temperatures, especially when combined with extended mixing times (e.g., 20 minutes), may have led to chain scission, further reducing ductility. These findings highlight that while MW improves dispersion and tensile performance, it can have adverse effects on flexibility. Optimal EAB values were observed under milder conditions, such as lower processing temperatures and shorter mixing times, which helped preserve ductile behavior.

RCS is a critical parameter for pigment-based masterbatches and was calculated using the Kubelka-Munk equation. The S/N ratio analysis (Figure 2.13) clearly identified MW as the most effective wax type for enhancing color strength, which is consistent with its high dispersion efficiency.

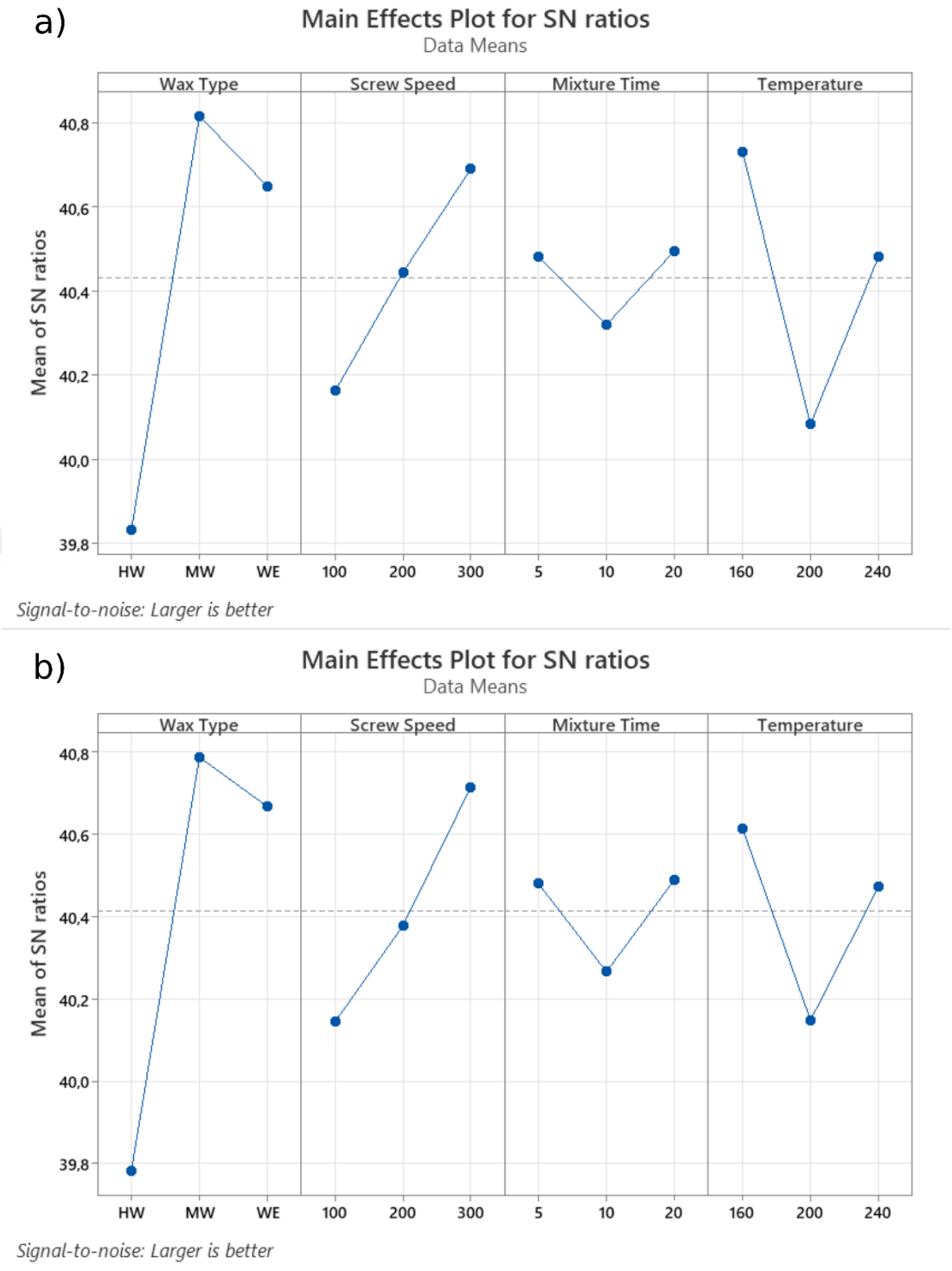

Figure 2.12: Signal-to-noise ratio graph for relative color strength: (a) biobased polyethylene and (b) petroleum-based polyethylene

Process-wise, a screw speed of 200 rpm and extrusion at 240°C maximized RCS values, due to the improved melting and wetting of pigment particles. However, as observed in EAB results, this benefit must be weighed against the potential for

mechanical degradation at high temperatures. The overall trends confirmed that RCS was less sensitive to mixing time compared to other outputs.

Based on the statistical findings, wax type -particularly micronized wax (MW)- had the most significant influence across all four output parameters for both Bio-PE and PB-PE matrices. The superior performance of MW is attributed to its fine particle size and high compatibility, which contributed to enhanced pigment wetting, lower filter resistance, and higher tensile strength.

However, it is important to note that MW negatively impacted elongation at break (EAB). The increased stiffness and reduced chain flexibility associated with MW formulations led to lower ductility values. This trade-off highlights the need to balance mechanical reinforcement with flexibility depending on the target application.

Among the process parameters, a screw speed of 200 rpm and a mixing time of 10 minutes were identified as optimal for most outputs. Regarding extrusion temperature, values between 200°C and 240°C offered performance-specific advantages. While higher temperatures (e.g., 240°C) enhanced pigment wetting and improved RCS, they also caused a reduction in EAB, due to thermal degradation.

The integration of the Taguchi design with analysis of variance and regression enabled the development of statistically robust models, as summarized in Table 2.7. The models for FPV, EAB, and RCS showed particularly high reliability, with coefficients of determination (R^2) exceeding 0.98.

Table 2.7: Summary of analysis of variance and regression results for all response variables

Output Parameter	Matrix	R^2 (ANOVA)	p-value	R^2 (Regression)
FPV	BIO-PE	99.28	< 0.001	99.98
FPV	PB-PE	97.54	< 0.001	99.39
UTS	BIO-PE	89.25	0.01	89.29
UTS	PB-PE	90.38	< 0.001	96.02
EAB	BIO-PE	99.86	< 0.001	99.93
EAB	PB-PE	98.93	< 0.001	98.93
RCS	BIO-PE	98.29	< 0.001	98.65
RCS	PB-PE	96.91	< 0.001	97.72

These findings provide a robust basis for optimizing masterbatch formulations in both biobased and petroleum-based polyethylene systems. The high coefficients of determination obtained from the statistical models underscore the reliability of the Taguchi-based design in predicting key performance indicators such as FPV, EAB, and RCS. This enables a more precise and systematic adjustment of formulation and processing parameters, facilitating the development of high-performance masterbatches that meet specific functional and end-use requirements across diverse application areas.

2.4 Conclusion

In all formulations containing wax emulsion, viscosity increased significantly, reaching up to 90%, has been observed. The lowest filter pressure values were obtained in samples containing micronized wax and processed at temperatures below 240°C. The next lowest filter pressure value was recorded in samples containing wax emulsion, processed at 160°C with an extruder speed of 300 rpm. In blown film samples, the lowest particle count was observed in samples made with micronized wax. No significant difference was observed in the overall color appearance of the samples. The highest color strength was observed in the samples with the lowest filter pressure values, indicating a correlation between dispersion quality and color

development. There was no significant change in tensile strength compared to pure polymer. However, elongation at break decreased significantly in all samples, with reductions reaching up to 98% compared to the pure polymer.

FTIR analysis revealed a spectral similarity of 99% between biobased and petroleum-based polymers. No distinct spectral peak was identified that could differentiate the wax types in the samples. All samples exhibited a spectral similarity of 98% or higher.

In SEM analysis, agglomerated particles of 10 micrometers and smaller were observed only in samples produced with micronized wax at 240°C or lower. In the Taguchi analysis for FPV, wax type was identified as the most influential factor, while the lowest values were associated with shorter mixing times. For UTS, temperature was identified as the most influential parameter, whereas screw speed had the least effect. For elongation at break, wax type was also the most significant factor, while screw speed once again had the least influence. For color strength, wax type had the most substantial impact, and lower values were observed in samples prepared with longer mixing times.

ANOVA and regression analyses, except for UTS (~90%), achieved a confidence level of 95% or higher for all samples. The results for all samples, except UTS ($p \approx 0.172–0.390$), were statistically significant at the 5% level ($p < 0.05$).

From a cradle-to-gate perspective, producing one kilogram of sugarcane-based biobased polyethylene results in the removal of approximately 2.12 kilograms of CO_2 equivalent, whereas the production of one kilogram of petroleum-based polyethylene emits around 3.10 kilograms of CO_2 equivalent. Replacing fossil-based polyethylene with its biobased counterpart therefore yields a net greenhouse gas benefit of nearly 5.2 kilograms of CO_2 equivalent per kilogram of polymer. When these resins are used in color masterbatch formulations, where polyethylene constitutes approximately 75 % by weight, each kilogram of biobased polyethylene-based masterbatch results in a net removal of approximately 1.6 kilograms of CO_2 equivalent. In contrast, a petroleum-based counterpart emits around 4.2 kilograms of CO_2 equivalent. These findings highlighted the environmental benefits of using biobased polyethylene and its masterbatches, which not only reduced overall carbon emissions but also contributed to atmospheric carbon capture.

Considering only the polymer content, the biobased polyethylene carrier masterbatch resulted in negative carbon emissions, while the petroleum based masterbatch contributed to net emissions. The high confidence levels obtained in all tests under these ratios indicated robust and reliable results.

Chapter 3

3 Biobased Polyethylene Films with Natural Pigments for Sustainable Packaging

3.1 Introduction

Plastic waste poses considerable environmental challenges due to limited recycling rates and prolonged degradation periods in natural settings, thereby burdening ecosystems and complicating waste management. In addition, substantial amounts of CO_2 and other greenhouse gases result from conventional plastic manufacturing, worsening climate change. Polymers derived from renewable resources address these challenges by offering a cleaner production pathway. Biobased polyethylene, produced from feedstocks such as sugarcane or corn, reduces carbon emissions and exhibits a lower carbon footprint than conventional polyethylene, while remaining compatible with traditional recycling methods (Agrawal et al., 2021; Benavides et al., 2020; Gandhi et al., 2021; Siracusa & Blanco, 2020; Tsiropoulos et al., 2015).

Natural pigments also play an important role in promoting eco-friendly strategies. Extracted from sustainable plant sources, these pigments serve as viable alternatives to synthetic pigments due to their biodegradability and low toxicity. Their safety profile has encouraged usage in fields including food, cosmetics, and textiles, and their pleasing visual properties, evident from their longstanding presence in artistic and cultural applications, highlight the benefits of merging functionality with environmental considerations (Aman Mohammadi et al., 2022; Ardila-Leal et al.,

2021; Dawson, 2009; De Carvalho et al., 2014; de Souza Mesquita et al., 2021; Galasso et al., 2017; Higuera-Ciapara et al., 2006; Jurić et al., 2022; Venil et al., 2020).

Türkiye's diverse flora includes numerous species known for their high pigment yields. Examples include Rubia tinctorum (madder), Punica granatum (pomegranate), Juglans regia (walnut), Reseda lutea (yellow mignonette), and Quercus infectoria (Aleppo oak). Madder has traditionally been used for vibrant red hues, pomegranate peel pigments appear in textile coloring and leather tanning, while walnut and Aleppo oak deliver deep brown or black tones. Yellow mignonette stands out for a bright yellow shade (Agnhage et al., 2016; Angelini et al., 2003; Bener et al., 2010; Choudhry & Akhtar, 2023; De Santis & Moresi, 2007; Derksen & Van Beek, 2002; Ko et al., 2021). Along with their lack of toxicity, these pigments undergo natural breakdown, making them attractive as eco-friendly alternatives to synthetic dyes (Bechtold & Mussak, 2009).

Existing literature confirms that certain plant-based pigments can be combined with polymer matrices; for instance, adding walnut shell pigments to plastics showed to yield consistent color results (Ferreira et al., 2004). However, investigations specifically targeting the mentioned pigments in plastic matrices remain limited, illustrating a clear opportunity for further exploration.

This study aims to address this research gap by blending biobased polyethylene with the five selected plant pigments from Türkiye's flora to create biocomposite films using the blown film extrusion method. Comprehensive evaluations of the optical, mechanical, and surface properties of these films were subsequently conducted. The main objective is to formulate eco-friendly packaging materials that curtail dependence on synthetic colorants and fossil-based resins, while preserving performance and visual appeal. To complete the life-cycle perspective on biobased polyethylene, Chapter 4 examines the performance of the material over successive mechanical recycling cycles, in comparison with its fossil-based counterpart.

3.2 Materials and Methods

3.2.1 Materials

Madder was obtained from local suppliers (Themazi, Türkiye), whereas pomegranate and walnut shells, along with yellow mignonette, were collected from their natural habitats in the Aegean region of Türkiye. Shells of Aleppo oak were sourced from the Marmara region. Each plant source was sun-dried for three to seven days, depending on the material thickness and weather conditions, ensuring that the process occurred in an open and well-ventilated environment.

The Bio-PE (SEB853/72) used in composite production was supplied by Braskem (Brazil), containing at least 95% biobased carbon content. With a melt flow index of 2.7 g/10 min (190 °C, 2.16 kg), it was formulated for compatibility with blown film extrusion processes.

3.2.2 Characterization of Plant Powders

3.2.2.1 Grinding and Particle Size Analysis

An appropriate volume of dried plant material was selected and subjected to an initial grinding stage using a vibratory disc mill (Retsch RS 200, Germany) operating at 1000 rpm for one minute. During milling, the powder temperature was routinely monitored, and cooling intervals were applied when necessary. A Retsch analysis sieve (100 μm) was subsequently used to eliminate coarse particles and residues. Following grinding, the particle size distribution was analyzed using a particle size analyzer (Malvern Mastersizer 3000, UK). The samples were stored in amber glass containers to minimize light exposure and preserve their quality.

3.2.2.2 Thermogravimetric Analysis

The thermal stability of the ground plant materials was evaluated with a thermogravimetric analyzer (SDT Q600, TA Instruments, USA). Approximately 10

mg of material was placed into an alumina crucible and heated from ambient temperature to 1200 °C at a rate of 10 °C/min, under a constant nitrogen flow.

3.2.2.3 Scanning Electron Microscopy

Scanning electron microscopy offered insights into the morphology of each sample. Prior to analysis, gold coating was applied to enhance conductivity and reduce charging effects on the surfaces. Micrographs were obtained using a Tescan Vega microscope (Czech Republic) at 20 kV in high-vacuum mode. Images were captured at multiple magnifications to study the size distribution of the particles, surface topographies, and dispersion characteristics in the resulting composite forms.

3.2.3 Composite Production Process

Pre-ground Bio-PE and powdered plant additives were combined in a laboratory-scale mixer (Labtech Engineering, Thailand) at 500 rpm for five minutes, maintaining a plant powder loading of 10% by weight. Table 3.1 presents the formulations and their corresponding mixing ratios.

Table 3.1: Formulations of biobased polyethylene composites containing plant-derived powders

Sample	Madder (wt.%)	Pomegranate (wt.%)	Walnut (wt.%)	Yellow mignonette (wt.%)	Aleppo oak (wt.%)	BIO-PE (wt.%)
BIO-MA	10	-	-	-	-	90
BIO-PO	-	10	-	-	-	90
BIO-WA	-	-	10	-	-	90
BIO-YM	-	-	-	10	-	90
BIO-AO	-	-	-	-	10	90

The composite samples were subsequently fed into a twin-screw extruder (Labtech Engineering, Thailand) with a screw diameter of 25 mm and an L/D ratio of 44:1, indicating a screw length 44 times its diameter. During processing, temperatures

ranged from 130 to 165 °C, while feed rate was maintained at 20 rpm and screw speed at 200 rpm.

3.2.4 Characterization of Composites

3.2.4.1 Physical Property Analysis

Density measurements were conducted according to ASTM D792, initially weighing samples in air and then in acetone (density = 0.791 g/cm^3). The density of each sample was calculated based on five independent measurements.

A melt flow instrument (Zwick/Roell Mflow, Germany) was used to assess the melt flow rate of each composite at 190 °C under a 2.16 kg load (ASTM D1238). Five measurements were conducted per formulation, and the average values were reported.

3.2.4.2 Differential Scanning Calorimetry

The thermal properties of each composite were analyzed using a Q2000 DSC system (TA Instruments, USA). Approximately 10 mg of the sample was sealed in a Tzero Aluminum Hermetic pan, then heated from 20 °C to 150 °C at 10 °C/min to eliminate prior thermal history. The sample was subsequently cooled to -20 °C and reheated to 150 °C at the same rate. The crystallization temperature (T_c), melting temperature (T_m), and associated enthalpies (ΔH_c and ΔH_m) were recorded. Crystallinity (χc) was calculated using 293 J/g as the reference enthalpy for a 100% crystalline polyethylene (Kong & Hay, 2003).

3.2.5 Blown Film Extrusion Process

Films were fabricated using a blown film extrusion line (Labtech Engineering, Thailand) equipped with a 20 mm screw diameter and an L/D ratio of 30. The processing temperature was maintained between 170 and 180 °C, with a screw speed of 90 rpm. Each composite was fed directly into the extruder, and the resulting film thickness was set at 100 micrometers.

3.2.6 Characterization of Blown Films

3.2.6.1 Optical Property Analysis

Optical measurements were performed using an X-Rite Ci64 spectrophotometer (USA) to determine the color parameters (L, a, b*) in accordance with ASTM E308-18, employing a D65/10° illumination geometry. Transmission and haze values were determined on an X-Rite Ci7600 bench spectrophotometer (USA).

Haze refers to the extent to which light is scattered as it passes through a material. A high haze level results in a cloudy appearance and reduced transparency. It is typically measured by comparing the amount of scattered light to the total transmitted light. Diffuse transmission refers to the portion of light that is scattered as it passes through a material, while total transmission includes both scattered and direct light, as described in Equation 3.1.

$$Haze\ (\%) = \frac{Diffuse\ Transmission}{Total\ Transmission} \times 100 \tag{3.1}$$

Transmission measurements indicate the amount of light that can pass through a material. The total light transmittance (T_{total}) is the combined amount of light that goes straight through (direct) and the light that scatters as it passes through (diffuse). This is calculated by dividing the total light intensity after passing through the material (I_{out}) by the total light intensity before it enters (I_{in}), as shown in Equation 3.2.

$$T_{total} = \frac{I_{\text{in}}}{I_{out}} \text{ x } 100 \tag{3.2}$$

3.2.6.2 Friction, Blocking, and Mechanical Analysis

The static and dynamic coefficients of friction (COF) of the specimens were measured with a tensile testing machine (Devotrans, Türkiye) equipped with a friction test fixture and in accordance with ISO 8295. The film surfaces were cleaned; one sample strip was attached to the moving clamp and another to the stationary clamp. The test was performed at a speed of 100 mm/min.

The static coefficient of friction (μ_s) is defined as the ratio of the maximum static friction force ($F_{s,max}$) to the normal force (N). Where $F_{s,max}$ is the maximum force that must be applied to an object to initiate movement. N is the normal force, which is the force pressing the two surfaces together (perpendicular to the contact surface), (Equation 3.3).

$$\mu_s = \frac{F_{s,max}}{N} \tag{3.3}$$

The static friction force (F_s) may vary from zero up to this maximum value, opposing any applied force that tends to cause motion, as long as the object remains at rest Equation 3.4):

$$F_s \leq \mu_s N \tag{3.4}$$

The dynamic or kinetic coefficient of friction is defined as the ratio of the kinetic friction force (F_k) to the normal force when the object is in motion (Equation 3.5).

$$\mu_k = \frac{F_k}{N} \tag{3.5}$$

Blocking tendencies were evaluated in accordance with ASTM D3354. Film parts were measured 5×5 cm, placed in the tester, aligning one film square on the upper clamp and another on the lower clamp. The pulling rate was set at 50 mm/min, and the force required to separate the layers (blocking force) was recorded.

Mechanical properties were evaluated using a universal testing machine (Devotrans, Türkiye) in accordance with ISO 527-3. Each specimen (10 × 150 mm) was tested at a crosshead speed of 50 mm/min to determine tensile modulus, tensile strength, and elongation at break.

3.3 Results and Discussion

3.3.1 Analysis of Plant Powders

Figure 3.1 presents images of the ground plant powders. The visual differences among the samples indicate that plant origin and cellular structure influence color shade, particle texture, and overall appearance. These distinctions suggest potential variations in downstream processing behavior and final film performance. Given that particle size and surface area govern filler–polymer interactions, detailed characterization was essential.

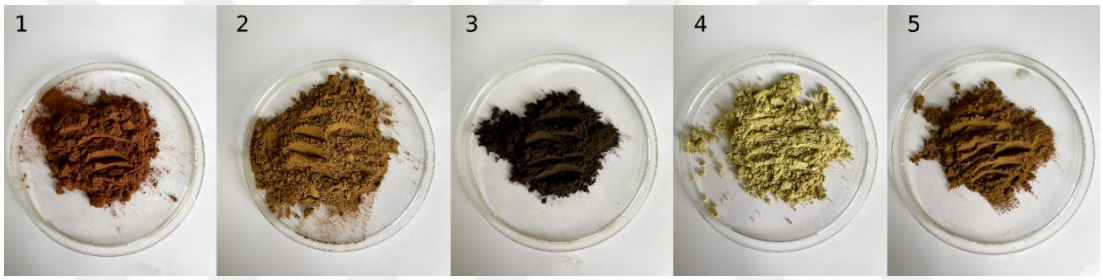

Figure 3.1: Images of the plant powders after grinding process (1. Madder, 2. Pomegranate, 3. Walnut, 4. Yellow mignonette, 5. Aleppo Oak)

The particle size distributions, displayed in Figure 3.2, are summarized through Dv (10), Dv (50), and Dv (90) parameters, which mark diameters below which 10 %, 50 %, and 90 % of the cumulative volume are found, respectively. Average particle size (Dv (50)) spanned roughly 39.1 µm to 49.1 µm. Pomegranate powder exhibited the largest mean diameter (49.1 µm), whereas Aleppo oak showed the smallest (39.1 µm). Distribution breadth differed by source: yellow mignonette recorded the widest span (3.121), indicating a broader particle size, while pomegranate exhibited the narrowest span (2.087), implying a more uniform population (Table 3.2).

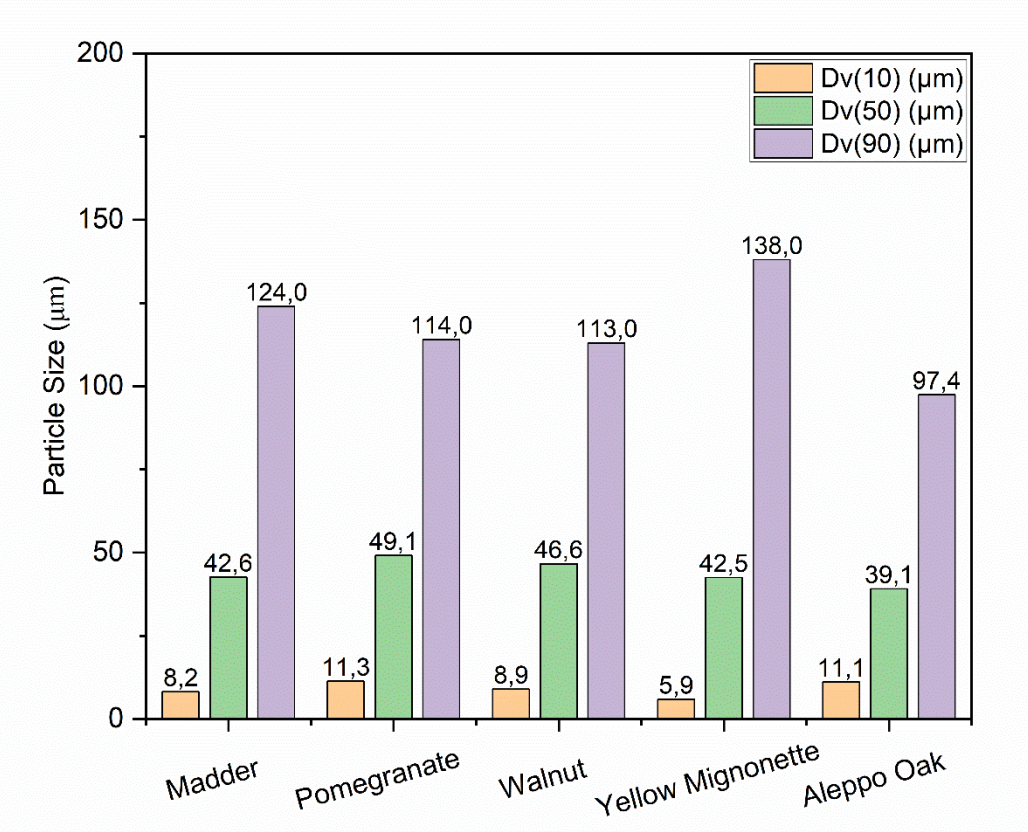

Figure 3.2: Particle-size distributions of plant powders

Table 3.2: Specific surface area and span values of plant powders

Sample Name	Specific Surface Area (m^2/kg)	Span
Madder	365.1	2.715
Pomegranate	229.6	2.087
Walnut	307.8	2.241
Yellow mignonette	435.3	3.121
Aleppo oak	281.9	2.208

The specific surface area, defined as the total particle surface per unit mass, is a key indicator of potential reactivity and interfacial bonding (Bardestani et al., 2019). The Yellow mignonette exhibited the highest surface area (435.3 m^2/kg), reflecting its relatively fine fraction despite the broad size distribution. At the other extreme, pomegranate showed the lowest value (229.6 m^2/kg). Together with the span data,

these findings indicate that yellow mignonette contains a high proportion of fine particles, which increase the overall surface area, while pomegranate has relatively more coarse particles with lower surface development.

Thermogravimetric analysis (Figure 3.3) monitored mass loss as the temperature increased from room temperature to 1200 °C. An initial mass reduction of 10–20% within the 200–300 °C range can be attributed to moisture release and volatilization of low-molecular constituents. More significant degradation was observed between 300 °C and 600 °C, corresponding to breakdown of cellulosic and hemicellulosic fractions (D. Chen et al., 2018; Poletto et al., 2015; Stevulova et al., 2017). In this region, madder and pomegranate powders lost nearly half their mass, while yellow mignonette and Aleppo oak remained slightly more stable. Above 600 °C, walnut powder retained a higher proportion of its initial mass than the other powders, a pattern consistent with its larger lignin-like fraction and the recognized thermal resilience of lignin structures (Blanco et al., 2017; Senneca et al., 2020; Vänskä et al., 2016). Beyond 800 °C, residual mass approached 5–10 % for all samples, representing mainly carbonaceous and mineral remnants.

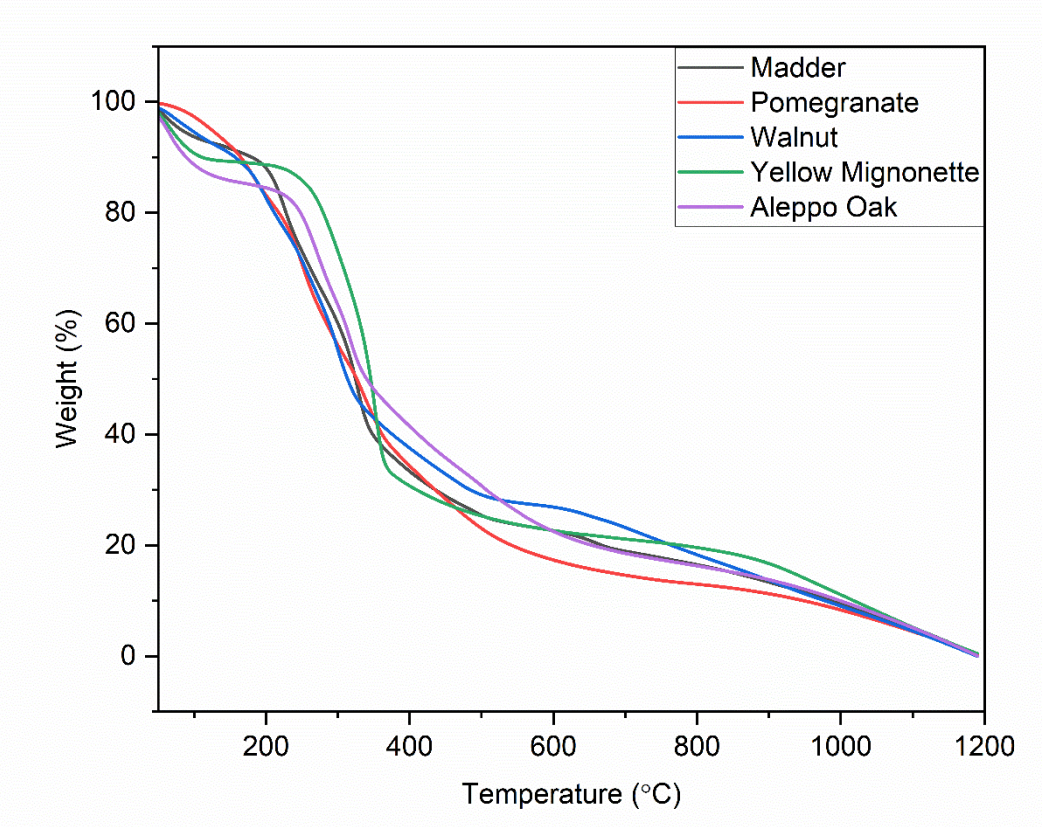

Figure 3.3: Thermogravimetric analysis curves illustrating the thermal stability and decomposition behavior of plant powders

Scanning electron micrographs (Figure 3.4) further highlight the morphological differences among the plant powders. Madder particles appeared irregular and rugged, with a wide particle size distribution. Pomegranate powder also displayed irregular geometry but with comparatively smoother surfaces. Walnut particles were larger and often showed distinct angular facets. Yellow mignonette exhibited a heterogeneous mixture of fine particles, characterized by visible micropores and surface grooves, while Aleppo oak powder tended to form dense clusters with less pronounced surface roughness. These surface traits influenced dispersion quality and adhesion once the powders were blended into BIO-PE.

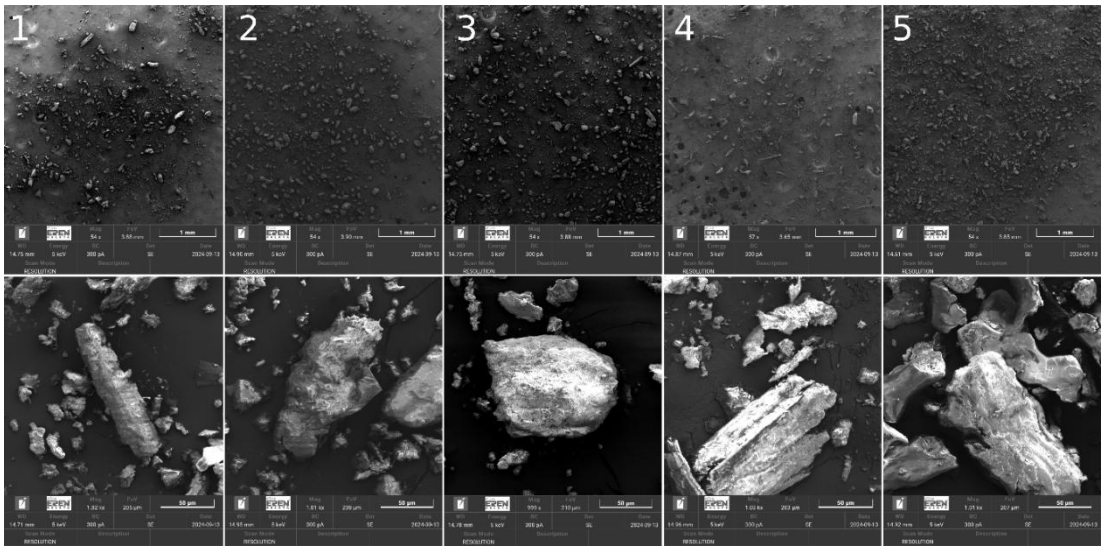

Figure 3.4: Scanning electron microscopy images of plant powders at two magnifications (1. Madder, 2. Pomegranate, 3. Walnut, 4. Yellow mignonette, 5. Aleppo Oak)

In summary, the five plant-based powders exhibited significant differences in particle size distribution, specific surface area, thermal stability, and morphology. Yellow mignonette exhibited the highest specific surface area and a broad particle size distribution, factors that can enhance pigment dispersion yet may raise melt viscosity. Walnut's greater thermal resilience and coarse morphology could affect processing temperature and mechanical performance. Such baseline information guided interpretation of subsequent composite and film results.

3.3.2 Analysis of Composites

Table 3.3 presents melt-flow index and density values for neat BIO-PE and the five plant-powder composites. All formulations maintained acceptable flow properties. Madder and pomegranate filled samples showed MFI values of 2.50 g/10 min, only slightly higher than neat BIO-PE (2.32 g/10 min); this similarity indicates no pronounced loss in processability. The walnut composite exhibited a modest increase to 2.80 g/10 min, suggesting that walnut powder may reduce melting viscosity through particle shape or interfacial effects. Small spherical features observed in Figure 3.4 may facilitate chain mobility by lowering internal friction.

Table 3.3: Melt-flow index and density of neat biobased polyethylene and biobased polyethylene composites

Sample	MFI (g/10 min)	Density (g/cm^3)
BIO-PE	2.32 ± 0.05^a	0.90 ± 0.02^a
BIO-MA	2.50 ± 0.04^b	0.81 ± 0.03^b
BIO-PO	2.50 ± 0.04^b	0.84 ± 0.02^b
BIO-WA	2.80 ± 0.06^c	0.85 ± 0.03^b
BIO-YM	2.48 ± 0.05^b	0.83 ± 0.02^b
BIO-AO	2.60 ± 0.05^c	0.82 ± 0.02^b

Note: Mean values ± standard deviation (n=5). Different superscript letters indicate statistically significant differences ($P < 0.05$) as determined by ANOVA and Tukey's HSD test.

Density results also changed within a narrow band. Whereas neat BIO-PE measured 0.90 g/cm^3, composite densities ranged between 0.81 g/cm^3 and 0.85 g/cm^3, reflecting partial replacement of polymer with lower-density plant powders. A reduction in mass per unit volume can benefit packaging applications by lowering the overall weight, though any change in mechanical strength must be verified experimentally. Statistical analysis (ANOVA followed by Tukey's HSD test) confirmed statistically significant differences ($p < 0.05$) among certain formulations for both MFI and density, underlining the influence of filler type and morphology.

Thermal transitions determined by DSC are summarized in Table 3.4. The melting temperature (T_m) of neat BIO-PE (113.0 °C) decreased only slightly after filler addition, remaining within 111.7-112.8 °C for all composites. Such minor shifts imply that none of the powders disrupted crystalline lamellae to a meaningful extent. In contrast, crystallization temperature (T_c) rose from 97.4 °C in neat BIO-PE to about 98.6–99.8 °C in filled samples. This indicates that powder particles function as nucleation sites, promoting faster crystal formation.

Table 3.4: Thermal parameters of neat biobased polyethylene and plant-powder composites obtained from differential scanning calorimetry thermograms

Sample	T_m (°C)	T_c (°C)	ΔH_c (J/g)	ΔH_m (J/g)	χ_c (%)
BIO-PE	113.00	97.41	75.26	72.85	24.86
BIO-MA	112.74	99.81	64.53	67.48	23.03
BIO-PO	111.70	99.63	65.19	63.64	21.72
BIO-WA	112.56	98.57	66.16	62.59	21.36
BIO-YM	112.10	99.64	78.16	87.61	29.90
BIO-AO	112.53	99.42	65.39	63.28	21.60

Enthalpy data provides further insight. The yellow mignonette composite exhibited the highest melting enthalpy (87.6 J/g) and crystallization enthalpy (78.2 J/g), yielding a crystallinity index of 29.9 %. These values surpass the 24.9 % of neat BIO-PE, suggesting that particles from this sample encourage a more ordered structure. In contrast, pomegranate and walnut fillers lowered crystallinity to around 21-22 %, presumably because their surface chemistry or particle geometry interferes with chain folding. A similar nucleation mechanism where added surfaces facilitate chain alignment, has been reported for semicrystalline polyethylene systems containing micro-powder inclusions (Queyroy & Monasse, 2012).

When considered collectively, the physical and thermal results demonstrate that every plant powder leaves a recognizable footprint on BIO-PE, yet the base resin remains fully processable by conventional extrusion. The moderate variations in melt flow index are particularly relevant to blown film production: values between 2.3 g/10 min and 2.8 g/10 min still fall within the operating window of most laboratory film lines, indicating that no major adjustments to screw design or die pressure are necessary. A slight MFI rise, observed for the walnut composite, can even ease bubble stability by reducing melt torque, though it may also lower melt strength and thus call for lower blow-up ratios during scale-up.

The density drop of 5–10 % across filled samples suggest direct mass saving. When converted to packaging thickness, this reduction means that a standard roll of film covers a larger surface area for the same roll weight. In high-volume sectors such as

produce bags or single-use liners, such savings translate into lower transport emissions and reduced disposal mass.

Crystallization behavior deserves closer attention, because it sets the cooling rate and the final microstructure of the film. The observed T_c increase of roughly 2 °C, common to all powders, means that BIO-PE begins to solidify sooner after leaving the die. In a blown-film tower, earlier solidification permits a shorter frost-line height, allowing faster line speeds or a more compact cooling section. The difference is most notable for yellow mignonette powder, whose strong nucleating effect increased crystallinity to nearly 30%. Higher crystalline rates typically enhance hardness and dimensional stability, which may reduce wrinkling in bags during subsequent use.

By contrast, pomegranate and walnut powders reduced χc to just above 21%. A lower degree of order usually softens the matrix, making the film more pliable but also more permeable to gases. Combined with their modest effect on MFI, these powders may be suitable for applications where flexibility and easy foldability matter more than barrier strengths such as wrap films for fresh bread or confectionery.

The small decline in melting temperature (approximately 1–2 °C) across all composites is unlikely to affect hot-fill or sealing operations, because BIO-PE grades intended for packaging often tolerate ±5 °C variation in sealing jaws. Still, processors may choose to lower zone-6-barrel settings by 5 °C to minimize pigment discoloration, especially for madder-filled formulations that show early mass loss in TGA studies.

Finally, the enthalpy values reveal an energy trade-off: yellow-mignonette raises both ΔH_c and ΔH_m, indicating a more energy-dense crystalline phase, while pomegranate and walnut lower these measures, signaling fewer tight crystal stems. These distinctions prefigure the mechanical data that follow. A higher ΔH_m tends to boost film modulus and yield stress, whereas reduced ΔH_m aligns with greater elongation but lower tensile strength. The later sections confirm these expectations, linking thermal history directly to tensile response and surface slip.

In summary, the melt flow index, density, and crystallinity together define a distinct processing profile for each pigment-polyethylene system. For instance, madder exhibits minimal MFI shift, slight density decreases, and moderate nucleation, making it suitable for colored carrier bags that require intermediate stiffness. Pomegranate

shows no change in MFI, moderate density drops, and the lowest crystallinity, making it ideal for flexible yet strong films with an acceptable beige tint. Walnut demonstrates the highest MFI, minimal density change, and low crystallinity, making it appropriate for lightweight liners, though a compatibilizer is needed for enhanced strength. Yellow mignonette, with nearly unchanged MFI, the highest surface area, and the greatest crystallinity and opacity, is favorable when light blocking and rigidity are required. Aleppo oak, showing a slight MFI rise, moderate density decreases, and mid-range crystallinity, strikes a balance between slip behavior and a warm brown tone. These processing insights not only inform extrusion parameters but also provide guidance for the intended end-use of each composite, laying the groundwork for the optical, mechanical, and surface analyses that follow.

3.3.3 Analysis of Packaging Films

Figure 3.5 presents the blown film samples produced from BIO-PE and each plant pigment. While the neat BIO-PE sample is colorless and highly transparent, adding the powders introduces characteristic colors that reflect the natural colors of the source plants. The BIO-MA film displays a light brown shade, BIO-PO is a deeper beige, BIO-WA appears grey-brown, BIO-YM presents a bright yellow tone, and BIO-AO exhibits a warm medium brown. These visual impressions are supported by the quantitative optical data presented in Table 3.5.

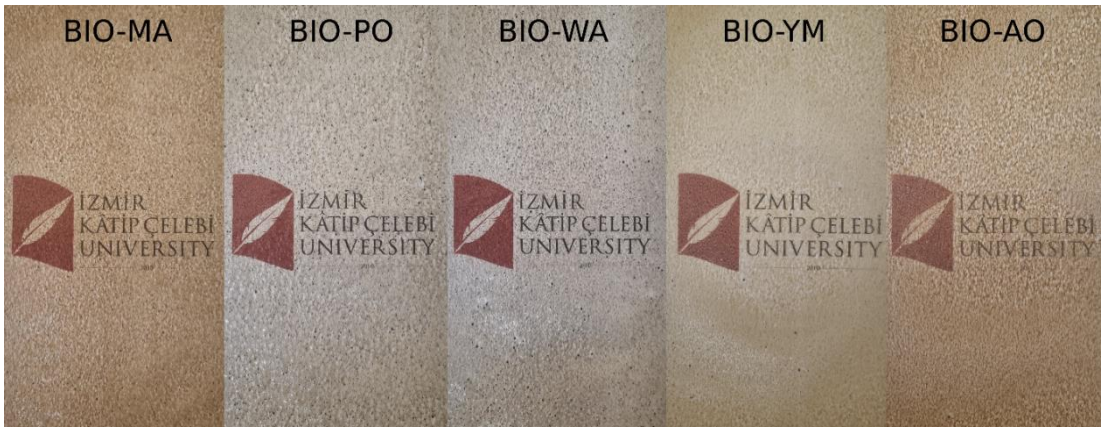

Figure 3.5: Photographs of biobased polyethylene composite films produced by blown film extrusion

According to Table 3.5, the reference BIO-PE film exhibited the lowest haze value (12.61 %) and the highest total light transmission (88.93 %), which is consistent with its clear appearance. Introducing madder increases haze to 55.46 % and reduces transmission to 45.42 %, yielding a semi-translucent film that still allows partial product visibility. Pomegranate and walnut powders raise haze further, to roughly 70 % and 83 % respectively, while yellow mignonette and Aleppo oak powders create nearly opaque structures with haze values of 99.77 % and 98.39 % and transmission below 51 %. These results demonstrate how plant-based pigments can modulate film opacity from transparent to fully light-blocking, a useful feature for packaging products that require differing degrees of light protection.

Table 3.5: Optical and colorimetric properties of biobased polyethylene composites

Sample	Haze (%)	Transmission (%)	L*	a*	b*
BIO-PE	12.61 ± 0.51^{a}	88.93 ± 2.22^{a}	92.51 ± 2.15^{a}	-0.39 ± 0.02^{a}	3.72 ± 0.02^{a}
BIO-MA	55.46 ± 1.14^{b}	45.42 ± 1.89^{b}	57.82 ± 1.58^{b}	10.72 ± 0.20^{b}	21.73 ± 0.50^{b}
BIO-PO	70.28 ± 6.50^{c}	62.94 ± 0.55^{c}	72.76 ± 0.55^{c}	2.41 ± 0.15^{c}	14.05 ± 0.24^{c}
BIO-WA	83.73 ± 0.51^{d}	49.04 ± 2.56^{d}	62.11 ± 0.98^{d}	2.89 ± 0.46^{c}	10.61 ± 0.29^{d}
BIO-YM	99.77 ± 1.24^{e}	50.49 ± 2.17^{d}	74.56 ± 2.46^{c}	3.96 ± 0.08^{d}	25.99 ± 0.34^{e}
BIO-AO	98.39 ± 2.91^{e}	38.61 ± 0.70^{e}	62.77 ± 0.64^{d}	6.66 ± 0.35^{e}	16.79 ± 0.05^{c}

Note: Mean values ± standard deviation (n=5). Different superscript letters indicate statistically significant differences ($P < 0.05$) as determined by ANOVA and Tukey's HSD test.

Color coordinates (L*, a*, b*) follow similar trends. The neat film's high lightness (L: 92.5) falls sharply for BIO-MA (57.8) and BIO-AO (62.8), mirroring the darker tones seen in Figure 3.5. Positive a and b values indicate a shift toward warmer color tones. Madder provides the strongest red component (a: 10.7), whereas yellow mignonette produces the highest positive b (26.0), consistent with its vivid yellow shade. The ANOVA results included with Table 3.5 show significant differences ($p < 0.05$) among formulations for every optical parameter (haze, transmission, L*, a*, b*). These optical differences enable packaging designers to strategically select pigments based on product protection and marketing requirements. For example,

high-opacity yellow-mignonette (BIO-YM) films can block photo-oxidative degradation in light-sensitive foods, while lightly tinted pomegranate (BIO-PO) films offer partial product visibility and UV filtering, balancing shelf appeal and preservation.

Figure 3.6 presents tensile modulus, tensile strength, and elongation at break of composite films. The tensile modulus of BIO-PO reached 246 MPa, surpassing that of all other filled films and indicating that pomegranate powder stiffens the matrix. A similar reinforcing effect of pomegranate pigment has been reported in various polyolefin and starch-based matrices (Ali et al., 2019; Banihani et al., 2021). The addition of madder resulted in the lowest modulus (≈ 168 MPa), suggesting less effective stress transfer, probably due to poorer interfacial bonding.

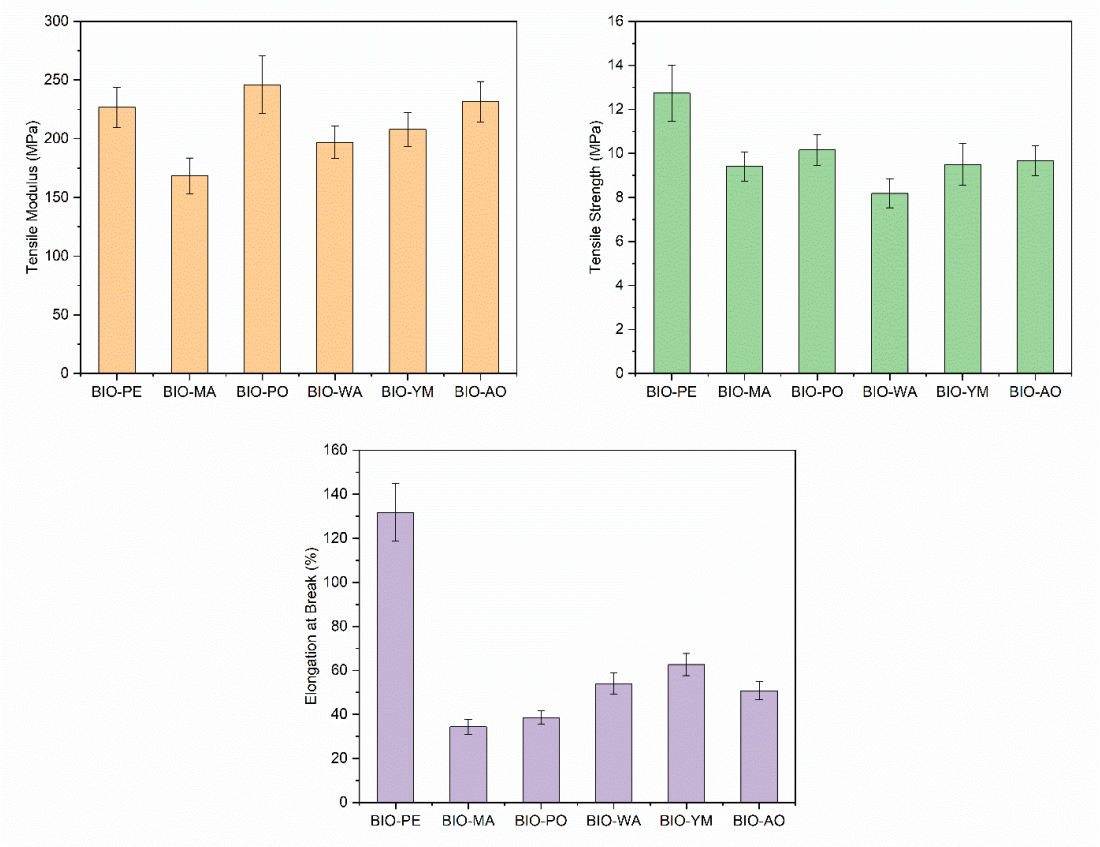

Figure 3.6: Effects of plant-powder pigments on tensile modulus, tensile strength, and elongation at break of biobased polyethylene films

Tensile strength exhibited a distinct trend: neat Bio-PE showed the highest value (12.7 ± 0.3 MPa). The reduction observed in the composites aligns with previous studies indicating that fillers create stress concentration sites, thereby reducing ultimate strength due to poor interfacial adhesion (Boronat et al., 2015; Kuciel et al., 2014). The BIO-WA composite showed the lowest tensile strength (8.2 ± 0.2 MPa), consistent with reports that untreated walnut particles debond under load, initiating cracks (Isam Bakr Albaker et al., 2021; Orue et al., 2020; Zheng et al., 2020). This suggests that compatibilizers may be needed to enhance BIO-WA's suitability for demanding packaging applications.

Elongation at break emphasized the changes in ductility. Unfilled polymer retained high elongation (≈ 132 %), whereas madder-filled film dropped to about 34 %, confirming increased brittleness. Yellow mignonette and Aleppo oak composites exhibited intermediate elongation values, suggesting that these powders disrupted chain mobility less severely and may be preferable when flexibility is critical. Plasticizers or reactive compatibilizers, such as epoxidized vegetable oils, could be introduced in future work to recover elongation without sacrificing modulus (Özgür Seydibeyoğlu et al., 2010).

In the coefficient of friction analysis (Figure 3.7), the BIO-PO composite exhibited the highest static coefficient of friction, measured at 0.27. This indicates that the BIO-PO surface has greater resistance to sliding and a stronger frictional force compared to the other composites. Following this, the BIO-YM composite showed slightly lower but still relatively high friction value of 0.24. On the other hand, the BIO-MA and BIO-AO composites had lower friction coefficients, both at 0.20, suggesting that their surfaces are more prone to sliding.

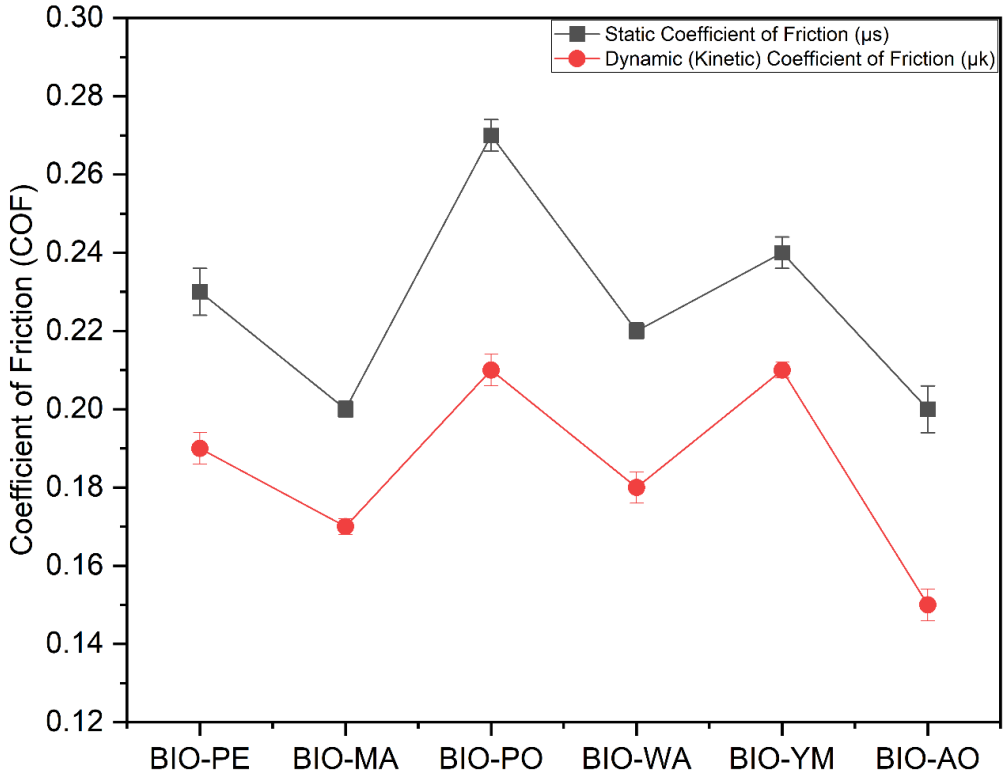

Figure 3.7: Static and dynamic coefficients of friction of biocomposite films

A similar trend was observed in the dynamic coefficient of friction results. The highest dynamic coefficient, 0.21, was observed for both the BIO-PO and BIO-YM composites, while the BIO-AO composite showed the lowest value at 0.15.

These variations in friction values are likely related to the surface microstructure of the composites and the interaction between the fillers and the matrix. Composites like BIO-PO and BIO-YM, which have higher friction coefficients, may have more microscopic contact points on their surfaces, which may increase resistance to sliding. In contrast, the lower values observed in BIO-MA and BIO-AO suggest smoother surfaces that allow easier movement.

In a study by Talikoti et al. (2015), the effect of filler interaction with the polymer matrix on the frictional behavior of composites was investigated. It was found that walnut shell powder increased the friction coefficient by enhancing the surface roughness. The incompatibility between the filler and matrix was shown to increase friction resistance by creating microscopic roughness on the surface. Additionally, in a study conducted by Yoon et al. (2022), the friction behavior of rice husk silica-filled

elastomer composites was examined. The study revealed that an increase in surface roughness and the interaction between the filler and the matrix resulted in an increase in the coefficient of friction. These results demonstrate that the microscopic roughness formed by the fillers on the surface contributes to the increase in the coefficient of friction and can improve the sliding resistance of such composites.

Blocking force results (Figure 3.8) quantify the tendency of adjacent film layers to adhere under mild pressure. The reference BIO-PE film required the greatest force to separate (530 gf/100 cm²), attributed to smooth polymer surfaces and higher surface energy. The incorporation of pigments reduced blocking, with values dropping to approximately 440 gF/100 cm^2 for pomegranate- and Aleppo-oak-based films.

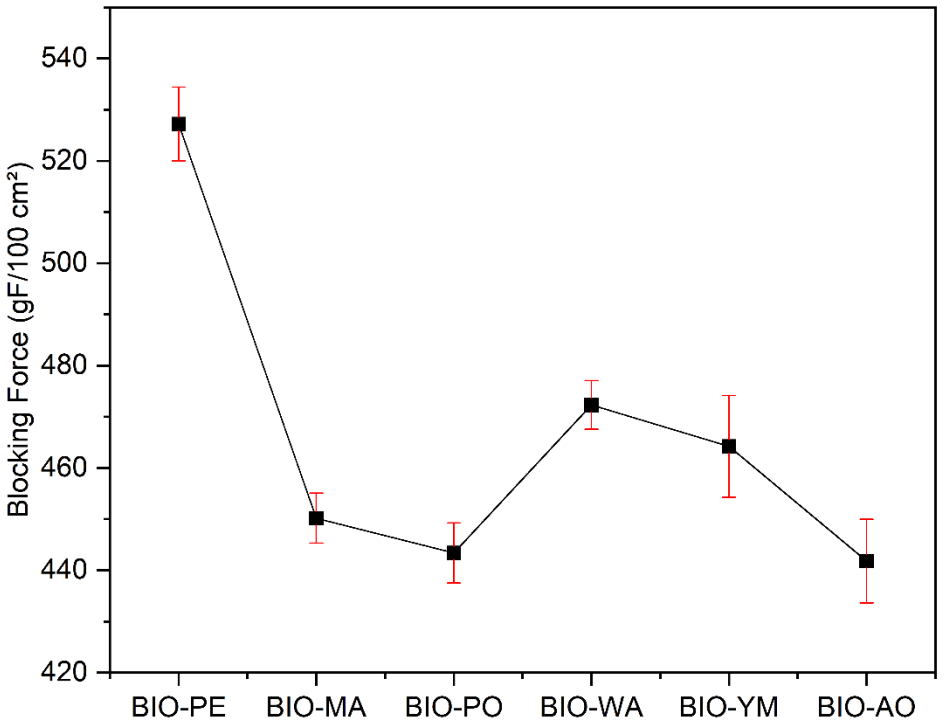

Figure 3.8: Blocking force of biocomposite films intended for packaging applications

Awaja et al. (2009) investigated the relationship between the adhesion behavior of polymer surfaces and their surface energy. The study found that polymers with higher surface energy exhibit stronger adhesion tendencies, resulting in increased blocking force. Higher surface energy leads to stronger adhesion between polymer layers,

thereby increasing the blocking tendency. This trend has also been reported in other similar studies. This behavior aligns with the principle that surface-protruding fillers reduce the real contact area and thereby decrease adhesion, as described in adhesion energy studies on polymer films (Deshmukh et al., 2013; Idumah & Obele, 2021). Reduced blocking is advantageous for roll handling and bag opening in packaging.

Overall, each plant powder generates a distinct balance of stiffness, toughness, slip, and blocking behavior. Pomegranate enhances stiffness and provides moderate opacity; yellow mignonette offers exceptional opacity along with elevated friction; Aleppo oak contributes to surface slip and low blocking; madder imparts a warm hue at the expense of ductility; walnut reduces density but also decreases tensile strength. Therefore, material selection should be based on the specific mechanical and optical requirements of the target application.

3.4 Conclusion

This study investigated the use of biobased polyethylene in combination with natural pigments derived from Türkiye's endemic plant species (Rubia tinctorum (madder), Punica granatum (pomegranate), Juglans regia (walnut), Reseda lutea (yellow mignonette), and Quercus infectoria (Aleppo oak)) to fabricate sustainable packaging films via blown film extrusion. The results confirmed that natural pigments significantly influence the functional performance of BIO-PE films, particularly with respect to their optical, mechanical, and surface characteristics.

Among the formulations, the yellow mignonette pigment exhibited the highest haze (99.77%) and significantly reduced light transmittance to 50.49%, enabling the development of films suitable for protecting light-sensitive products. The pomegranate pigment reinforced the matrix, increasing the tensile modulus to 246 MPa and thereby enhancing mechanical strength without compromising film processability. Although a decrease in elongation at break was observed due to the presence of particulate fillers, all films maintained sufficient structural integrity and flexibility for packaging applications.

Surface evaluations revealed enhanced frictional behavior, with coefficients ranging from 0.15 (BIO-AO) to 0.27 (BIO-PO), which contributed to improved stackability

and handling. Additionally, the blocking force, which affects usability in multilayer formats, was significantly reduced in several composites, particularly in the BIO-AO formulation (440 gf/100 cm^2), facilitating better roll separation and user experience.

The use of natural pigments, sourced from renewable and abundant plants, offers a promising alternative to synthetic colorants, many of which pose environmental and health concerns. These pigments are inherently non-toxic and biodegradable, supporting safer application in consumer-facing packaging, particularly in the food industry, where color, functionality, and safety must be carefully balanced.

In conclusion, the incorporation of natural pigments into biobased polyethylene provides a viable strategy for producing recyclable, functionally robust, and visually distinctive films with a reduced environmental impact. This approach aligns with the growing demand for cleaner, renewable, and safer materials in the packaging sector. Future research should focus on optimizing formulation parameters and assessing the long-term performance of these films under real-world conditions.

Chapter 4

4 Comparative Recycling Performance of Biobased and Petroleum-Based Polyethylene

4.1 Introduction

Polyethylene is among the most widely used thermoplastic polymers worldwide, with applications spanning various sectors such as packaging, piping, film coatings, and consumer goods. Its high mechanical strength, chemical resistance, and ease of processing make it a preferred material in industrial applications. Conventional polyethylene is produced from fossil fuels through petrochemical processes, which raises concerns regarding ecological sustainability due to carbon emissions and the depletion of natural resources (Chawla et al., 2022; Evode et al., 2021; Maraveas, 2020; Papo & Corona, 2022; Yao et al., 2022).

In response to these concerns, biobased polyethylene has been developed as a sustainable alternative to conventional polyethylene. It is derived from renewable resources, specifically plant biomass such as sugarcane or corn. This production method reduces both the carbon footprint and dependence on fossil resources. Since biobased polyethylene exhibits physical and chemical properties similar to those of its petroleum-based counterpart, it can potentially be integrated into existing production and recycling systems (Belboom & Léonard, 2016; Benavides et al., 2020; Helmes et al., 2022; Tsiropoulos et al., 2015; Wang et al., 2020).

Alterations in the physical and chemical attributes of polyethylene following multiple recycling cycles directly influence its performance and lifespan, highlighting the importance of maintaining stability during repeated processing. The performance of polyethylene, particularly in terms of its mechanical properties, thermal stability, and molecular weight distribution, is critical for its use in industries such as packaging, textiles, and automotive, where material reuse and recycling are indispensable (Badia et al., 2017; Lambert & Wagner, 2017; Moshood et al., 2022).

Although considerable research has been conducted on polyethylene and its recyclability, previous studies have primarily focused on conventional, petroleum-based polyethylene. These investigations examined degradation under conditions such as accelerated weathering and repeated extrusion cycles, revealing changes in crystallinity, density, hardness, mechanical strength, and melt flow due to oxidation and thermal effects (Dostál et al., 2008; Gulmine et al., 2003; Marsh et al., 2006; Mendes et al., 2011; Tsenoglou et al., 2001).

Nevertheless, the long-term recycling behavior of biobased polyethylene remains relatively underexplored. Addressing this knowledge gap is essential for the development of sustainable materials capable of maintaining stability and performance over multiple processing cycles. The primary aim of this study is to compare the changes in polymer characteristics of biobased and petroleum-based polyethylene after repeated use. The study evaluates the mechanical properties, thermal behavior, molecular weight distribution, melt flow index, and optical properties of both materials. It is anticipated that the resulting data will enhance the current understanding of biobased polyethylene recyclability and provide valuable insights for expanding its industrial applications.

4.2 Materials and Methods

4.2.1 Materials

The low-density biobased polyethylene (BBPE), (SEB853/72) used in this study was obtained from renewable resources provided by Braskem (Brazil) and contains 95% biobased carbon content. BBPE exhibits a melt flow index of 2.7 g/10 min (at 190 °C

under a 2.16 kg load), a density of 0.923 g/cm^3, and a melting point of 110 °C. Low-density petroleum-based polyethylene (PBPE) was supplied by Petkim (Türkiye) and exhibits a melt flow index of 2.5 g/10 min (at 190 °C under a 2.16 kg load), a density of 0.920 g/cm^3, and a melting point of 110 °C.

4.2.2 Multiple Cycle Extrusion Process

To investigate the material behavior across multiple reprocessing cycles, a twin-screw laboratory extruder (Labtech Engineering, Thailand) with a 20 mm diameter and an L/D ratio of 44:1 was used. The screw configuration featured a modular design to ensure effective mixing of the polymer melt. Throughout the process, all heating zones were maintained at 150 °C, the screw speed was held constant at 200 rpm, and the feed rate was set to 20 rpm. A total of five reprocessing cycles were performed for each raw material, allowing for the monitoring of property changes over successive cycles. The initial material was designated as Cycle 0, with each subsequent re-extrusion labeled as Cycle 1 through Cycle 5. This methodology enabled a comprehensive analysis of thermal and physical property variations resulting from repeated processing.

4.2.3 Preparation of Specimens for Mechanical and Optical Testing

The tensile test specimens required for mechanical strength measurements were prepared using an injection molding machine (Haitian, China) with a clamping force of 600 kN, employing a mold conforming to the ASTM D638 Type I standard. Injection molding parameters were kept constant to investigate the influence of multiple recycling cycles and processing conditions. Additionally, film samples with a thickness of 100 µm for optical property assessments were produced using a single screw blown film machine (Labtech Engineering, Thailand). All films were processed under identical conditions to ensure uniformity for accurate evaluation of optical properties.

4.2.4 Characterization and Performance Analysis

Material characterization and testing procedures were carried out using various analytical techniques. To ensure test repeatability, samples were conditioned under controlled temperature (23 °C ± 2 °C) and relative humidity (50% ± 5%) for 24–48 hours.

Mechanical properties were evaluated through tensile tests performed on a universal testing machine (Devotrans, Türkiye) in accordance with the ISO 527-3 standard. Test specimens (10 × 150 mm) were tested at a speed of 50 mm/min using a 10 kN load cell. Each test was repeated five times to determine the elastic modulus, tensile strength, and elongation at break.

Thermal properties were characterized using differential scanning calorimetry (DSC, TA Instruments Q2000, USA). Approximately 10 mg of each sample was placed in a hermetically sealed aluminum pan, heated from 20 °C to 150 °C at a rate of 10 °C/min, cooled to −20 °C, and then reheated to 150 °C. The melting temperature (Tm), crystallization temperature (T_c), enthalpy of melting (ΔH_m), and enthalpy of crystallization (ΔH_c) were recorded. The enthalpy of fusion for a fully crystalline polyethylene was taken as 293 J/g (Kong & Hay, 2003).

The melt flow behavior of the samples was evaluated using a melt flow index tester (Zwick Roell, Germany) operated at 190 °C under a constant load of 2.16 kg. Each sample was tested five times, and the average MFI values were calculated and reported.

Molecular weight distribution, including number-average molecular weight (M_n), weight-average molecular weight (M_w), and polydispersity index (PDI), was determined using gel permeation chromatography (GPC). The analysis was conducted with a Tosoh EcoSEC high-temperature GPC system equipped with a refractive index (RI) detector and a viscometer. The system was calibrated using a narrow-distribution polystyrene standard (Mw = 96,400 Da, 1.5 mg/mL). Prior to analysis, the samples were stored in solid form at room temperature and dissolved in 1,2,4-trichlorobenzene (TCB) at 145 °C, then filtered through a 0.96 µm filter. Each sample (300 µL injection

volume) was processed at a flow rate of 1 mL/min for a total analysis time of 45 minutes.

The chemical structure and functional groups were identified using Fourier transform infrared spectroscopy. The analysis was performed using a Bruker ALPHA-II (Germany), and spectra were collected in the range of 4000–450 cm^{-1}.

Spectrophotometric measurements were obtained using X-Rite Ci64 and Ci7600 (USA) instruments. Values for lightness (L*), redness (a*), yellowness (b*), and color difference (ΔE, representing the difference between reference and sample) were determined according to ASTM E308-18 using the CIE Lab D65/10° color system. Additionally, the yellowing index (ASTM E313), haze, and light transmission were measured.

For each optical parameter (haze, transmission, L*, a*, b*, and ΔE), mean and standard deviation values were calculated. One-way ANOVA was used to determine whether significant differences existed among groups. Tukey's HSD test was subsequently applied to identify pairwise differences at a significance level of $p < 0.05$.

4.3 Results and Discussion

4.3.1 Mechanical Properties

The data presented in Figure 4.1 show that the elastic modulus of BBPE is initially higher than that of PBPE (157.3 MPa versus 112.0 MPa). As the number of recycling cycles increases, the modulus of BBPE rises, reaching 203.9 MPa by Cycle 3. In contrast, the elastic modulus of PBPE increases more gradually, reaching 154.7 MPa at the same cycle. These results suggest that phenomena such as chain alignment during reprocessing and enhanced partial crystallization contribute to the modulus increase in BBPE. However, the elastic modulus of BBPE declines by Cycle 5, indicating that thermal degradation and chain scission begin to influence the material at later recycling stages (González-Aguilar et al., 2025; Saikrishnan et al., 2020).

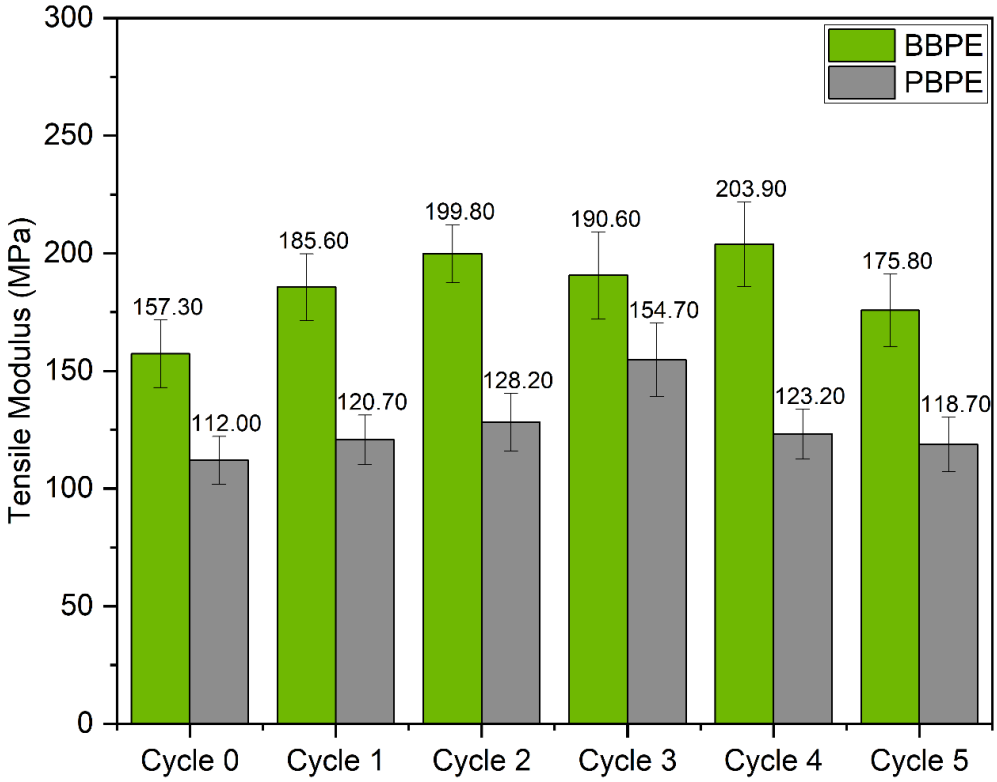

Figure 4.1: Tensile modulus of biobased polyethylene and petroleum-based polyethylene during five extrusion cycles

BBPE exhibited an initial tensile strength of 8.42 MPa (Cycle 0), which increased to 10.36 MPa by Cycle 4 (Figure 4.2). In contrast, PBPE showed a lower initial strength of 7.23 MPa and reached a maximum of 9.37 MPa, remaining consistently below that of BBPE. These results indicate that the mechanical strength of BBPE is retained throughout the recycling process due to partial crystallization and chain alignment, while PBPE exhibited a more stable but limited improvement.

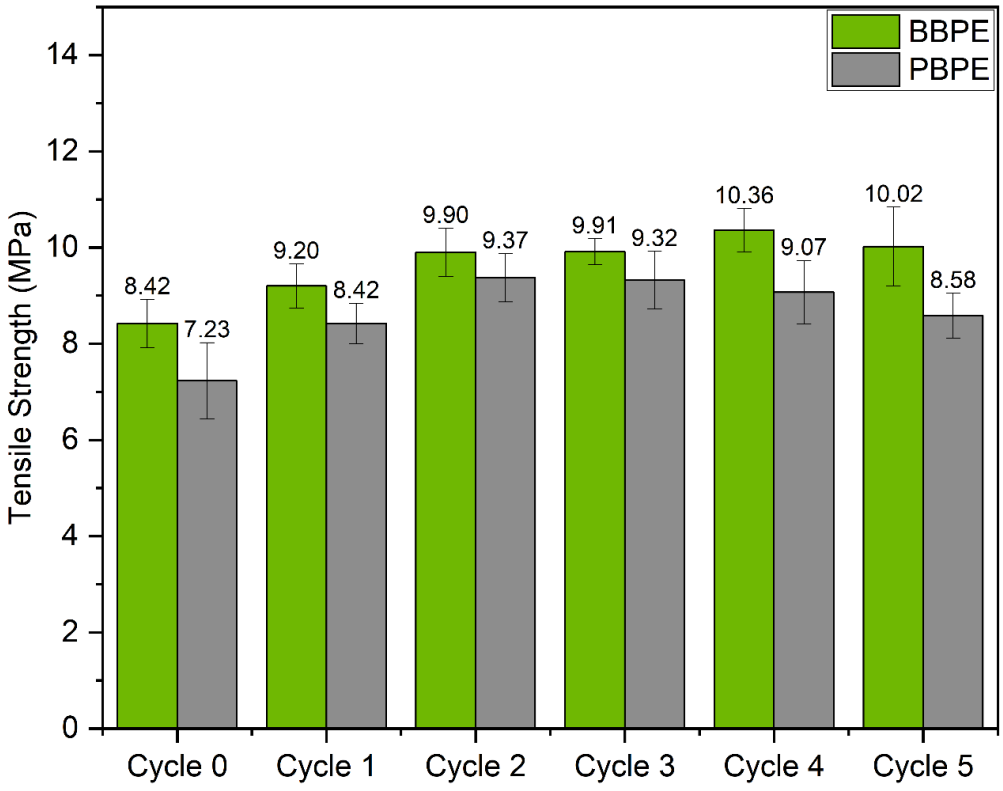

Figure 4.2: Tensile strength of biobased polyethylene and petroleum-based polyethylene during five extrusion cycles

Across all cycles, BBPE consistently exhibited lower elongation at break values compared to PBPE, with both materials displaying a decreasing trend (Figure 4.3). The initial elongation of BBPE in Cycle 0 was 107.19%, which decreased to 88.73% by Cycle 5. In contrast, PBPE showed a significantly higher initial elongation of 177.78%, which declined to 143.62% in Cycle 5. These results indicate that BBPE possesses inherently lower elasticity relative to PBPE. Although both materials experience a reduction in elongation as a result of recycling, PBPE retains higher ductility throughout the cycles.

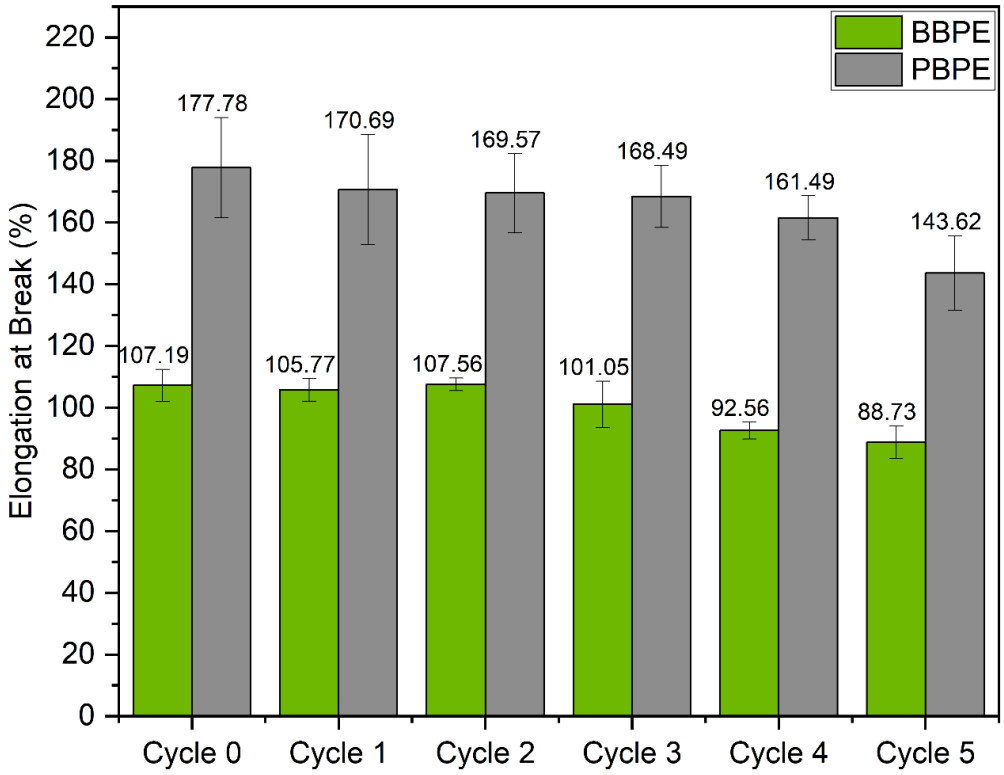

Figure 4.3: Elongation at break of biobased polyethylene and petroleum-based polyethylene during five extrusion cycles

In summary, the stiffness of BBPE initially increases, likely due to enhanced crystallinity, but then declines as chain scission becomes more pronounced. In contrast, PBPE maintains more consistent stiffness throughout the recycling cycles. Abad et al. (2004) reported that chain scission is the dominant degradation mechanism in HDPE, while crosslinking is more prevalent in LDPE. In both cases, the observed trends of decreasing elongation at break and increasing elastic modulus indicate that recycling adversely affects mechanical performance. Similarly, Saikrishnan et al. (2020) demonstrated that in PP/LDPE blends, chain scission following multiple extrusions reduced the mechanical strength of the PP phase and led to a decrease in elongation at break. Nevertheless, the crosslinking tendency in the LDPE phase does not entirely compromise the overall strength of the material, as it can contribute to increased toughness and flexibility.

4.3.2 Thermal Analysis (Differential Scanning Calorimetry)

The DSC data presented in Table 4.1 show the variations in melting temperature (Tm), crystallization temperature (T_c), enthalpy of melting (ΔH_m), enthalpy of crystallization (ΔH_c), and degree of crystallinity (χ_c) of BBPE and PBPE samples across the recycling cycles.

Table 4.1: Thermal properties of biobased polyethylene and petroleum-based polyethylene samples determined by differential scanning calorimetry

Sample	T_m (°C)	T_c (°C)	ΔH_c (J/g)	ΔH_m (J/g)	χ_c (%)
BBPEC0	113.32	97.04	79.42	69.50	23.72
BBPEC1	113.91	99.07	75.80	78.76	26.88
BBPEC2	112.71	99.61	68.84	78.93	26.94
BBPEC3	113.80	99.59	71.83	73.99	25.25
BBPEC4	112.46	99.41	79.15	71.48	24.40
BBPEC5	113.06	100.07	77.58	77.87	26.58
PBPEC0	112.78	96.80	62.92	63.14	21.55
PBPEC1	111.87	98.30	69.42	69.40	23.69
PBPEC2	111.99	98.07	61.09	63.40	21.64
PBPEC3	111.58	97.94	54.09	65.63	22.40
PBPEC4	112.78	97.68	66.23	67.70	23.11
PBPEC5	112.50	97.30	60.48	66.69	22.76

Notably, while the Tm value remained relatively constant in both materials, the Tc value in BBPE samples showed a slight increase during the recycling process, accompanied by a corresponding rise in the degree of crystallinity (χc) up to a certain point. The increase in elastic modulus and tensile strength of BBPE appears to correlate with this crystallization behavior, which is likely driven by partial chain alignment and the formation of crystalline domains during reprocessing. In contrast, PBPE exhibited a more moderate increase in tensile properties, attributed to its limited

improvement in crystallinity despite multiple cycles. However, analysis of the DSC and mechanical data of BBPE at Cycle 5 indicates that crystalline development plateaued and even slightly regressed, due to the onset of thermal degradation and chain scission. This suggests that although BBPE initially benefits from improved stiffness and strength, it may experience internal structural degradation that increases the risk of embrittlement in later cycles. Conversely, PBPE retained its higher elasticity; however, the increase in strength remained limited due to its relatively low crystallinity. When DSC and mechanical results are evaluated together, it becomes evident that chain alignment and increased crystallinity initially enhance recycling performance, but in later cycles, the dominant effects of chain scission and thermal degradation reduce the material's final properties.

Consistent with previous research on recycled polyethylene, the melting temperature remained nearly constant after multiple extrusions, as degradation primarily affects the amorphous regions rather than the crystalline domains. Meanwhile, the crystallization temperature and crystallinity of BBPE exhibited slight increases during the early cycles, indicating the formation of additional crystallites, followed by a plateau or slight decrease by Cycle 5, as degradation and chain scission became more pronounced. Abad et al. (2004) reported that repeated extrusion caused degradation mainly in the amorphous phase and at chain ends, with minimal impact on the crystalline phase, explaining why key DSC parameters such as melting temperature did not change significantly. In this study, DSC analyses confirmed that the melting temperatures of both BBPE and PBPE remained largely stable across cycles, though moderate fluctuations were observed in T_c and χ_c. These results are in agreement with findings by Jin et al. (2012), who showed that repeated extrusion of LDPE did not significantly alter the melting temperature but caused a reduction in crystallinity beyond the 40th cycle. This reduction was attributed to crosslinking and structural irregularities resulting from continued reprocessing, which partially hinder the regular packing of polymer chains.

4.3.3 Melt Flow Behavior of Biobased and Petroleum-Based Polyethylene during Recycling

The melt flow index values presented in Figure 4.4 illustrate the variations in the flow behavior of BBPE and PBPE materials across multiple cycles. MFI is a key parameter that determines a polymer's viscosity and characterizes its flow behavior during processing.

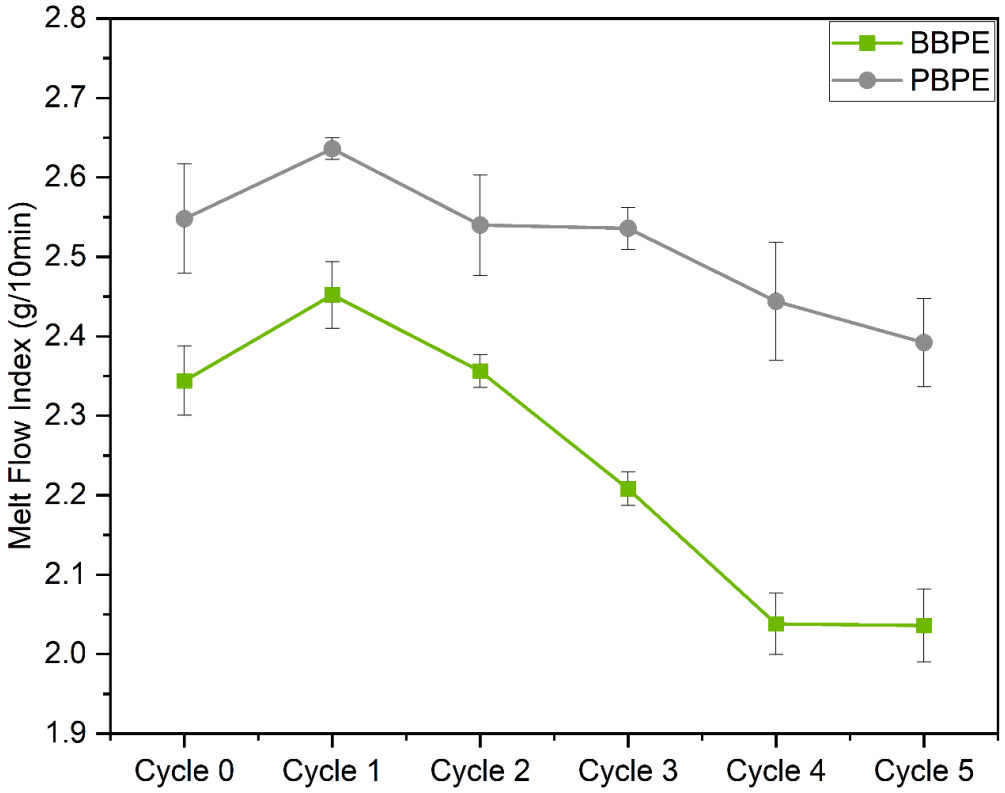

Figure 4.4: Melt-flow index of biobased polyethylene and petroleum-based polyethylene during five extrusion cycles

In Cycle 0, the MFI values of BBPE and PBPE were measured as 2.34 g/10 min and 2.55 g/10 min, respectively. The slightly lower initial viscosity of BBPE suggests reduced processability compared to PBPE. After a modest increase in Cycle 1, the MFI of BBPE showed a notable overall decline, reaching a minimum of 2.0 g/10 min by Cycle 5. This reduction indicates that chain scission and a decrease in molecular

weight occurred during recycling. As a result, the polymer's viscosity increased, diminishing its flowability due to the shortening of molecular chains (Oblak et al., 2015). Therefore, higher processing temperatures or pressures may be required for recycled BBPE.

In contrast, the MFI values of PBPE remained relatively stable throughout the recycling cycles. The value increased slightly to 2.6 g/10 min in Cycle 1 and then gradually decreased to 2.4 g/10 min by Cycle 5. This behavior suggests that PBPE underwent less chain scission and retained a more stable molecular weight distribution compared to BBPE. The consistent flow behavior of PBPE provides a processing advantage by maintaining its melt processability over multiple recycling steps. In comparison, the approximately 14% reduction in BBPE's MFI by Cycle 5 supports the observation that BBPE experienced more significant structural changes during recycling, likely involving a greater degree of crosslinking.

Previous studies also reported a decrease in MFI for reprocessed LDPE due to crosslinking, while an increase in MFI was observed in HDPE as a result of chain scission. These contrasting trends in MFI are largely dependent on the chemical structure of the polyethylene and the dominant degradation mechanism. Similar findings were reported by Jin et al. (2012) in their study on low-density polyethylene, which showed that up to 100 repeated extrusions resulted in significant reductions in MFI, particularly beyond the 40th cycle. This decline was primarily attributed to increased crosslinking, which restricts chain mobility and reduces flow capacity. These results confirm that the MFI of BBPE deteriorates more rapidly during recycling compared to PBPE. The greater reduction in BBPE's MFI suggests a higher degree of degradation, likely to involve both crosslinking and chain scission. In contrast, PBPE retained its flowability to a greater extent, indicating less severe structural changes. The reduced MFI of BBPE may cause processing difficulties in molding, extrusion, and film production due to increased viscosity. In practical applications, recycled BBPE may require higher temperatures or pressures to achieve sufficient melt flow. Conversely, the stable MFI values of PBPE suggest improved fluidity and ease of processing over multiple recycling cycles. Nevertheless, considering the environmental benefits of BBPE, future research should explore ways to enhance its MFI performance through the use of chain stabilizers or suitable additives.

4.3.4 Molecular Weight Distribution and Degradation Behavior via Gel Permeation Chromatography

The molecular weight distribution and intrinsic viscosity (IV) of the polymer samples were determined using GPC analysis. The results are summarized in Table 4.2. The number average molecular weight (M_n) represents the arithmetic mean of the molecular weight distribution, while the weight average molecular weight (M_w) gives greater emphasis to larger molecules. The polydispersity index (PDI), calculated as M_w/M_n, indicates the breadth of the molecular weight distribution, with higher values signifying broader distributions. Intrinsic viscosity (IV) reflects the hydrodynamic volume of polymer chains in solutions and is related to molecular weight and chain conformation.

Table 4.2: Molecular weight distribution of biobased polyethylene and petroleum-based polyethylene samples from gel permeation chromatography analysis (mean values, CV: coefficient of variation % in parentheses)

Sample	Mw (g/mol)	PDI (Mw/Mn)	IV (dL/g)
BBPEC0	155,105 (1.79%)	6.29	0.781
BBPEC5	126,288 (1.18%)	4.13	0.690
PBPEC0	169,574 (1.52%)	3.76	0.812
PBPEC5	155,113 (0.56%)	3.73	0.802

As expected, molecular weight decreased due to thermal exposure and shear stress during reprocessing. Initial measurements showed that PBPEC0 exhibited the highest weight average molecular weight (169,574 g/mol), indicating longer polymer chains. In contrast, BBPEC0 displayed the highest polydispersity index (PDI = 6.29), reflecting a broader molecular weight distribution. A gradual decline in M_w was observed with increasing extrusion cycles, with decreases of approximately 8.5% and 18.6% recorded for PBPEC5 and BBPEC5, respectively. Meanwhile, intrinsic viscosity values remained relatively unchanged, suggesting that the branching and entanglement structures of the polymer chains were largely preserved.

GPC analyses revealed that although a significant reduction in molecular weight occurred in BBPE samples due to chain scission, the formation of high molecular weight fractions resulting from crosslinking may also have taken place during repeated extrusion. However, the PDI of BBPE at Cycle 5 was lower than its initial value, indicating that the molecular weight distribution became narrower as extreme high or low molecular weight chains were diminished. These findings suggest that chain scission was the dominant degradation mechanism within the first five cycles, although a limited extent of crosslinking may have occurred concurrently. In the case of PBPE, the decrease in M_w was less significant, and the PDI remained relatively stable (around 3.7), implying a more uniform degradation pattern.

Jin et al. (2012) reported that repeated mechanical recycling of LDPE led to simultaneous chain scission and crosslinking, resulting in an increase in PDI after the 50th cycle due to structural degradation. In contrast, BBPE in the present study exhibited a reduction in molecular weight after just five cycles, along with a decrease in PDI, indicating that chain scission was the predominant degradation mechanism, with minimal contribution from crosslinking. PBPE, on the other hand, maintained a more stable PDI throughout the recycling process, suggesting a more consistent and uniform molecular weight degradation behavior.

It is well-established in polymer science that molecular weight and its distribution are critical factors influencing mechanical properties. Longer polymer chains improve load transfer under tensile stress, strengthen intermolecular interactions, and enhance overall mechanical performance. In the present study, although the reduction in M_w contributed to diminished elongation capacity, PBPE samples exhibited a more stable molecular structure than BBPE, showing less degradation across the recycling cycles. The greater loss of M_w observed in BBPE correlated with a more pronounced reduction in elongation, resulting in increased brittleness. In contrast, the smaller M_w reduction in PBPE helped preserve ductility, reinforcing the relationship between GPC results and mechanical behavior.

4.3.5 Chemical Structure Analysis by Fourier Transform Infrared Spectroscopy

The FTIR spectra (Figure 4.5) reveal notable differences between the initial (Cycle 0) and final (Cycle 5) states of both materials. The broad bands observed particularly in the 3000-3500 cm^{-1} range (3395, 3350, and 3188 cm^{-1} in BBPE; 3364 and 3188 cm^{-1} in PBPE) correspond to -OH/N-H stretching vibrations resulting from moisture, hydroxyl groups, or potential stabilizer/antioxidant presence in the polymer. The alteration in the intensity and position of these bands in Cycle 5 samples is attributed to the partial depletion or transformation of antioxidants or variations in the polymer's surface/total moisture content under high-temperature and multiple extrusion conditions (Gulmine et al., 2002).

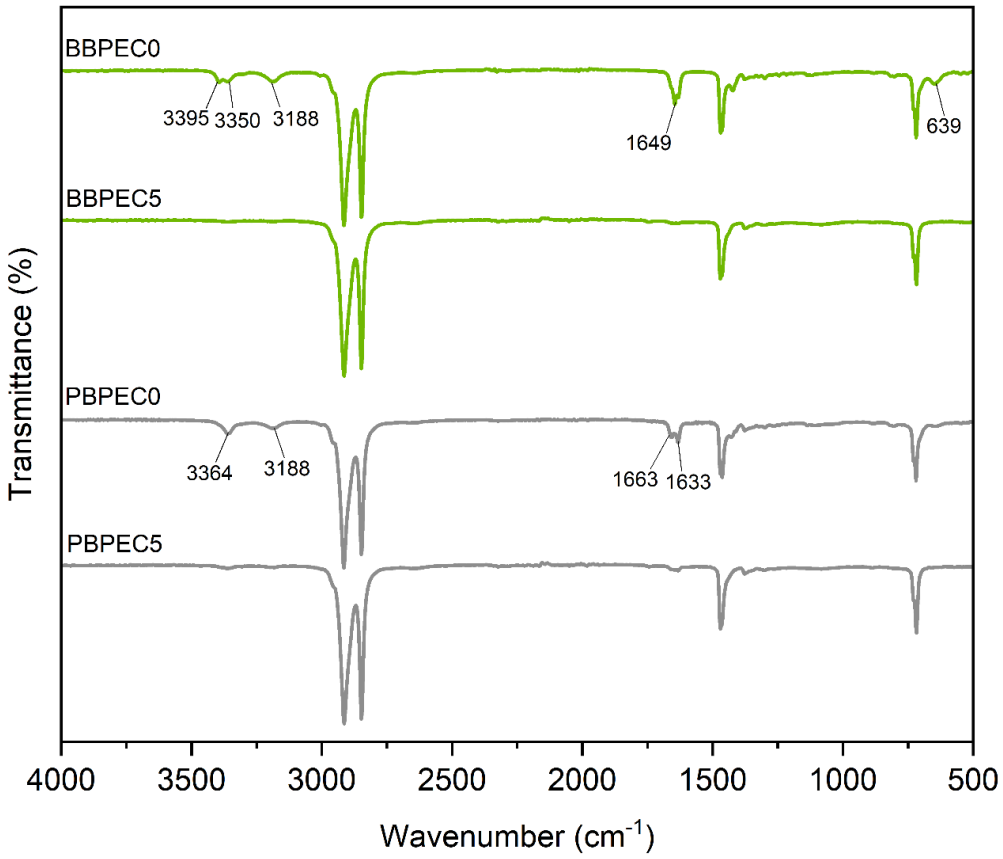

Figure 4.5: Fourier transform infrared spectroscopy spectra of biobased polyethylene and petroleum-based polyethylene for Cycle 0 and Cycle 5

Furthermore, the 1649 cm^{-1} band and the peak near 639 cm^{-1} in BBPE samples, as well as the 1663-1633 cm^{-1} band in PBPE samples, are noteworthy. Peaks in these regions generally indicate vibrations from carbonyl (C=O) or unsaturated bonds (C=C), or the existence of adducts (such as additives or oxidation products). The increase or change in the position of these peaks in the Cycle 5 spectra suggests the formation of new functional groups due to oxidative degradation and chain breakage induced by multiple extrusions (Hirsch et al., 2017). Notably, the prominent peaks in BBPE, consistent with prior mechanical and rheological findings, indicate that BBPE is more susceptible to oxidative and structural changes compared to PBPE.

The reduction or disappearance of antioxidant-related peaks suggests that these additives are significantly depleted or transformed during repeated processing under high-temperature and shear conditions (Abad et al., 2004). The weakening of the peaks

associated with antioxidants (primarily located in the O–H and N–H stretching regions), observed in the Cycle 5 FTIR spectra, indicates that the antioxidants have largely fulfilled their stabilizing function and were subsequently degraded or eliminated from the system. Although these changes were more pronounced in BBPE, the findings imply that PBPE may also undergo similar degradation processes during extended recycling.

4.3.6 Analysis of Optical Properties in Recycled Biobased and Petroleum-Based Polyethylene

The assessment of optical properties is essential for evaluating the material's performance in both aesthetic and functional contexts. Parameters such as haze, light transmission, and color demonstrate notable variations in BBPE and PBPE samples across different cycles (Table 4.3). Furthermore, the total color difference (ΔE) values are a significant parameter in determining the impact of recycling cycles on optical attributes. Therefore, the Cycle 0 sample of each polymer was utilized as a reference in comparison with its subsequent cycles.

Table 4.3: Optical properties of biobased polyethylene and petroleum-based polyethylene samples

Sample	Haze (%)	Transmission (%)	L* (Lightness)	a* (Redness)	b* (Yellowness)	ΔE
BBPEC0	14.07 ± 0.26^{a}	87.76 ± 3.65^{a}	55.26 ± 1.26^{a}	0.94 ± 0.01^{a}	2.49 ± 0.07^{a}	-
BBPEC1	14.71 ± 0.70^{a}	87.49 ± 0.93^{a}	54.93 ± 2.16^{a}	0.90 ± 0.01^{a}	2.69 ± 0.02^{a}	0.38 ± 0.02^{a}
BBPEC2	15.61 ± 0.57^{a}	85.47 ± 0.78^{b}	55.03 ± 0.55^{a}	0.92 ± 0.03^{a}	2.79 ± 0.14^{a}	0.38 ± 0.02^{a}
BBPEC3	19.03 ± 0.57^{b}	84.67 ± 0.78^{b}	55.18 ± 1.42^{a}	1.02 ± 0.02^{b}	3.48 ± 0.13^{b}	0.99 ± 0.03^{b}
BBPEC4	22.26 ± 0.17^{c}	83.77 ± 1.27^{c}	55.18 ± 1.63^{a}	1.03 ± 0.01^{b}	3.50 ± 0.16^{b}	1.02 ± 0.04^{b}
BBPEC5	22.71 ± 0.18^{c}	83.69 ± 2.20^{c}	54.35 ± 0.13^{a}	1.03 ± 0.03^{b}	4.01 ± 0.18^{c}	1.77 ± 0.05^{c}
PBPEC0	14.76 ± 0.04^{a}	88.91 ± 1.94^{d}	55.98 ± 1.70^{b}	1.29 ± 0.01^{c}	3.41 ± 0.10^{b}	-
PBPEC1	14.91 ± 0.65^{a}	88.01 ± 1.28^{a}	56.28 ± 0.48^{b}	1.25 ± 0.06^{c}	3.87 ± 0.18^{c}	0.55 ± 0.02^{d}
PBPEC2	16.22 ± 0.49^{a}	86.68 ± 2.62^{b}	56.56 ± 0.18^{b}	1.35 ± 0.02^{d}	4.11 ± 0.02^{c}	0.91 ± 0.03^{e}
PBPEC3	20.41 ± 0.72^{b}	85.72 ± 0.60^{b}	56.63 ± 2.69^{b}	1.45 ± 0.05^{d}	4.26 ± 0.04^{c}	1.08 ± 0.03^{e}
PBPEC4	21.22 ± 0.02^{c}	85.81 ± 1.25^{b}	57.00 ± 2.75^{b}	1.39 ± 0.02^{d}	4.65 ± 0.01^{d}	1.21 ± 0.04^{f}
PBPEC5	22.13 ± 1.22^{c}	85.51 ± 1.55^{b}	56.73 ± 2.29^{b}	1.25 ± 0.03^{c}	4.72 ± 0.08^{d}	1.51 ± 0.05^{f}

Mean values ± standard deviation (n=5). Different superscript letters indicate statistically significant differences ($P < 0.05$) as determined by ANOVA and Tukey's HSD test.

In BBPE samples, haze values increased progressively with the number of recycling cycles. The haze value, initially measured as 14.07% in BBPEC0, rose to 22.71% by Cycle 5. This increase is likely due to microstructural changes within the material, including increased surface roughness and the formation of irregular crystalline regions caused by chain scission. The depletion of antioxidants during repeated extrusion may also accelerate oxidative degradation and morphological disruption, thereby contributing to increased haze and reduced optical clarity (Lagaron et al., 2001; Mahendran et al., 2008). In parallel, the rise in melt viscosity observed in BBPE may enhance light scattering and diminish transparency by deteriorating surface uniformity.

PBPE samples also exhibited a low initial haze level that increased with successive recycling cycles. Haze values rose from 14.76% in PBPEC0 to 22.13% in PBPEC5. Compared to PBPE, BBPE showed a slightly more pronounced haze increase after five cycles, suggesting greater light scattering caused by degradation by-products in BBPE.

Light transmission decreased in both materials as the number of cycles increased. In BBPE, the transmittance dropped from 87.76% in Cycle 0 to 83.69% in Cycle 5. PBPE began with a slightly higher initial transmittance of 88.91%, which declined to 85.51% after five cycles of reprocessing.

An analysis of the color parameters (L*, a*, and b*) revealed that in BBPE samples, the L* value decreased with increasing recycling cycles, while the a* and b* values increased. The reduction in L* indicates a loss of brightness, which can be attributed to surface oxidation and changes in crystallinity. Increases in a* and b* suggest a shift toward red and yellow tones, respectively. In particular, the b* value rose from 2.49 in BBPEC0 to 4.01 in BBPEC5, indicating pronounced yellowing due to oxidative degradation.

In PBPE samples, the L* value remained relatively stable throughout the recycling process, while the b* value increased to 4.72 by Cycle 5. This final b* value was slightly higher than that measured in BBPE. Although PBPE initially exhibited greater yellowness, likely due to its additive content or the inherent coloration of the base polymer, its color remained more consistent throughout the recycling cycles. The increase in b* in PBPE is attributed to additive degradation and the formation of

oxidation products; however, both the rate and extent of color change were lower than in BBPE.

The total color difference values provide a quantitative measure of the effects of recycling on the optical properties of the materials. In BBPE, the ΔE value increased to 1.77 in Cycle 5, indicating a noticeable color deviation. This level of change may present limitations in applications where color uniformity is critical. In comparison, PBPE exhibited a ΔE value of 1.51 in Cycle 5, suggesting that it maintained more consistent color performance throughout the recycling cycles.

The images of the granules in Figure 4.6 show that both BBPEC0 and PBPEC0 samples initially exhibited a bright, uniform, and white appearance. After five recycling cycles, however, noticeable yellowing and surface haze were observed in both materials.

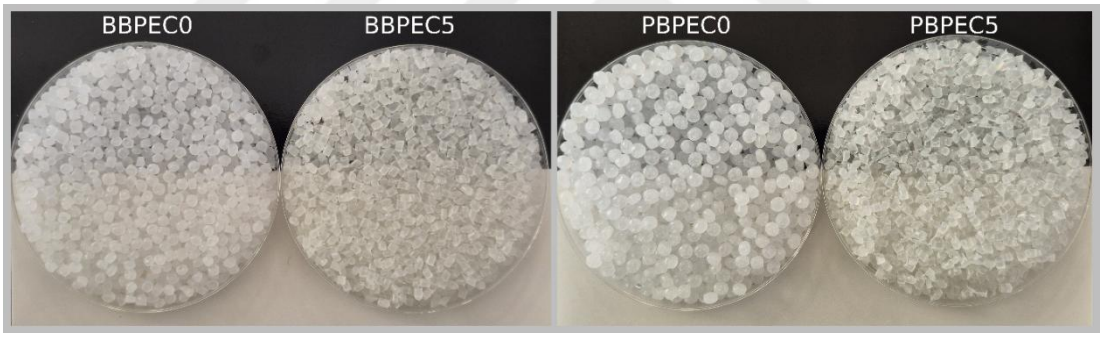

Figure 4.6: Photographs of BBPE and PBPE pellets before and after five extrusion cycles showing yellowing and surface changes

This visual change is supported by the yellowness index (YI) values presented in Figure 4.7. The YI for BBPE increased from an initial value of 8.49 to 13.10 after five extrusion cycles. For PBPE, the initial YI was 11.43 and increased to 14.88 in Cycle 5. These increases indicate that both materials are subject to oxidative degradation during recycling, with the decomposition of stabilizing additives playing a significant role in the discoloration process.

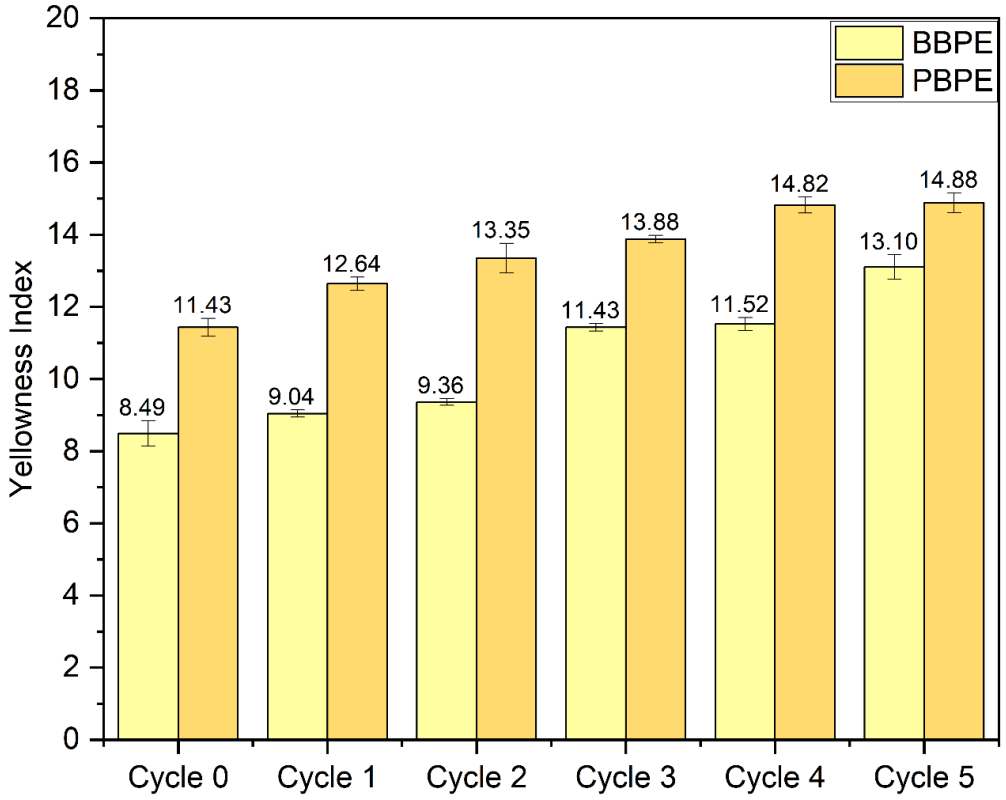

Figure 4.7: Yellowness index of biobased polyethylene and petroleum-based polyethylene during five extrusion cycles

Although BBPE initially exhibited a lower yellowness index compared to PBPE, its percentage increase over five recycling cycles was considerably higher, reaching 54.3% compared to 30.2% for PBPE. This result suggests that BBPE is more prone to oxidative degradation and undergoes a greater loss of stabilizer effectiveness over time. The effect became particularly evident in Cycle 5, where the rapid increase in yellowing was accompanied by visible surface deterioration.

In contrast, although PBPE started with a higher initial yellowness, it showed a smaller percentage increase, indicating that it preserved its optical properties more effectively throughout the recycling process. This stability implies that PBPE experienced less degradation overall, which contributed to maintaining its structural and optical integrity in long-term applications.

These findings underscore the influence of repeated recycling on both the aesthetic and functional performance of polyethylene materials. They also highlight the

importance of implementing appropriate stabilization strategies based on the intended end-use of the product.

4.4 Conclusion

This study examined the performance differences between biobased polyethylene (BBPE) and petroleum-based polyethylene (PBPE) over multiple recycling cycles. Although BBPE initially exhibited a higher elastic modulus, its mechanical strength declined during recycling due to progressive chain scission. While PBPE exhibited more stable mechanical properties across cycles, BBPE retained higher absolute tensile strength in all cycles despite a sharper decline, highlighting different degradation dynamics. Thermal analysis indicated that the degree of crystallinity in BBPE increased in the early cycles, but degradation became the dominant mechanism in later stages. PBPE, by comparison, demonstrated more stable thermal behavior, which offers advantages for long-term use.

From a rheological perspective, BBPE displayed a decreasing melt flow index, while PBPE maintained a relatively consistent MFI and preserved its processability. BBPE also exhibited a more rapid decrease in molecular weight, contributing to increased brittleness during reprocessing. FTIR analysis confirmed that BBPE was more prone to oxidative degradation, whereas PBPE showed greater resistance, likely due to the presence of stabilizing additives. In terms of optical characteristics, BBPE became increasingly hazy and yellowed with repeated cycles, while PBPE retained comparatively better clarity and color stability.

From an industrial perspective, the renewable origin of BBPE offers a distinct sustainability advantage. However, its accelerated degradation during recycling poses challenges for long-term usability and highlights the need for effective stabilization approaches to support repeated processing. In contrast, PBPE demonstrated more consistent mechanical and optical properties throughout recycling, while BBPE, despite its higher initial clarity, exhibited more rapid deterioration. These results underscore the importance of developing tailored stabilization strategies for BBPE, while also reaffirming the environmental drawbacks associated with the continued use of fossil-based PBPE.

Overall, BBPE and PBPE exhibit distinct recycling behaviors. BBPE, with lower initial discoloration but a higher degradation rate, may be more suitable for short-term applications where visual appearance is critical. PBPE, on the other hand, maintains greater structural and optical stability, making it a more appropriate choice for applications requiring long-term durability.

It is important to note that this study was conducted under controlled laboratory conditions involving five consecutive extrusion cycles. Future research should address the effects of real-world recycling variables such as contamination, environmental exposure, and the role of different stabilizer systems on the recyclability and long-term performance of both materials.

Chapter 5

5 General Conclusion

This doctoral thesis presented a multi-faceted investigation into the properties and processing of biobased polyethylene in comparison to petroleum-based polyethylene, encompassing masterbatch preparation, the use of natural pigments, and the evaluation of recycling performance. The collective findings of this research contribute significantly to a deeper understanding of the potential and challenges associated with biobased polymers in the pursuit of sustainable plastic materials. By integrating experimental results across these three domains, the study provides a coherent framework for assessing both the technical feasibility and environmental viability of substituting conventional polyethylene with biobased alternatives.

The first phase of the research examined the optimization of pigment dispersion within masterbatches produced using both biobased and petroleum-based polyethylene as carrier resins. A design of experiments approach based on the Taguchi method was employed to systematically assess the effects of wax type, mixing time, screw speed, and extrusion temperature on color strength, dispersion efficiency, and filter pressure performance. Among the tested conditions, micronized waxes significantly improved pigment wetting and distribution, resulting in higher color strength and substantially lower filter pressure values, particularly in BBPE systems. The influence of processing parameters was further supported by statistical analysis, revealing that wax type and screw speed were the most critical factors in determining pigment performance.

Mechanical testing of the masterbatches showed that improved dispersion could be achieved without compromising stiffness, although a moderate decrease in elongation at break was observed due to pigment-induced rigidity. Scanning electron microscopy confirmed that better-dispersed pigments were associated with fewer agglomerates and a more uniform matrix, particularly in formulations processed at lower temperatures

and higher screw speeds. Additionally, FTIR spectra demonstrated that optimized conditions minimized thermal degradation during processing. From a sustainability perspective, cradle-to-gate life cycle analysis indicated that the use of BBPE-based masterbatches offered a carbon savings of approximately 5.2 kg CO_2 eq per kilogram of product compared to their PBPE counterparts. These findings collectively support the technical and environmental feasibility of producing high-quality, color-controlled masterbatches based on biobased polyethylene.

The second phase of the research focused on the development of sustainable food packaging films by incorporating natural plant-based pigments into biobased polyethylene matrices. Pigments extracted from madder, pomegranate, walnut, yellow mignonette, and Aleppo oak were selected for their vivid coloration, biodegradability, and historical use in natural dyeing. These additives served as renewable alternatives to synthetic colorants and aligned with the broader objective of reducing environmental toxicity in packaging materials. While their incorporation resulted in desirable improvements such as enhanced opacity, reduced blocking force, and lower coefficients of friction, a trade-off was observed in mechanical performance. Tensile testing revealed a consistent reduction in elongation at break, primarily attributed to particle rigidity and limited interfacial adhesion between the pigment particles and the polymer matrix.

Optical property measurements demonstrated that the films exhibited a wide range of visual outcomes, from translucent to nearly opaque, depending on the pigment type and dispersion quality. Yellow mignonette-based films, for example, achieved the highest haze and opacity levels, making them ideal candidates for light-sensitive packaging applications. Conversely, Aleppo oak formulations presented a balanced combination of moderate stiffness and surface slip, enhancing processability and handling. Scanning electron microscopy and particle size analysis further confirmed that pigment morphology and particle size distribution critically influenced dispersion behavior and film uniformity. These findings underscore the importance of pigment selection and reinforce the need for compatibilization strategies or surface functionalization techniques to minimize brittleness while preserving visual appeal and sustainability.

The third phase of the study evaluated the recyclability of biobased and petroleum-based polyethylene by subjecting both materials to five successive extrusion cycles that simulated industrial reprocessing. A wide range of material characteristics, including mechanical strength, melt flow behavior, thermal stability, optical properties, and chemical structure, were systematically monitored after each cycle. The results showed that both materials experienced degradation over time, but the degree and nature of the deterioration differed substantially. Biobased polyethylene exhibited a more rapid decline in molecular weight and a sharper increase in melt flow index, indicating a higher sensitivity to chain scission and a more significant loss in viscosity under thermal and shear stress.

These molecular changes were reflected in macroscopic properties, including reduced elongation at break and an increase in haze and yellowing. In contrast, petroleum-based polyethylene maintained greater stability in mechanical and rheological behavior throughout the recycling process. Although it exhibited a slightly higher initial yellowness, it preserved tensile performance and visual clarity more effectively across cycles. FTIR analysis revealed more pronounced oxidative degradation in BBPE, although this observation may also be influenced by differences in antioxidant systems used in the commercial formulations, rather than the biobased nature of the polymer itself. Differential scanning calorimetry also indicated variations in crystallinity and crystallization temperature, particularly in the later cycles. Despite these challenges, the recyclability of BBPE remains technically feasible. However, enhancing its stability may require the use of renewable antioxidant packages or mild chain-extending agents to preserve long-term performance.

Taken together, the findings of this thesis demonstrate that biobased polyethylene represents a promising alternative to petroleum-based polyethylene, particularly for applications focused on reducing environmental impact. The material was evaluated across three critical domains, namely masterbatch preparation, film development with natural pigments, and mechanical recycling. Under optimized processing conditions, BBPE exhibited favorable characteristics such as high dispersion quality, functional film performance, and a significantly lower carbon footprint compared to its fossil-based counterpart. However, it also revealed limitations, including reduced mechanical durability and increased susceptibility to oxidative degradation during

repeated processing. These drawbacks were evident in the form of molecular weight loss, declining elongation at break, and more pronounced color instability.

In contrast, petroleum-based polyethylene maintained superior stability in its mechanical and thermal properties during recycling, preserving tensile strength and visual clarity over multiple cycles. Despite this advantage, its environmental burden due to fossil origin remains a key concern. The results also highlighted that upstream formulation choices, such as the type of wax, screw speed, and pigment properties, played a decisive role in determining overall material performance. These factors directly affected the efficiency of pigment dispersion, filtration pressure, and film surface behavior. Consequently, while biobased polyethylene has the potential to satisfy performance requirements in targeted applications, future improvements in formulation strategies, additive systems, and processing design will be necessary to enhance its long-term viability.

The outcomes of this thesis provide a foundation for advancing the industrial application of biobased polyethylene through targeted process optimization and material design strategies. To fully assess recyclability under realistic conditions, future studies should replicate field-level variables such as mixed polymer waste streams, environmental aging, and variable residence times in extrusion. These factors are expected to influence oxidative degradation, chain scission, and optical stability in ways that differ from laboratory conditions. In addition, the mechanical fragility introduced by natural pigments indicates the need for compatibilization approaches that can reinforce interfacial bonding. Potential methods include surface modification of pigment particles, reactive extrusion using graft copolymers, or the use of renewable plasticizers to balance opacity with flexibility.

Furthermore, the performance of biobased masterbatches and films should be validated under full-scale production scenarios, including blown film and cast film lines operating at industrial throughput levels. Such validation would allow for a better understanding of pigment dispersion dynamics, energy consumption, and material yield under commercial processing parameters. The accelerated oxidative degradation observed in biobased polyethylene also highlights the necessity of formulating improved stabilization systems, preferably using bio-derived antioxidants or mild chain extenders to preserve molecular integrity during repeated use. Finally, an

integrated cradle-to-grave sustainability assessment should be incorporated into future work. This includes evaluating not only greenhouse gas emissions but also resource efficiency, end-of-life options, and the displacement ratio of recycled versus virgin polymer. Together, these recommendations can support the development of durable, high-performance, and environmentally responsible polyethylene products that meet both industrial standards and sustainability goals.

References

Abad, M. J., Ares, A., Barral, L., Cano, J., Díez, F. J., García-Garabal, S., López, J., & Ramírez, C. (2004). Effects of a mixture of stabilizers on the structure and mechanical properties of polyethylene during reprocessing. *Journal of Applied Polymer Science*, *92*(6). https://doi.org/10.1002/app.20420

Agnhage, T., Perwuelz, A., & Behary, N. (2016). Eco-innovative coloration and surface modification of woven polyester fabric using bio-based materials and plasma technology. *Industrial Crops and Products*, *86*. https://doi.org/10.1016/j.indcrop.2016.04.016

Agrawal, P., Araújo, A. P. M., Brito, G. F., Cavalcanti, S. N., Alves, A. M., Freitas, D. M. G., & Mélo, T. J. A. (2021). Rheological and Mechanical Properties of Poly(lactic acid)/Bio-Based Polyethylene/Clay Biocomposites Containing Montmorillonite and Vermiculite Clays. *Journal of Polymers and the Environment*, *29*(6). https://doi.org/10.1007/s10924-020-02015-z

Aguado, R., Espinach, F. X., Vilaseca, F., Tarrés, Q., Mutjé, P., & Delgado-Aguilar, M. (2022). Approaching a Zero-Waste Strategy in Rapeseed (Brassica napus) Exploitation: Sustainably Approaching Bio-Based Polyethylene Composites. *Sustainability (Switzerland)*, *14*(13). https://doi.org/10.3390/su14137942

Ali, A., Chen, Y., Liu, H., Yu, L., Baloch, Z., Khalid, S., Zhu, J., & Chen, L. (2019). Starch-based antimicrobial films functionalized by pomegranate peel. *International Journal of Biological Macromolecules*, *129*. https://doi.org/10.1016/j.ijbiomac.2018.09.068

AlMaadeed, M. A., Labidi, S., Krupa, I., & Ouederni, M. (2015). Effect of waste wax and chain structure on the mechanical and physical properties of

polyethylene. *Arabian Journal of Chemistry*, *8*(3). https://doi.org/10.1016/j.arabjc.2014.01.006

Alsadi, J. (2021). Experimental assessment of pigment dispersion in compounding of plastics: Rheological characterization at the crossover points. *Materials Today: Proceedings*, *45*. https://doi.org/10.1016/j.matpr.2021.01.014

Aman Mohammadi, M., Ahangari, H., Mousazadeh, S., Hosseini, S. M., & Dufossé, L. (2022). Microbial pigments as an alternative to synthetic dyes and food additives: a brief review of recent studies. In *Bioprocess and Biosystems Engineering* (Vol. 45, Issue 1). https://doi.org/10.1007/s00449-021-02621-8

Andrew, F. P., & Ajibade, P. A. (2018a). Synthesis, characterization and anticancer studies of bis-(N-methyl-1-phenyldithiocarbamato) Cu(II), Zn(II), and Pt(II) complexes: single crystal X-ray structure of the copper complex. *Journal of Coordination Chemistry*, *71*(16–18), 2776–2786. https://doi.org/10.1080/00958972.2018.1489537

Andrew, F. P., & Ajibade, P. A. (2018b). Synthesis, characterization and anticancer studies of bis-(N-methyl-1-phenyldithiocarbamato) Cu(II), Zn(II), and Pt(II) complexes: single crystal X-ray structure of the copper complex. *Journal of Coordination Chemistry*, *71*(16–18), 2776–2786. https://doi.org/10.1080/00958972.2018.1489537

Angelini, L. G., Bertoli, A., Rolandelli, S., & Pistelli, L. (2003). Agronomic potential of Reseda luteola L. as new crop for natural dyes in textiles production. *Industrial Crops and Products*, *17*(3). https://doi.org/10.1016/S0926-6690(02)00099-7

Ardila-Leal, L. D., Poutou-Piñales, R. A., Pedroza-Rodríguez, A. M., & Quevedo-Hidalgo, B. E. (2021). A brief history of colour, the environmental impact of synthetic dyes and removal by using laccases. In *Molecules* (Vol. 26, Issue 13). https://doi.org/10.3390/molecules26133813

Awaja, F., Gilbert, M., Kelly, G., Fox, B., & Pigram, P. J. (2009). Adhesion of polymers. In *Progress in Polymer Science (Oxford)* (Vol. 34, Issue 9). https://doi.org/10.1016/j.progpolymsci.2009.04.007

Badia, J. D., Gil-Castell, O., & Ribes-Greus, A. (2017). Long-term properties and end-of-life of polymers from renewable resources. In *Polymer Degradation and Stability* (Vol. 137). https://doi.org/10.1016/j.polymdegradstab.2017.01.002

Bajpai, P. (2019). Environmental impact of biobased polymers. In *Biobased Polymers*. https://doi.org/10.1016/b978-0-12-818404-2.00007-2

Banihani, S., Al-Oqla, F. M., & Mutawe, S. (2021). Mechanical performance investigation of lignocellulosic coconut and pomegranate / LDPE biocomposite green materials. *Journal of the Mechanical Behavior of Materials*, *30*(1). https://doi.org/10.1515/jmbm-2021-0026

Barbas, J. M., Machado, A. V., & Covas, J. A. (2014). Processing Conditions Effect on Dispersion Evolution in a Twin-Screw Extruder: Polypropylene-Clay Nanocomposites. *Chemical Engineering and Technology*, *37*(2). https://doi.org/10.1002/ceat.201300303

Bardestani, R., Patience, G. S., & Kaliaguine, S. (2019). Experimental methods in chemical engineering: specific surface area and pore size distribution measurements—BET, BJH, and DFT. In *Canadian Journal of Chemical Engineering* (Vol. 97, Issue 11). https://doi.org/10.1002/cjce.23632

Bardet, R., Belgacem, M. N., & Bras, J. (2013). Different strategies for obtaining high opacity films of MFC with TiO2 pigments. *Cellulose*, *20*(6). https://doi.org/10.1007/s10570-013-0025-1

Bechtold, T., & Mussak, R. (2009). Handbook of Natural Colorants. In *Handbook of Natural Colorants*. https://doi.org/10.1002/9780470744970

Belboom, S., & Léonard, A. (2016). Does biobased polymer achieve better environmental impacts than fossil polymer? Comparison of fossil HDPE and

biobased HDPE produced from sugar beet and wheat. *Biomass and Bioenergy*, *85*. https://doi.org/10.1016/j.biombioe.2015.12.014

Benavides, P. T., Lee, U., & Zarè-Mehrjerdi, O. (2020). Life cycle greenhouse gas emissions and energy use of polylactic acid, bio-derived polyethylene, and fossil-derived polyethylene. *Journal of Cleaner Production*, *277*. https://doi.org/10.1016/j.jclepro.2020.124010

Bener, M., Özyürek, M., Güçlü, K., & Apak, R. (2010). Polyphenolic contents of natural dyes produced from industrial plants assayed by HPLC and novel spectrophotometric methods. *Industrial Crops and Products*, *32*(3). https://doi.org/10.1016/j.indcrop.2010.06.020

Bigger, S. W., & Delatycki, O. (1989). The effects of pigments on the photostability of polyethylene. *Journal of Materials Science*, *24*(6). https://doi.org/10.1007/BF02385404

Blanco, I., Cicala, G., Latteri, A., Saccullo, G., El-Sabbagh, A. M. M., & Ziegmann, G. (2017). Thermal characterization of a series of lignin-based polypropylene blends. *Journal of Thermal Analysis and Calorimetry*, *127*(1). https://doi.org/10.1007/s10973-016-5596-2

Boronat, T., Fombuena, V., Garcia-Sanoguera, D., Sanchez-Nacher, L., & Balart, R. (2015). Development of a biocomposite based on green polyethylene biopolymer and eggshell. *Materials and Design*, *68*. https://doi.org/10.1016/j.matdes.2014.12.027

Bos, H. L., Meesters, K. P. H., Conijn, S. G., Corré, W. J., & Patel, M. K. (2012). Accounting for the constrained availability of land: A comparison of bio-based ethanol, polyethylene, and PLA with regard to non-renewable energy use and land use. *Biofuels, Bioproducts and Biorefining*, *6*(2). https://doi.org/10.1002/bbb.1320

Buccella, M., Dorigato, A., Rizzola, F., Caldara, M., & Fambri, L. (2018). Influence of the Processing Parameters on the Dispersion and Coloration

Behavior of a Halogenated Copper Phthalocyanine-Based Masterbatch. *Advances in Polymer Technology*, *37*(3). https://doi.org/10.1002/adv.21721

Burelo, M., Hernández-Varela, J. D., Medina, D. I., & Treviño-Quintanilla, C. D. (2023). Recent developments in bio-based polyethylene: Degradation studies, waste management and recycling. In *Heliyon* (Vol. 9, Issue 11). https://doi.org/10.1016/j.heliyon.2023.e21374

Calabrò, E., & Magazù, S. (2013). Demicellization of Polyethylene Oxide in Water Solution under Static Magnetic Field Exposure Studied by FTIR Spectroscopy. *Advances in Physical Chemistry*, *2013*(1), 485865. https://doi.org/10.1155/2013/485865

Chawla, S., Varghese, B. S., A, C., Hussain, C. G., Keçili, R., & Hussain, C. M. (2022). Environmental impacts of post-consumer plastic wastes: Treatment technologies towards eco-sustainability and circular economy. In *Chemosphere* (Vol. 308). https://doi.org/10.1016/j.chemosphere.2022.135867

Chen, C. yao, Gu, J., Weng, Y. xuan, Huang, Z. gang, Qiu, D., & Shao, S. xi. (2018). Optimization of the preparation process of biodegradable masterbatches and characterization of their rheological and application properties. *Polymer Testing*, *70*. https://doi.org/10.1016/j.polymertesting.2018.08.011

Chen, D., Gao, A., Cen, K., Zhang, J., Cao, X., & Ma, Z. (2018). Investigation of biomass torrefaction based on three major components: Hemicellulose, cellulose, and lignin. *Energy Conversion and Management*, *169*. https://doi.org/10.1016/j.enconman.2018.05.063

Cheng, J., Gao, R., Zhu, Y., & Lin, Q. (2024). Applications of biodegradable materials in food packaging: A review. In *Alexandria Engineering Journal* (Vol. 91). https://doi.org/10.1016/j.aej.2024.01.080

Choudhry, A., & Akhtar, N. (2023). Formulation, characterization of Quercus infectoria (Olivier) emulsions, and in vitro, in vivo evaluation as

cosmeceutical formulation. *Journal of Cosmetic Dermatology*, *22*(12). https://doi.org/10.1111/jocd.15865

Christie, R., & Abel, A. (2022). Quinacridone pigments. *Physical Sciences Reviews*, *7*(2). https://doi.org/10.1515/psr-2020-0195

Dawson, T. L. (2009). Biosynthesis and synthesis of natural colours. *Coloration Technology*, *125*(2), 61–73. https://doi.org/10.1111/J.1478-4408.2009.00177.X

De Carvalho, J. C., Cardoso, L. C., Ghiggi, V., Woiciechowski, A. L., De Souza Vandenberghe, L. P., & Soccol, C. R. (2014). Microbial Pigments. *Biotransformation of Waste Biomass into High Value Biochemicals*, *9781461480051*, 73–97. https://doi.org/10.1007/978-1-4614-8005-1_4

De Santis, D., & Moresi, M. (2007). Production of alizarin extracts from Rubia tinctorum and assessment of their dyeing properties. *Industrial Crops and Products*, *26*(2). https://doi.org/10.1016/j.indcrop.2007.02.002

de Souza Mesquita, L. M., Martins, M., Pisani, L. P., Ventura, S. P. M., & de Rosso, V. V. (2021). Insights on the use of alternative solvents and technologies to recover bio-based food pigments. *Comprehensive Reviews in Food Science and Food Safety*, *20*(1). https://doi.org/10.1111/1541-4337.12685

Demir, M. M., & Wegner, G. (2012). Challenges in the preparation of optical polymer composites with nanosized pigment particles: A review on recent efforts. In *Macromolecular Materials and Engineering* (Vol. 297, Issue 9). https://doi.org/10.1002/mame.201200089

Derksen, G. C. H., & Van Beek, T. A. (2002). Rubia tinctorum L. *Studies in Natural Products Chemistry*, *26*(PART G). https://doi.org/10.1016/S1572-5995(02)80016-3

Deshmukh, K., Khatake, S. M., & Joshi, G. M. (2013). Surface properties of graphene oxide reinforced polyvinyl chloride nanocomposites. *Journal of Polymer Research*, *20*(11). https://doi.org/10.1007/s10965-013-0286-2

Desidery, L., & Lanotte, M. (2021). Effect of waste polyethylene and wax-based additives on bitumen performance. *Polymers*, *13*(21). https://doi.org/10.3390/polym13213733

Dolza, C., Fages, E., Gonga, E., Gomez-Caturla, J., Balart, R., & Quiles-Carrillo, L. (2021). Development and characterization of environmentally friendly wood plastic composites from biobased polyethylene and short natural fibers processed by injection moulding. *Polymers*, *13*(11). https://doi.org/10.3390/polym13111692

Dostál, J., Kašpárková, V., Zatloukal, M., Muras, J., & Šimek, L. (2008). Influence of the repeated extrusion on the degradation of polyethylene. Structural changes in low density polyethylene. *European Polymer Journal*, *44*(8). https://doi.org/10.1016/j.eurpolymj.2008.05.028

Ersoy, O., & Köse, H. (2020). Comparison of the effect of reactive and nonreactive treatments on the dispersion characteristics of a calcium carbonate (calcite) filler in a polypropylene matrix composite. *Polymer Composites*, *41*(9). https://doi.org/10.1002/pc.25634

Evode, N., Qamar, S. A., Bilal, M., Barceló, D., & Iqbal, H. M. N. (2021). Plastic waste and its management strategies for environmental sustainability. *Case Studies in Chemical and Environmental Engineering*, *4*. https://doi.org/10.1016/j.cscee.2021.100142

Ferreira, E. S. B., Hulme, A. N., McNab, H., & Quye, A. (2004). The natural constituents of historical textile dyes. *Chemical Society Reviews*, *33*(6). https://doi.org/10.1039/b305697j

Foschi, E., & Bonoli, A. (2019). The commitment of packaging industry in the framework of the european strategy for plastics in a circular economy. *Administrative Sciences*, *9*(1). https://doi.org/10.3390/admsci9010018

Galasso, C., Corinaldesi, C., & Sansone, C. (2017). Carotenoids from marine organisms: Biological functions and industrial applications. In *Antioxidants* (Vol. 6, Issue 4). https://doi.org/10.3390/antiox6040096

Gandhi, N., Farfaras, N., Wang, N. H. L., & Chen, W. T. (2021). Life cycle assessment of recycling high-density polyethylene plastic waste. *Journal of Renewable Materials*, *9*(8). https://doi.org/10.32604/jrm.2021.015529

Garcia-Garcia, D., Carbonell-Verdu, A., Jordá-Vilaplana, A., Balart, R., & Garcia-Sanoguera, D. (2016). Development and characterization of green composites from bio-based polyethylene and peanut shell. *Journal of Applied Polymer Science*, *133*(37). https://doi.org/10.1002/app.43940

Giuliani, A., Cerretani, L., & Cichelli, A. (2015). Colors: Properties and Determination of Natural Pigments. In *Encyclopedia of Food and Health*. https://doi.org/10.1016/B978-0-12-384947-2.00189-6

González-Aguilar, S. E., Robledo-Ortíz, J. R., Arellano, M., Martín del Campo, A. S., Rodrigue, D., & Pérez-Fonseca, A. A. (2025). Mechanical recycling of biobased polyethylene-agave fiber composites. *Journal of Thermoplastic Composite Materials*, *38*(1), 140–160. https://doi.org/10.1177/08927057241248045

Granados-Carrera, C. M., Castro-Criado, D., Jiménez-Rosado, M., Romero, A., & Perez-Puyana, V. M. (2025). Reinforcement of soy protein-based bioplastics as potential sustainable packaging solutions. *Future Foods*, *11*. https://doi.org/10.1016/j.fufo.2024.100524

Gulmine, J. V., Janissek, P. R., Heise, H. M., & Akcelrud, L. (2002). Polyethylene characterization by FTIR. *Polymer Testing*, *21*(5). https://doi.org/10.1016/S0142-9418(01)00124-6

Gulmine, J. V., Janissek, P. R., Heise, H. M., & Akcelrud, L. (2003). Degradation profile of polyethylene after artificial accelerated weathering. *Polymer Degradation and Stability*, *79*(3). https://doi.org/10.1016/S0141-3910(02)00338-5

Hellvig, E. L. F., & Flores-Sahagun, T. H. S. (2023). Investments in Braskem green polymers: Extraordinary profits or decarbonization of the

environment. *International Journal of Sustainable Development Research*, *7*(1).

Helmes, R. J. K., Goglio, P., Salomoni, S., van Es, D. S., Vural Gursel, I., & Aramyan, L. (2022). Environmental Impacts of End-of-Life Options of Biobased and Fossil-Based Polyethylene Terephthalate and High-Density Polyethylene Packaging. *Sustainability (Switzerland)*, *14*(18). https://doi.org/10.3390/su141811550

Higuera-Ciapara, I., Félix-Valenzuela, L., & Goycoolea, F. M. (2006). Astaxanthin: A review of its chemistry and applications. In *Critical Reviews in Food Science and Nutrition* (Vol. 46, Issue 2). https://doi.org/10.1080/10408690590957188

Hirsch, S. G., Barel, B., Shpasser, D., Segal, E., & Gazit, O. M. (2017). Correlating chemical and physical changes of photo-oxidized low-density polyethylene to the activation energy of water release. *Polymer Testing*, *64*. https://doi.org/10.1016/j.polymertesting.2017.10.005

Ibáñez-García, A., Berbegal-Pina, R., Vidal, R., & Martínez-García, A. (2024). Sustainability in the Development of Natural Pigment-Based Colour Masterbatches and Their Application in Biopolymers. *Polymers 2024, Vol. 16, Page 2116*, *16*(15), 2116. https://doi.org/10.3390/POLYM16152116

Idumah, C. I., & Obele, C. M. (2021). Understanding interfacial influence on properties of polymer nanocomposites. In *Surfaces and Interfaces* (Vol. 22). https://doi.org/10.1016/j.surfin.2020.100879

Isam Bakr Albaker, R., Kocaman, S., Marti, M. E., & Ahmetli, G. (2021). Application of various carboxylic acids modified walnut shell waste as natural filler for epoxy-based composites. *Journal of Applied Polymer Science*, *138*(31). https://doi.org/10.1002/app.50770

Jaiswal, D., De Souza, A. P., Larsen, S., Lebauer, D. S., Miguez, F. E., Sparovek, G., Bollero, G., Buckeridge, M. S., & Long, S. P. (2017). Brazilian

sugarcane ethanol as an expandable green alternative to crude oil use. *Nature Climate Change*, *7*(11). https://doi.org/10.1038/nclimate3410

Javadi, Y., Hosseini, M. S., & Aghjeh, M. K. R. (2014). The effect of carbon black and HALS hybrid systems on the UV stability of high-density polyethylene (HDPE). *Iranian Polymer Journal (English Edition)*, *23*(10), 793–799. https://doi.org/10.1007/S13726-014-0275-2/TABLES/3

Jin, H., Gonzalez-Gutierrez, J., Oblak, P., Zupančič, B., & Emri, I. (2012). The effect of extensive mechanical recycling on the properties of low density polyethylene. *Polymer Degradation and Stability*, *97*(11). https://doi.org/10.1016/j.polymdegradstab.2012.07.039

Joo, C., Lee, J., Lim, J., Kim, J., & Cho, H. (2024). A genetic algorithm-based optimal selection and blending ratio of plastic waste for maximizing economic potential. *Process Safety and Environmental Protection*, *186*, 715–727. https://doi.org/10.1016/j.psep.2024.03.114

Jorda-Reolid, M., Gomez-Caturla, J., Ivorra-Martinez, J., Stefani, P. M., Rojas-Lema, S., & Quiles-Carrillo, L. (2021). Upgrading argan shell wastes in wood plastic composites with biobased polyethylene matrix and different compatibilizers. *Polymers*, *13*(6). https://doi.org/10.3390/polym13060922

Jurić, S., Jurić, M., Król-Kilińska, Ż., Vlahoviček-Kahlina, K., Vinceković, M., Dragović-Uzelac, V., & Donsì, F. (2022). Sources, stability, encapsulation and application of natural pigments in foods. In *Food Reviews International* (Vol. 38, Issue 8). https://doi.org/10.1080/87559129.2020.1837862

Kannan, D., Reddy, M. V., Mohanakrishna, G., Sarkar, O., Isha, I., Rohit, M. V, Patel, A., & Chang, Y.-C. (2025). *Advances in Microbial and Plant Based Biopolymers: Synthesis and Applications in Next-Generation Materials*. https://doi.org/10.20944/preprints202502.0548.v1

Karlsen, E. M., & Spanget-Larsen, J. (2009). FTIR investigation of the reaction between pyridine and iodine in a polyethylene host. Formation of N-

iodopyridinium polyiodide. *Chemical Physics Letters*, *473*(4–6), 227–232. https://doi.org/10.1016/J.CPLETT.2009.04.005

Kikuchi, Y., Hirao, M., Narita, K., Sugiyama, E., Oliveira, S., Chapman, S., Arakaki, M. M., & Cappra, C. M. (2013). Environmental performance of biomass-derived chemical production: A case study on sugarcane-derived polyethylene. *Journal of Chemical Engineering of Japan*, *46*(4). https://doi.org/10.1252/jcej.12we227

Ko, K., Dadmohammadi, Y., & Abbaspourrad, A. (2021). Nutritional and bioactive components of pomegranate waste used in food and cosmetic applications: A review. In *Foods* (Vol. 10, Issue 3). https://doi.org/10.3390/foods10030657

Kong, Y., & Hay, J. N. (2003). The enthalpy of fusion and degree of crystallinity of polymers as measured by DSC. *European Polymer Journal*, *39*(8). https://doi.org/10.1016/S0014-3057(03)00054-5

Kuan, H. T. N., Tan, M. Y., Shen, Y., & Yahya, Mohd. Y. (2021). Mechanical properties of particulate organic natural filler-reinforced polymer composite: A review. *Composites and Advanced Materials*, *30*. https://doi.org/10.1177/26349833211007502

Kuciel, S., Jakubowska, P., & Kuźniar, P. (2014). A study on the mechanical properties and the influence of water uptake and temperature on biocomposites based on polyethylene from renewable sources. *Composites Part B: Engineering*, *64*. https://doi.org/10.1016/j.compositesb.2014.03.026

Lagaron, J. M., Giménez, E., & Saura, J. J. (2001). Degradation of high barrier ethylene-vinyl alcohol copolymer under mild thermal-oxidative conditions studied by thermal analysis and infrared spectroscopy. *Polymer International*, *50*(6). https://doi.org/10.1002/pi.674

Lambert, S., & Wagner, M. (2017). Environmental performance of bio-based and biodegradable plastics: The road ahead. In *Chemical Society Reviews* (Vol. 46, Issue 22). https://doi.org/10.1039/c7cs00149e

Lapčík, L., Maňas, D., Lapčíková, B., Vašina, M., Staněk, M., Čépe, K., Vlček, J., Waters, K. E., Greenwood, R. W., & Rowson, N. A. (2018). Effect of filler particle shape on plastic-elastic mechanical behavior of high density poly(ethylene)/mica and poly(ethylene)/wollastonite composites. *Composites Part B: Engineering*, *141*. https://doi.org/10.1016/j.compositesb.2017.12.035

Lee, J. Y., Lee, S. E., & Lee, D. W. (2022). Current status and future prospects of biological routes to bio-based products using raw materials, wastes, and residues as renewable resources. *Critical Reviews in Environmental Science and Technology*, *52*(14), 2453–2509. https://doi.org/10.1080/10643389.2021.1880259

Leong, Y. W., Abu Bakar, M. B., Ishak, Z. A. M., Ariffin, A., & Pukanszky, B. (2004). Comparison of the mechanical properties and interfacial interactions between talc, kaolin, and calcium carbonate filled polypropylene composites. *Journal of Applied Polymer Science*, *91*(5). https://doi.org/10.1002/app.13542

Leppäkoski, L., Lopez, G., Uusitalo, V., Nieminen, H., Järviö, N., Kosonen, A., Koiranen, T., Laari, A., Breyer, C., & Ahola, J. (2023). Climate and biodiversity impacts of low-density polyethylene production from CO2 and electricity in comparison to bio-based polyethylene. *Science of the Total Environment*, *882*. https://doi.org/10.1016/j.scitotenv.2023.163628

Lertwimolnun, W., & Vergnes, B. (2006). Effect of processing conditions on the formation of polypropylene/organoclay nanocomposites in a twin screw extruder. *Polymer Engineering and Science*, *46*(3). https://doi.org/10.1002/pen.20458

Liang, J. Z., & Li, R. K. Y. (2000). Effect of filler content and surface treatment on the tensile properties of glass-bead-filled polypropylene composites. *Polymer International*, *49*(2). https://doi.org/10.1002/(SICI)1097-0126(200002)49:2<170::AID-PI322>3.0.CO;2-U

Lomax, S. Q. (2005). Phthalocyanine and quinacridone pigments: their history, properties and use. *Studies in Conservation*, *50*(sup1). https://doi.org/10.1179/sic.2005.50.supplement-1.19

Maalihan, R. D., & Pajarito, B. B. (2015). Effect of Colorant on Tensile Strength and Carbonyl Index of Oxo-Biodegradable Low-Density Polyethylene Films during Thermal Aging. *Advanced Materials Research*, *1125*. https://doi.org/10.4028/www.scientific.net/amr.1125.235

Mahdi, E., & Dean, A. (2020). The effect of filler content on the tensile behavior of polypropylene/cotton fiber and poly(vinyl chloride)/cotton fiber composites. *Materials*, *13*(3). https://doi.org/10.3390/ma13030753

Mahendran, A. R., Aust, N., Vijayakumar, C. T., & Lederer, K. (2008). Preparation and characterization of partially degraded high-density polyethylene in an internal mixer. *Polymer - Plastics Technology and Engineering*, *47*(11). https://doi.org/10.1080/03602550802391623

Maraveas, C. (2020). Environmental sustainability of plastic in agriculture. In *Agriculture (Switzerland)* (Vol. 10, Issue 8). https://doi.org/10.3390/agriculture10080310

Marsh, R., Griffiths, A. J., Williams, K. P., & Evans, S. L. (2006). Thermal degradation of polyethylene film materials due to successive recycling. *Proceedings of the Institution of Mechanical Engineers, Part C: Journal of Mechanical Engineering Science*, *220*(8). https://doi.org/10.1243/09544062JMES178

Martin, C. (2013). *Twin Screw Extrusion for Pharmaceutical Processes*. https://doi.org/10.1007/978-1-4614-8432-5_2

McKeown, N. B. (1998). Phthalocyanine materials: synthesis, structure, and function. In *Chemistry of Solid State Materials*. Cambridge University Press.

Mecking, S. (2020). Polyethylene-like materials from plant oils: PE-like materials from plant oils. *Philosophical Transactions of the Royal Society*

A: Mathematical, Physical and Engineering Sciences, *378*(2176). https://doi.org/10.1098/rsta.2019.0266

Mendes, A. A., Cunha, A. M., & Bernardo, C. A. (2011). Study of the degradation mechanisms of polyethylene during reprocessing. *Polymer Degradation and Stability*, *96*(6). https://doi.org/10.1016/j.polymdegradstab.2011.02.015

Mendieta, C. M., Vallejos, M. E., Felissia, F. E., Chinga-Carrasco, G., & Area, M. C. (2020). Review: Bio-polyethylene from Wood Wastes. In *Journal of Polymers and the Environment* (Vol. 28, Issue 1). https://doi.org/10.1007/s10924-019-01582-0

Moshood, T. D., Nawanir, G., Mahmud, F., Mohamad, F., Ahmad, M. H., & AbdulGhani, A. (2022). Sustainability of biodegradable plastics: New problem or solution to solve the global plastic pollution? In *Current Research in Green and Sustainable Chemistry* (Vol. 5). https://doi.org/10.1016/j.crgsc.2022.100273

Neo, P. K., Kitada, Y., Deeying, J., Thumsorn, S., Soon, M. F., Goh, Q. S., Leong, Y. W., & Ito, H. (2023). Influence of Compounding Parameters on Color Space and Properties of Thermoplastics with Ultramarine Blue Pigment. *Polymers*, *15*(24). https://doi.org/10.3390/polym15244718

Oblak, P., Gonzalez-Gutierrez, J., Zupančič, B., Aulova, A., & Emri, I. (2015). Processability and mechanical properties of extensively recycled high density polyethylene. *Polymer Degradation and Stability*, *114*. https://doi.org/10.1016/j.polymdegradstab.2015.01.012

Orue, A., Eceiza, A., & Arbelaiz, A. (2020). The use of alkali treated walnut shells as filler in plasticized poly(lactic acid) matrix composites. *Industrial Crops and Products*, *145*. https://doi.org/10.1016/j.indcrop.2019.111993

Özgür Seydibeyoğlu, M., Misra, M., & Mohanty, A. (2010). Synergistic improvements in the impact strength and % elongation of polyhydroxybutyrate-co-valerate copolymers with functionalized soybean

oils and poss. *International Journal of Plastics Technology*, *14*(1). https://doi.org/10.1007/s12588-010-0005-3

Papo, M., & Corona, B. (2022). Life cycle sustainability assessment of non-beverage bottles made of recycled High Density Polyethylene. *Journal of Cleaner Production*, *378*. https://doi.org/10.1016/j.jclepro.2022.134442

Pérez, E., Alvarez, V., Pérez, C. J., & Bernal, C. (2013). A comparative study of the effect of different rigid fillers on the fracture and failure behavior of polypropylene based composites. *Composites Part B: Engineering*, *52*. https://doi.org/10.1016/j.compositesb.2013.03.035

Petrielli, G. P., Nogueira, G. P., Henzler, D. de S., de Souza, N. R. D., Bruno, K. M. B., Luciano, A. C. dos S., le Maire, G., & Hernandes, T. A. D. (2023). Integrating carbon footprint to spatialized modeling: The mitigation potential of sugarcane ethanol production in the Brazilian Center-South. *Resources, Conservation and Recycling*, *189*. https://doi.org/10.1016/j.resconrec.2022.106725

Poletto, M., Ornaghi Jnior, H. L., & Zattera, A. J. (2015). Thermal Decomposition of Natural Fibers: Kinetics and Degradation Mechanisms. In *Reactions and Mechanisms in Thermal Analysis of Advanced Materials*. https://doi.org/10.1002/9781119117711.ch21

Queyroy, S., & Monasse, B. (2012). Effect of the molecular structure of semicrystalline polyethylene on mechanical properties studied by molecular dynamics. *Journal of Applied Polymer Science*, *125*(6). https://doi.org/10.1002/app.36560

Quiles-Carrillo, L., Montanes, N., Jorda-Vilaplana, A., Balart, R., & Torres-Giner, S. (2019). A comparative study on the effect of different reactive compatibilizers on injection-molded pieces of bio-based high-density polyethylene/polylactide blends. *Journal of Applied Polymer Science*, *136*(16). https://doi.org/10.1002/app.47396

Rahman, M. H., & Bhoi, P. R. (2021). An overview of non-biodegradable bioplastics. In *Journal of Cleaner Production* (Vol. 294). https://doi.org/10.1016/j.jclepro.2021.126218

Rodriguez-Amaya, D. B. (2019). Update on natural food pigments - A mini-review on carotenoids, anthocyanins, and betalains. *Food Research International*, *124*. https://doi.org/10.1016/j.foodres.2018.05.028

Saeaung, K., Phusunti, N., Phetwarotai, W., Assabumrungrat, S., & Cheirsilp, B. (2021). Catalytic pyrolysis of petroleum-based and biodegradable plastic waste to obtain high-value chemicals. *Waste Management*, *127*, 101–111. https://doi.org/10.1016/J.WASMAN.2021.04.024

Saikrishnan, S., Jubinville, D., Tzoganakis, C., & Mekonnen, T. H. (2020). Thermo-mechanical degradation of polypropylene (PP) and low-density polyethylene (LDPE) blends exposed to simulated recycling. *Polymer Degradation and Stability*, *182*. https://doi.org/10.1016/j.polymdegradstab.2020.109390

Salem, M. A., Farouk, H., & Kashif, I. (2002). Physicochemical changes in UV-exposed low- density polyethylene films. *Macromolecular Research*, *10*(3), 168–173. https://doi.org/10.1007/BF03218267/METRICS

Senneca, O., Cerciello, F., Russo, C., Wütscher, A., Muhler, M., & Apicella, B. (2020). Thermal treatment of lignin, cellulose and hemicellulose in nitrogen and carbon dioxide. *Fuel*, *271*. https://doi.org/10.1016/j.fuel.2020.117656

Shen, M., Huang, W., Chen, M., Song, B., Zeng, G., & Zhang, Y. (2020). (Micro)plastic crisis: Un-ignorable contribution to global greenhouse gas emissions and climate change. In *Journal of Cleaner Production* (Vol. 254). https://doi.org/10.1016/j.jclepro.2020.120138

Shirvanimoghaddam, K., Balaji, K. V., Yadav, R., Zabihi, O., Ahmadi, M., Adetunji, P., & Naebe, M. (2021). Balancing the toughness and strength in polypropylene composites. In *Composites Part B: Engineering* (Vol. 223). https://doi.org/10.1016/j.compositesb.2021.109121

Siracusa, V., & Blanco, I. (2020). Bio-Polyethylene (Bio-PE), Bio-Polypropylene (Bio-PP) and Bio-Poly(ethylene terephthalate) (Bio-PET): Recent Developments in Bio-Based Polymers Analogous to Petroleum-Derived Ones for Packaging and Engineering Applications. *Polymers*, *12*(8). https://doi.org/10.3390/polym12081641

Soo, X. Y. D., Muiruri, J. K., Wu, W. Y., Yeo, J. C. C., Wang, S., Tomczak, N., Thitsartarn, W., Tan, B. H., Wang, P., Wei, F., Suwardi, A., Xu, J., Loh, X. J., Yan, Q., & Zhu, Q. (2024). Bio-Polyethylene and Polyethylene Biocomposites: An Alternative toward a Sustainable Future. In *Macromolecular Rapid Communications* (Vol. 45, Issue 14). John Wiley and Sons Inc. https://doi.org/10.1002/marc.202400064

Stevulova, N., Estokova, A., Cigasova, J., Schwarzova, I., Kacik, F., & Geffert, A. (2017). Thermal degradation of natural and treated hemp hurds under air and nitrogen atmosphere. *Journal of Thermal Analysis and Calorimetry*, *128*(3). https://doi.org/10.1007/s10973-016-6044-z

Suarez, A., Ford, E., Venditti, R., Kelley, S., Saloni, D., & Gonzalez, R. (2023). Is sugarcane-based polyethylene a good alternative to fight climate change? *Journal of Cleaner Production*, *395*. https://doi.org/10.1016/j.jclepro.2023.136432

Talikoti, C. B., Hawal, T. T., Kakkamari, P. P., Patil, M. S., Tech, M., & Engineering, M. (2015). Preparation and Characterization of Epoxy Composite Reinforced With Walnut Shell Powder. *International Research Journal of Engineering and Technology (IRJET)*, *2*(5).

Trucillo, P., Rizzo, M., Errico, D., & Di Maio, E. (2024). Social, Economic, and Environmental Impacts of Bio-Based Versus Fossil-Derived Polyethylene Production. *Advanced Sustainable Systems*, *9*(1), 2400392. https://doi.org/10.1002/ADSU.202400392;WGROUP:STRING:PUBLICATION

Tsenoglou, C., Kartalis, C. N., Papaspyrides, C. D., & Pfaendner, R. (2001). Modeling the role of stabilizing additives during melt recycling of high-

density polyethylene. *Journal of Applied Polymer Science*, *80*(12). https://doi.org/10.1002/app.1324

Tsiropoulos, I., Faaij, A. P. C., Lundquist, L., Schenker, U., Briois, J. F., & Patel, M. K. (2015). Life cycle impact assessment of bio-based plastics from sugarcane ethanol. *Journal of Cleaner Production*, *90*. https://doi.org/10.1016/j.jclepro.2014.11.071

Vanli, A. S., & Karakaya, C. (2025). *Investigation of the Use of Sustainable Polymers in the Industry and the Effects of Olive Seed Additives on Polymer Properties*. https://doi.org/10.20944/preprints202501.1338.v1

Vänskä, E., Vihelä, T., Peresin, M. S., Vartiainen, J., Hummel, M., & Vuorinen, T. (2016). Residual lignin inhibits thermal degradation of cellulosic fiber sheets. *Cellulose*, *23*(1). https://doi.org/10.1007/s10570-015-0791-z

Venil, C. K., Velmurugan, P., Dufossé, L., Devi, P. R., & Ravi, A. V. (2020). Fungal pigments: Potential coloring compounds for wide ranging applications in textile dyeing. In *Journal of Fungi* (Vol. 6, Issue 2). https://doi.org/10.3390/jof6020068

Wagner, J. R., Mount, E. M., & Giles, H. F. (2013). Extrusion: The Definitive Processing Guide and Handbook. In *Extrusion: The Definitive Processing Guide and Handbook*. https://doi.org/10.1016/C2010-0-67040-4

Wang, Z., Ganewatta, M. S., & Tang, C. (2020). Sustainable polymers from biomass: Bridging chemistry with materials and processing. In *Progress in Polymer Science* (Vol. 101). https://doi.org/10.1016/j.progpolymsci.2019.101197

Weinmann, M. (2007). Masterbatch production on co-rotating twin screw extruders. *Plastics, Additives and Compounding*, *9*(2). https://doi.org/10.1016/S1464-391X(07)70028-4

Wijesekara, T., & Xu, B. (2024). A critical review on the stability of natural food pigments and stabilization techniques. *Food Research International*, *179*. https://doi.org/10.1016/j.foodres.2024.114011

Wong, A. C. Y., Ng, N. S. K., & Ng, V. L. F. (1997). Colouring of moulded plastic products by the addition of colour masterbatches. *Journal of Materials Processing Technology*, *63*(1–3). https://doi.org/10.1016/S0924-0136(96)02666-0

Wu, T., Li, Y., Wu, Q., Wu, G., & Tan, H. M. (2005). Study on the nonisothermal crystallization process of mLLDPE/EVA blends using FTIR micro-spectroscopy. *Journal of Applied Polymer Science*, *96*(2), 261–267. https://doi.org/10.1002/APP.20953

Yao, Z., Seong, H. J., & Jang, Y. S. (2022). Environmental toxicity and decomposition of polyethylene. In *Ecotoxicology and Environmental Safety* (Vol. 242). https://doi.org/10.1016/j.ecoenv.2022.113933

Yoon, B., Kim, S., Lang, A., Egelkamp, C., Meier, J., Giese, U., Kim, B., Kim, J. H., Bae, J. W., Um, G. Y., Kim, S. H., Kim, D. Il, Kim, S. J., & Suhr, J. (2022). Friction behaviors of rice husk silica-reinforced elastomer composites in contact with rough self-affine surfaces. *Polymer Testing*, *116*. https://doi.org/10.1016/j.polymertesting.2022.107764

Yücetürk, M., & Seydibeyoğlu, M. Ö. (2020). Understanding dispersion of copper phthalocyanine alpha blue pigment in polyethylene masterbatch with the use of wax. *Coloration Technology*, *136*(6). https://doi.org/10.1111/cote.12506

Zaman, A., & Newman, P. (2021). Plastics: are they part of the zero-waste agenda or the toxic-waste agenda? *Sustainable Earth*, *4*(1). https://doi.org/10.1186/S42055-021-00043-8

Zheng, H., Sun, Z., & Zhang, H. (2020). Effects of walnut shell powders on the morphology and the thermal and mechanical properties of poly(lactic acid). *Journal of Thermoplastic Composite Materials*, *33*(10). https://doi.org/10.1177/0892705719828801

Curriculum Vitae

Mert Yücetürk

Education

Ph.D. in Materials Science and Engineering

İzmir Kâtip Çelebi University, 2020 – 2025 (GPA: 3.95/4.00)

Thesis Title: Investigation of Process Conditions in the Preparation of Biobased Polyethylene Masterbatch and Development of Innovative Masterbatches

Focus areas: Biobased polymers, pigment dispersion, recycling technologies, advanced characterization techniques

B.Sc. in Materials Science and Engineering

İzmir Kâtip Çelebi University, 2015 – 2019 (GPA: 3.70/4.00, Ranked 1st in class)

Thesis Title: Dispersion of Phthalocyanine Blue Pigments in Polyethylene Masterbatch

B.A. in Business Administration

Anadolu University, 2005 – 2009 (GPA: 2.61/4.00)

Work Experience

R&D Manager, BudinGroup – Masterbatches & Printing Inks Manufacturer

March 2018 – Present, İzmir, Türkiye

- Managed R&D and quality control operations in masterbatch, plastic compound, and thermoplastic composite production
- Led multiple TÜBİTAK and KOSGEB-supported R&D projects
- Specialized in color measurement, formulation optimization, and performance testing of polymer products
- Skilled in polymer processing and characterization techniques, including extrusion, blown film, FTIR, DSC, and MFI analysis

R&D and Quality Control Specialist, BudinGroup

September 2007 – March 2018, İzmir, Türkiye

- Conducted pigment dispersion and polymer material testing
- Implemented quality assurance protocols in manufacturing processes

Publications Derived from Ph.D. Dissertation

1. Yücetürk, M., Aksoy, E., & Seydibeyoğlu, M. Ö. (2025). Development of Eco-Friendly Food Packaging Films Using Bio-Based Polyethylene and Natural Pigments. Packaging Technology and Science, 38(3), 241-253.

2. Yücetürk, M., & Seydibeyoğlu, M. Ö. (2024). Bio-based polyethylene masterbatch preparation and investigation of the effect of process conditions on pigment dispersion. Coloration Technology.

3. Yücetürk, M., & Seydibeyoğlu, M. Ö. (2025) (Under Review). Comparative analysis on the recycling performance of biobased and petroleum-based polyethylene. Journal of Applied Polymer Science. Manuscript ID: app.20250915

Other Publications

4. Yilmaz Atay, G., Mergen, B., Sakan, E., Yücetürk, B., & Yücetürk, M. (2024). Improving mechanical properties of huntite hydromagnesite reinforced flame retardant

polymer composites with calcite and zeolite minerals. Vietnam Journal of Chemistry, 62(1), 114-121.

5. Yücetürk, M., Yücetürk, B., & Yılmaz Atay, G. (2024). Investigation of combustion and mechanical properties of huntite-hydromagnesite and intumescent flame retardants in polypropylene composites. Journal of Composite Materials, 58(2), 181-191.

6. Yücetürk, M., Yücetürk, B., & Yegane, G. (2024). Investigation of flame retardancy and physical-mechanical properties of mineral-based polyethylene composites. Journal of Thermoplastic Composite Materials, 37(7), 2377-2390.

7. Aksoy, Ö., Doğru, A., Yücetürk, M., Alyamaç, E., & Seydibeyoglu, M. O. (2022). Rheology of nanocomposites. In Nanoparticle-Based Polymer Composites (pp. 109-118). Woodhead Publishing.

8. Yücetürk, M., Kuru, B., & Seydibeyoğlu, M. Ö. (2021). Synergistic effect of natural clinoptilolite with non-lethal repellents in anti-rodent dry food packaging. Packaging Technology and Science, 34(11-12), 683-692.

9. Yücetürk, M., & Seydibeyoğlu, M. Ö. (2020). Understanding dispersion of copper phthalocyanine alpha blue pigment in polyethylene masterbatch with the use of wax. Coloration Technology, 136(6), 526-534.